

# UC Riverside

## UC Riverside Electronic Theses and Dissertations

### Title

Genetically Encoded FRET-Based Probes for Live Cell Imaging

### Permalink

<https://escholarship.org/uc/item/0n95n65h>

### Author

Youssef, Suzan Ali

### Publication Date

2016

Peer reviewed|Thesis/dissertation

UNIVERSITY OF CALIFORNIA  
RIVERSIDE

Genetically Encoded FRET-Based Probes for Live Cell Imaging

A Dissertation submitted in partial satisfaction  
of the requirements for the degree of

Doctor of Philosophy

in

Chemistry

by

Suzan Ali Youssef

June 2016

Dissertation Committee:

Dr. Huiwang Ai, Chairperson

Dr. Q. Jason Cheng

Dr. Wenwan Zhong

Copyright by  
Suzan Ali Youssef  
2016

The Dissertation of Suzan Ali Youssef is approved:

---

---

---

Committee Chairperson

University of California, Riverside

## ACKNOWLEDGEMENTS

During my PhD journey, I have had great opportunity to learn and grow as both a scientist and a person. There are many people responsible for where I am, and without their help and encouragement this would not have been possible.

My gratitude first goes to Dr. Huiwang Ai, my advisor, chair of the committee. I was very fortunate to join his laboratory in 2011. His much needed guidance and encouragement have been a great source of inspiration for me during my PhD journey. His patience and kindness have greatly enforced my persistence on pursuing goals on scientific research. Thank you Dr. Ai, your precious training and guidance is much appreciated.

Next, I would like to express my gratitude to my committee, Professors Jason Cheng and Wenwan Zhong. I appreciate all your efforts in taking time reading my dissertation and offering your suggestions. Thank you!

Also, I would like to take a moment to thank all the members of the Ai lab. My research would not have been possible without your discussions, and useful comments and suggestions on problems I encountered along the way with my research projects.

Finally, my heartiest love, respect and thanks goes to my parents, Ali Youssef and Jamila Sawan, and to my husband, Ziad Saleh whose immense love, support, and confidence in me paved my way to successfully accomplish my goal.

## **DEDICATIONS**

To my parents Ali Youssef and Jamila Sawan for all their love and support and putting me through the best education possible. I appreciate their sacrifices and I wouldn't have been able to get to this stage without them.

To my husband Ziad Saleh for his unending support, level-headedness and love. I wouldn't have gotten through this doctorate if it wasn't for him.

To my kids, Amer Saleh, Majd Saleh, and Mohamad Saleh.

## ABSTRACT OF THE DISSERTATION

Genetically Encoded FRET-Based Probes for Live Cell Imaging

by

Suzan Ali Youssef

Doctor of Philosophy, Graduate Program in Chemistry  
University of California, Riverside, June 2016  
Dr. Huiwang Ai, Chairperson

Biosensors based on the principle of Förster resonance energy transfer (FRET) have proven to be powerful tools for biological research. Aided by the plethora of color variants to green fluorescent proteins, numerous FRET-based probes have been developed for study of molecular interactions, enzyme activities, and small molecules in live mammalian cells with high spatial and temporal resolution. In this dissertation, I focus on the development of genetically encoded FRET-based probes for cellular processes related to hydrogen sulfide and hypoxic signaling.

Hydrogen sulfide ( $\text{H}_2\text{S}$ ) has been recently identified as an important gasotransmitter playing crucial roles in cell signaling. We developed the first genetically encoded FRET-based biosensor, hsCY, for live-imaging cellular  $\text{H}_2\text{S}$ . We utilized blue and fluorescent proteins (EBFP and cpGFP, respectively), and genetically modified the cpGFP with *p*-azidophenylalanine as the  $\text{H}_2\text{S}$ -sensory element. We validated hsCY *in vitro* and mammalian cells and demonstrated the use of hsCY for selective, ratiometric

imaging of H<sub>2</sub>S. hsCY thus represents a valuable addition to the toolbox for H<sub>2</sub>S detection and imaging.

Oxygen is vital for all aerobic life forms. Oxygen-dependent hydroxylation of hypoxia-inducible factor (HIF)-1 $\alpha$  by prolyl hydroxylase domain enzymes (PHDs) is an important step for controlling the expression of oxygen-regulated genes in metazoan species, thereby constituting a molecular mechanism for oxygen sensing and response. Herein, we report a genetically encoded dual-emission ratiometric fluorescent sensor, ProCY, which responds to PHD activities *in vitro* and in live cells. We demonstrated that ProCY could monitor hypoxia in mammalian cells. By targeting this novel genetically encoded biosensor to the cell nucleus and cytosol, we determined that the HIF-prolyl hydroxylase activity was mainly confined to the cytosol of HEK 293T cells under normoxic conditions. The results collectively suggest broad applications of ProCY on evaluating cellular hypoxia and PHD activities and understanding of pathways for the control of hypoxic responses.

As HIF-prolyl hydroxylases have emerged as promising drug targets for a variety of diseases, such as myocardial infarction, stroke, cancer, diabetes, and severe anemia, we also explored the use of ProCY in high-throughput assays to identify inhibitors or activators of PHDs. Our preliminary study supports the feasibility of this approach. A lentiviral system has been developed for transduction of HEK 293T and establishment of ProCY-expressing stable cells.



## Table of Contents

DEDICATIONS.....	v
ACKNOWLEDGEMENTS.....	iv
ABSTRACT OF THE DISSERTATION.....	vi
Chapter 1.....	1
Introduction.....	1
1.1. Theory of FRET.....	1
1.2. Why Fluorescent Protein-FRET Based Sensors? .....	2
1.3. Genetically Encoded Fluorescent Sensors.....	4
1.4. Green Fluorescent Proteins and Evolution .....	6
1.4.1. The Green Fluorescent Protein .....	6
1.4.2. Circular Permutation of the Green Fluorescent Protein.....	9
1.5. The Genetic Code and Expansion.....	10
1.5.1. The Genetic Code .....	10
1.5.2. Genetic Code Expansion.....	11
1.6. Cell Signaling via Hydrogen Sulfide and HIF-1 $\alpha$ .....	16
1.6.1. Hydrogen Sulfide and Cell Signaling .....	16
1.6.2. Signaling via HIF-1 $\alpha$ .....	18
1.7. Scope of this Dissertation .....	19
References.....	22
Chapter 2.....	28
2.1. Abstract.....	28
2.2. Introduction.....	29
2.3 Experimental Section.....	31
2.3.1. Materials, Reagents, and General Methodology.....	31
2.3.2. Construction of Escherichia coli Expression Plasmids and Libraries. ....	31
2.3.3. Library Screening.....	33
2.3.4 Protein Expression and Purification.....	36

2.3.5. In Vitro Characterization. ....	36
2.3.6. Construction of Mammalian Expression Plasmids .....	37
2.3.7. Mammalian Cell Culture and Imaging. ....	38
2.4 Results and Discussion .....	38
2.4.1. Laboratory Engineering of hsCY .....	38
2.4.2 Spectroscopic Responses of hsCY to H <sub>2</sub> S .....	42
2.4.3 Expression of hsCY in live Live Mammalian Cells .....	48
2.5 Conclusion .....	48
References .....	50
Chapter 3 .....	55
3.1. Abstract .....	55
3.2. Introduction .....	55
3.3. Experimental Section .....	58
3.3.1. Materials, Reagents, and General Methodology .....	58
3.3.2. Construction of E. Coli Expression Plasmids .....	59
3.3.3. Optimization of FRET Efficiency by Linker Modification .....	61
3.3.4. Protein Expression and Purification in E. coli .....	61
3.3.5. Spectroscopic Characterization .....	62
3.3.6. PHD2 Activity Assay .....	63
3.3.7. Construction of Mammalian Reporter Plasmids .....	63
3.3.8. Experimental Design of Hypoxia Chambers .....	64
3.3.9. Mammalian Cell Culture and Imaging .....	65
3.3.10. Western blotting .....	66
3.4. Results and Discussion .....	66
3.5. Conclusion .....	78
References .....	80
Chapter 4 .....	85
4.1. Abstract .....	85
4.2. Introduction .....	86

4.3.1 Materials, Reagents, and General Methodology.....	89
4.3.2. Mammalian Cell Culture, Imaging, and Screening.....	90
4.3.3. Construction of the Lentivirus Reporter Plasmid.....	90
4.3.4. Lentivirus Production and Purification.....	91
4.4. Results and Discussion.....	91
4.5. Conclusion and Future Direction.....	94
Reference.....	96
Chapter 5.....	98
Concluding Remarks and Future Direction.....	98
Appendix A.....	101
Supporting Information for Chapter 2.....	101
Appendix B.....	103
Supporting Information for Chapter 3.....	104
Appendix C.....	107
Supporting Information for Chapter 4.....	107

## Table of Figures

Figure 1.1.....	5
Steps involved in engineering of a genetically encoded fluorescent sensor by the cell machinery.	
Figure 1.2.....	8
Structure of the Green Fluorescent Protein from the <i>jellyfish Aequorea Victoria</i> .	
Figure 1.3.....	13
Steps involved in chromophore maturation of the GFP.	
Figure 1.4.....	15
Schematic diagram showing a general method for genetic incorporation of unnatural acids (UAAs) in live cells.	
Figure 1.5.....	16
Chemical structure of p-Azido-L-phenylalanine (pAzF).	
Figure 2.1.....	35
Illustration of the FRET change of the genetically encoded dual-emission ratiometric fluorescent sensor, hsCY.	
Figure 2.2.....	40
Sequence alignment of hsCY and the different designs developed in this study.	
Figure 2.3.....	43
Fluorescence emission spectra of hsCY (1 $\mu\text{M}$ ) in response to various concentrations of $\text{H}_2\text{S}$ .	
Figure 2.4.....	44
GFP/BFP ratio changes of hsCY (1 $\mu\text{M}$ ) in response to 1 mM $\text{H}_2\text{S}$ , 100 $\mu\text{M}$ , 50 $\mu\text{M}$ , 20 $\mu\text{M}$ , and 0 $\mu\text{M}$ from top to bottom.	
Figure 2.5.....	45
GFP/BFP Ratios of hsCY (1 $\mu\text{M}$ ) to $\text{H}_2\text{S}$ up to 100 $\mu\text{M}$ .	

Figure 2.6.....	46
GFP/BFP Ratios of hsCY (1 $\mu$ M) to H <sub>2</sub> S up to 100 $\mu$ M.	
Figure 2.7.....	47
Live cell imaging of HEK 293T cells expressing hsCY	
Figure 3.1.....	57
Schematic illustration of the regulation of HIF-1 $\alpha$ .	
Figure 3.2.....	68
Illustration of the FRET change of the genetically encoded dual-emission ratiometric fluorescent sensor, ProCY, upon the actions of PHDs.	
Figure 3.3.....	69
Chemical reaction for conversion of proline into 4-hydroxyproline by prolyl hydroxylase domain enzymes (PHDs). (B) Interactions between a VHL domain (residues 60-154) and a HIF-1 $\alpha$ derived peptide, showing several interfacial H-bonds through the hydroxyl group of 4-hydroxyproline (residue 564).	
Figure 3.4.....	70
Domain arrangements of biosensors constructed in this study.	
Figure 3.5.....	71
Fluorescent emission spectra for (A) ProCY-B, (B) ProCY-C, (C) ProCY-D, and (D) ProCY-E before (blue) and after (orange) treatment with a catalytically active PHD2 fragment.	
Figure 3.6.....	72
Domain arrangements of ProCY and the negative-control probe, ProCY-N (A). Fluorescent emission spectra for ProCY before (blue) and after (orange) treatment with a catalytically active PHD2 fragment (B). Fluorescent emission spectra for ProCY-N, showing no response to PHD2 treatment (C).	
Figure 3.7.....	74
Pseudocolored ratio images of representative ProCY-expressing HEK 293T cells without (A-C) or with (D-F) overexpression of PHD2.	

Figure 3.8.....	75
The FRET ratios of ProCY or ProCY-N in HEK 293T cells under the corresponding conditions (A). Western blot of PHD2 and HIF-1 $\alpha$ for cells under hypoxia or normoxia (B).	
Figure 3.9.....	76
Pseudocolored ratio images of representative ProCY-N expressing HEK 293T cells under normoxia (A and B) or hypoxia (C and D).	
Figure 3.10.....	77
Microscopic images of representative HEK 293T cells expressing nuclear or cytosolic ProCY.	
Figure 4.1.....	87
The reaction catalyzed by the HIF prolyl hydroxylases in the hypoxic response.	
Figure 4.2.....	89
Assay Development Cycle for HTS.	
Figure 4.3.....	93
Microscopic images of representative HEK 293T cells expressing ProCY. The cells were cultured under normoxia in a 96-well plate and treated with IOX2.	

## **Chapter 1**

### **Introduction**

Recent advancements in fluorescence microscopy coupled with fluorescent proteins have transformed Fluorescence (Förster) Resonance Energy Transfer (FRET) into a powerful technique to study the dynamics of signaling molecules with high spatial and temporal resolution. Unlike single intensity-based probes, FRET-based sensors provide a signal that is not sensitive to fluctuations in sensor concentration, optical path length or excitation intensity. FRET between two fluorescent proteins can be exploited to create fully genetically encoded sensors and thus subcellularly targetable sensors for the study and evaluation of cell signaling biomolecules such as hydrogen sulfide and prolyl hydroxylase domains. Since cell signaling is the basis of development, tissue repair, immunity and normal tissue homeostasis, sensors that targets cell signaling molecules are important to understand cell signaling pathways and to treat diseases effectively.

#### **1.1. Theory of FRET**

Fluorescence resonance energy transfer (FRET) is an important physical phenomenon describing energy transfer between two light-sensitive fluorophores. It was first described over 50 years ago and it is being used to study important biological events such as protein-protein interactions, conformational changes in soluble and membrane-

associated complexes, cellular and molecular imaging, DNA analysis, to name a few. Today, FRET is used more and more in biomedical research and drug discovery.<sup>1</sup> FRET involves a transfer of energy from a donor chromophore in its excited state to a nearby acceptor chromophore in a non-radiative fashion through long-range dipole-dipole interactions. The donor molecule is the molecule that initially absorbs energy upon irradiation and the acceptor chromophore is the molecule to which the energy is subsequently transferred. This energy transfer causes a reduction in the donor's fluorescence intensity and excited state life time, and a subsequent increase in the acceptor's fluorescence emission intensity. In theory, the excited fluorophore can be treated as an oscillating dipole that can undergo an energy transfer with a second dipole having a similar oscillating frequency. For FRET to occur, some conditions need to be met; First, the donor and acceptor molecules must be in close proximity (10-100 Å). Second, the absorption or excitation spectrum of the acceptor must overlap the fluorescence emission spectrum of the donor. Also, the orientation of the donor and acceptor transition dipoles should be approximately parallel.<sup>2</sup> Therefore, FRET is a sensitive phenomenon that is capable to inform us whether the donor and the acceptor molecules are close to one another on a molecular scale (usually within 1-10 nm), and whether they are moving relative to each other.

## **1.2. Why Fluorescent Protein-FRET Based Sensors?**

Fluorescence resonance energy transfer between two differently colored fluorescent proteins have gained popularity because of the ease of GFP targeting. Two fluorescent proteins of different hues are used as the donor and acceptor fluorophores in



the design and construction of FRET-based biosensors for a variety of biologically relevant ions, molecules, and specific enzymatic activities to answer numerous questions in cell biology.<sup>3</sup> While intensity-based FP sensors highly depend on the excitation source and sensor concentration, FP-FRET can eliminate or reduce the effect of these factors by self-calibration of the two emission bands. Two different types of FP-FRET have been utilized. The first type is based on intramolecular FRET between FPs fused to opposite ends of an environmentally sensitive peptide or protein. Such sensors have been developed to measure intracellular metal ions such as  $\text{Ca}^{2+}$ , and  $\text{Zn}^{2+}$ , study of cAMP activity, protease activity and many other cellular events. The second type is based on intermolecular FRET between two FP-labeled proteins and is mainly used to study protein-protein interactions.<sup>4</sup> Choosing a donor/acceptor pair for fluorescent protein-based FRET applications is facile due to the plethora of color variants reported that show improved spectral properties and have good overlap. Yet, the critical and challenging element for high FRET efficiency is the proximity of the pairs. One pair of fluorescent proteins originally used for FRET was a blue fluorescent protein (BFP) donor and a GFP acceptor. The BFP donor is a GFP mutant with a Tyr66His mutation. BFP initially used had a low quantum yield and bleaches easily.<sup>5</sup> Improved versions of BFP have been reported that were brighter than BFP. However, EBFP2, one of the improved versions of BFP, have been proved to be the blue FP of choice for use in live cell fluorescence imaging due to its higher photostability.<sup>6</sup> Therefrom, in Chapter 2 of this dissertation, we utilized EBFP2 as the FRET donor along with a circularly permuted green fluorescent protein (cpGFP) originally derived the  $\text{Ca}^{2+}$  sensor, inverse pericam, and further

improved in our laboratory by mutagenesis methods<sup>7,8</sup> for designing a FP-Based sensor for H<sub>2</sub>S imaging. Another FP-FRET pair widely used for a variety of applications involves the cyan-(Tyr66Trp-based chromophore) and the yellow-(Thr203Tyr-based substitution) emitting variants of GFP as the FRET donor and acceptor, respectively. ECFP and YPet, the improved versions of the cyan and the yellow FPs respectively, have been proved to remarkably enhance the sensitivity of the different ECFP/YPet FRET biosensors reported. Thus, we utilized ECFP/YPet pair in chapter 3 of this dissertation to design our FP-FRET sensor for hypoxia and prolyl hydroxylases. To quantify FRET in FP-FRET probes such as the sensors we developed in this thesis, the ratio change of fluorescence emission intensity of the acceptor to the donor is measured. Such quantification method is simple and ideal for FP-FRET sensors when appropriate controls are used since the fluorescence intensity signal is collected using emission filters chosen for both the donor and the acceptor fluorescence.

### **1.3. Genetically Encoded Fluorescent Sensors**

Genetically encoded fluorescent protein probes are sensors that are encoded by a nucleic acid sequence and are synthesized entirely by a cell.<sup>9</sup> These sensors are incorporated into the cell or organism as plasmid DNA, and expressed into a functional sensor by the cell machinery. Once the sensor is incorporated into the system of interest, a long-term optical signal is generated in response to a cellular event, such as binding of a molecule to a sensing domain or change in protein conformation which can then be detected by a microscope (Figure 1.1).<sup>10</sup> Genetically encoded fluorescent sensors are

attractive tools because they provide an insight into the real-time biochemistry of living cells and organisms.

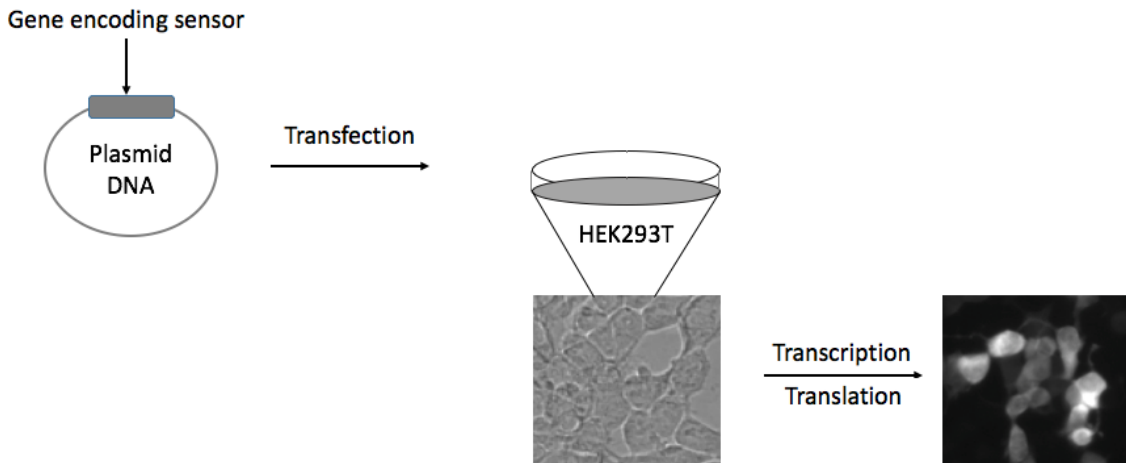


**Figure 1.1.** Steps involved in engineering of a genetically encoded fluorescent sensor by the cell machinery.

Many genetically encoded fluorescent probes that utilize single fluorescent proteins and fluorescence resonance energy transfer (FRET) have been developed to address the spatiotemporal regulation of various biological processes in cells. Examples include sensors for ions,<sup>11,12</sup> molecules,<sup>13,14</sup> enzymatic activities,<sup>15,16</sup> oxidation-reduction events,<sup>17</sup> changes in membrane potential and channel conformation,<sup>18</sup> and other events. One of the major advantages of genetically encoded sensors is that they can be targeted to subcellular compartments by fusing them to a signal sequence or protein that localizes to

a specific region in the cell.<sup>19</sup> This approach enables the analysis of many proteins and cellular signals occurring at different locations within the complex cell while preserving the spatiotemporal control of protein function and signaling cascades. Another important advantage is that these sensors do not require cell-invasive procedures and can be easily incorporated into cells, tissues, and even organisms by transfection of plasmid DNA or transgenic technologies. Moreover, genetically encoded sensors can be easily modified through mutagenesis and directed evolution approaches.<sup>20</sup>

## **1.4. Green Fluorescent Proteins and Evolution**

### *1.4.1. The Green Fluorescent Protein*

Genetically encoded fluorescent sensors use the Green Fluorescent Protein (GFP) from the jellyfish *Aequorea victoria*, its siblings from other organisms, and engineered variants of the members of the “GFP-family” as autofluorescent proteins.<sup>21</sup> GFP and its related variants have become an important tool as genetic tags to monitor gene expression, protein localization and dynamics, protein-protein interactions, intracellular transport pathways, cell division and other phenomena in living cells and organisms.<sup>22</sup> The wild-type GFP from the jellyfish *Aequorea Victoria* is a monomeric protein composed of 238-amino acid residues (26.9 kDa) which exhibit green fluorescence when exposed to light in the blue to ultraviolet range. The excitation spectrum of this protein has a major maximum at about 395 nm and a significantly smaller peak at about 475 nm due to the neutral and anionic chromophores, respectively. The emission spectrum has a sharp maximum at about 505 nm and a shoulder around 540 nm.<sup>23-25</sup> The anionic

chromophore is generated from the neutral chromophore through an excited-state proton transfer mechanism when irradiated. Crystal structure of GFP shows a barrel formed by 11-stranded  $\beta$  sheets that accommodates an internal distorted helix with the chromophore located in the center of this barrel (Figure 1.2). The fluorescent chromophore of the wild-type GFP is generated spontaneously by peptide cyclization of residues Ser65 and Gly67 to form a five-membered imidazolinone ring, followed by oxidation and dehydration of the  $\alpha$ - $\beta$  bond of Tyr66. Two mechanisms have been proposed for the maturation process that differ in the order of the oxidation and hydration steps as seen in Figure 1.3.<sup>26</sup> The barrel structure, and the mechanism of chromophore formation is thought to be similar in all fluorescent proteins, regardless of the source. Gene sequences of the now over 100 naturally available FPs show that only four amino acid residues are absolutely conserved. The first residue is the Tyr66 which can be replaced with any aromatic residue by mutagenesis methods. This finding led to the discovery of the widespread blue (BFP) and cyan (CFP) variants which involve the Tyr66His and Tyr66Trp mutations, respectively. The second residue is the Gly67 that is essential for cyclization of the chromophore. The last two conserved amino acid residues are Arg96 and Glu222 that are positioned near the chromophore and play an important catalytic role in chromophore maturation.<sup>27,28</sup> Studies also showed that although the chromophore is formed by the aforementioned three amino acid residues, nearly the entire sequence is required to generate a functional chromophore as it protects the chromophore from the surrounding environment. Because it is a protein,

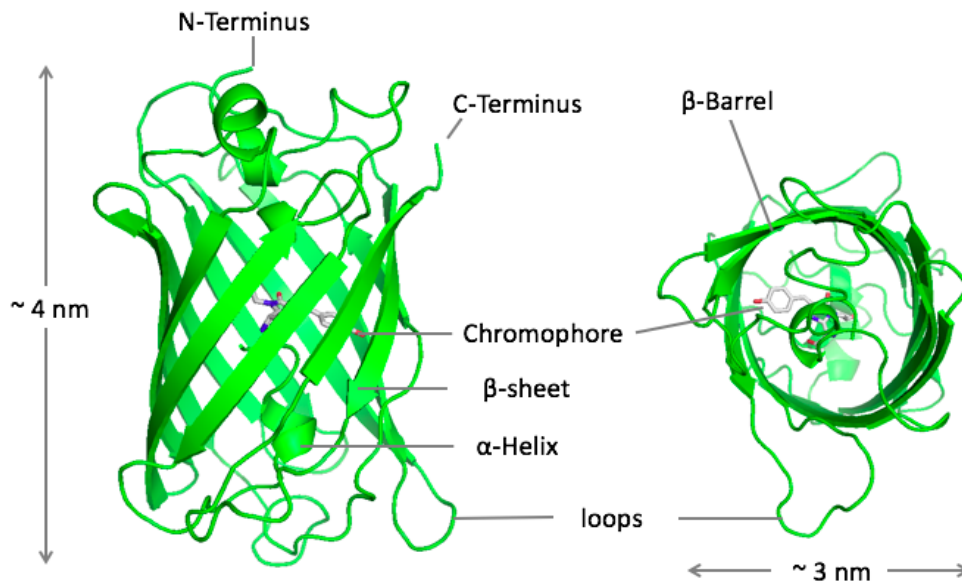


**Figure 1.2.** Structure of the Green Fluorescent Protein from the *jellyfish Aequorea Victoria*. GFP has a beta barrel structure consisting of 11- $\beta$  sheets, with an  $\alpha$ -helix containing the covalently bonded chromophore located in the middle. The cylinder has a diameter of about 3 nm and a length of about 4 nm.

FP gene sequence, and therefore its structure and properties, can be conveniently manipulated using standard molecular biology tools. These techniques led to the development of a wide color palette that span the entire visible spectrum from deep blue to deep red, providing a wide choice of genetically encoded markers to be used simultaneously when coupled with the advanced imaging instruments.<sup>29</sup> GFP and its variants are important tools not only because they are fluorescent, but also due to their high stability to thermal and chemical denaturation resistance to proteolysis, and the fact that chromophore maturation does not require cofactors or enzymes (only molecular oxygen).<sup>30-32</sup>

#### *1.4.2. Circular Permutation of the Green Fluorescent Protein*

The vast majority of GFP mutants generated were the result of mutagenesis methods performed on the natural, linear genetic sequence of GFP. Circular permutation of GFP is an alternative method of protein engineering compared to these standard mutagenesis procedures. It involves linking the original N- and C- terminal ends directly, or through a short linker and subsequently generating new termini at sites within the folding of FPs.<sup>33</sup> In practice, this is performed on the genetic sequence encoding the corresponding protein using polymerase chain reaction (PCR) technology. Due to its tight interwoven three-dimensional structure, and the fact that the chromophore is formed after a series of posttranslational modification (Figure 1.3), one may expect that circular permutation of GFP would prevent fluorescence. In fact, circular permutation of GFP have been extensively studied for its impact on chromophore maturation. Baird et al.<sup>34</sup>

have showed that several circularly permuted GFPs are still fluorescent despite rearrangement. For example, by linking the original N- and C- termini with a hexapeptide linker and generating a new N-terminal at Y145 site so that the fluorescent protein sequence begins at Y145, the fluorescence intensity was not affected. The generated N- and C- termini are close to the chromophore, and therefore the chromophore would be more accessible to small molecules such as hydrogen sulfide. For this reason, we utilized a circularly permuted GFP that starts at Y145 to develop the hydrogen sulfide sensor described in Chapter 2.

## **1.5. The Genetic Code and Expansion**

### *1.5.1. The Genetic Code*

The genetic code is a set of rules that defines how information encoded within DNA or RNA is translated into the 20-letter code of amino acids that constitute the building blocks of proteins. The sequence of the bases or nucleotides in the gene determines the sequence and the content of those amino acids in proteins. With some exceptions,<sup>35</sup> each codon, represented by a three-nucleotide sequence, is specific for only one amino acid, while a single amino acid may be coded for by more than one codon. There are four different nucleotides allowing for 64 possible combinations of codons to be made. Of these 64 possible codons, 61 represent the 20 natural amino acids, while the rest three codons are stop signals. Decoding of the genetic message occurs in the ribosome and depends on the presence of an aminoacyl-tRNA whose anticodon matches the mRNA codon, with the cognate amino acid esterified to the tRNA's 3'- terminal



adenosine. Ribosomal protein synthesis also depends on the aminoacyl-tRNA synthetase (aaRSs); an enzyme responsible for the esterification of the cognate amino acid to the corresponding tRNA species. Once the codon in an mRNA is recognized by a specific tRNA anticodon that is aminoacylated with the appropriate amino acid, a new amino acid is added into the peptide chain. A chain of amino acids is formed as the ribosome moves along the mRNA which is released once a stop codon that is not recognized by any tRNA is encountered.<sup>36,37</sup>

### 1.5.2. Genetic Code Expansion

With few exceptions, such as selenocysteine<sup>38</sup> and pyrrolysine,<sup>39</sup> the genetic code is preserved in all known organisms and encodes the same 20 amino acids. The biosynthesis of proteins containing modified amino acids has long been a subject of interest as it helps manipulating protein structures and functions. Site-directed mutagenesis methodology is a powerful conventional method used by researchers to explore protein structures and roles by replacing amino acid residues in proteins of interest.<sup>40,41</sup> However, the number of mutations that can be made using site-directed methods are limited. An alternative approach involves developing methods to incorporate unnatural amino acids into proteins to precisely alter their steric and electronic properties, or introduce spectroscopic probes, posttranslational modifications, metal chelators, photoaffinity labels, or other chemical functional groups. Such methods enable the evolution of proteins with new or enhanced properties and allows to explore protein structure and function both *in vitro* and *in vivo*.<sup>42</sup> Multiple methods have been developed for this purpose, for example proteins can be

modified at their side chains,<sup>43</sup> but this method can only be applied to certain amino acid residues and can lead to non selective and non-quantitative derivatization. Solid-phase peptide synthesis has also been developed to introduce unnatural amino acids or modify peptide/protein backbone. However, this method is best suited for peptides and small proteins.<sup>44</sup> To produce larger proteins, chemical<sup>45</sup>, and intein-mediated peptide ligations can be utilized.<sup>46</sup> In addition to the chemical methods used to incorporate unnatural amino acids into proteins, researchers have developed a general *in vitro* biosynthetic method which uses nonsense suppressor tRNA that are chemically misacylated with the amino acid.<sup>47</sup> An alternative to the aforementioned methods is the incorporation of an unnatural amino acid directly at a defined site in proteins in living organisms. This methodology provides a powerful tool to study protein structure and function both *in vitro* and *in vivo*. It also overcomes the challenges with the above methods owing to its fidelity, higher yields and technical ease.<sup>42</sup> In fact, Schultz and others developed a genetic code expansion method to site-specifically introduce a non-canonical amino acid in proteins.<sup>42,48</sup> The method requires an ‘orthogonal’ aminoacyl tRNA synthetase/tRNA pair, that is, a synthetase that aminoacylates the orthogonal tRNA but none of the endogenous tRNAs, and a tRNA that does not encode any of the 20 canonical amino acids and only deliver the novel amino acid in response to a unique codon. In addition, an unnatural amino acid that is not identified by the endogenous synthetase is required (Figure 1.4). The unnatural amino acid should also be cell permeable, non-toxic, and stable to endogenous metabolic enzymes.

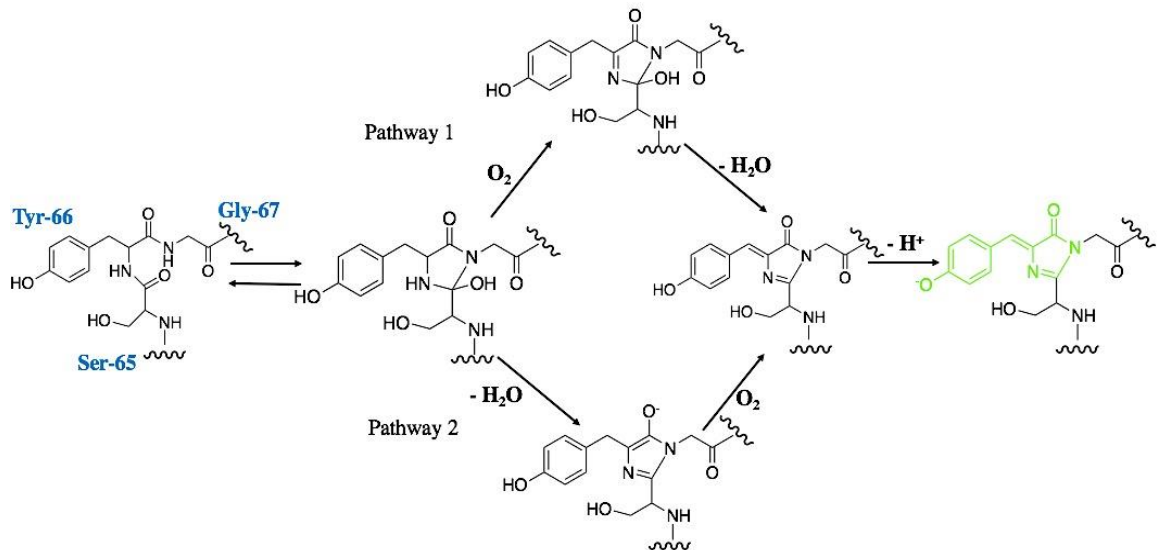


**Figure 1.3.** Steps involved in chromophore maturation of the GFP. Two proposed mechanisms for chromophore maturation from three residues in the wild-type GFP. After peptide cyclization, the five-membered imidazolinone intermediate then undergoes dehydration (left) or oxidation (right) followed by formation of an  $\alpha$ - $\beta$  double bond in Tyr66. The green anionic chromophore is generated from the neutral chromophore through an excited-state proton transfer when irradiated.

In a typical experiment, a pre-engineered orthogonal tRNA with its anticodon complementary to a stop codon or a 4-based codon, and a pre-engineered aminoacyl tRNA synthetase that charges only the unnatural amino acid to the orthogonal tRNA, are co-expressed in cells. The unnatural amino acid is added to the culture media. The host cells then use its protein synthesis machinery to link the amino acid with the suppressor tRNA and synthesize modified proteins containing site-specifically incorporated unnatural amino acids.

Methods are well established to identify the orthogonal synthetase-tRNA pair which involve a two-step procedure. In the first step, the synthetase-tRNA pair is isolated from an orthologous organism to the host of interest. In the second step, the specificity of the synthetase enzyme is altered to only recognize the unnatural amino acid. This can be achieved by a two-step positive and negative selection methods in which large libraries of mutations in the active site of the synthetase are created, and then synthetases that only identify the non-canonical amino acid are selected. Using this methodology, four synthetase-tRNA pairs have been developed and successfully used to incorporate more than 90 unnatural amino acids with distinct chemical reactive groups into the genetic codes of the *Escherichia coli*, yeast, mammalian cells, and *C. elegans*.<sup>36,42,49</sup> For example, *p*-Azido-L-phenylalanine (*p*AzF) (Figure 1.5) was efficiently incorporated into proteins expressed in *E. coli* in response to the amber (TAG) codon with high translational fidelity using the *Methanococcus jannaschii* tyrosyl tRNA and tyrosyl-tRNA synthetase pair

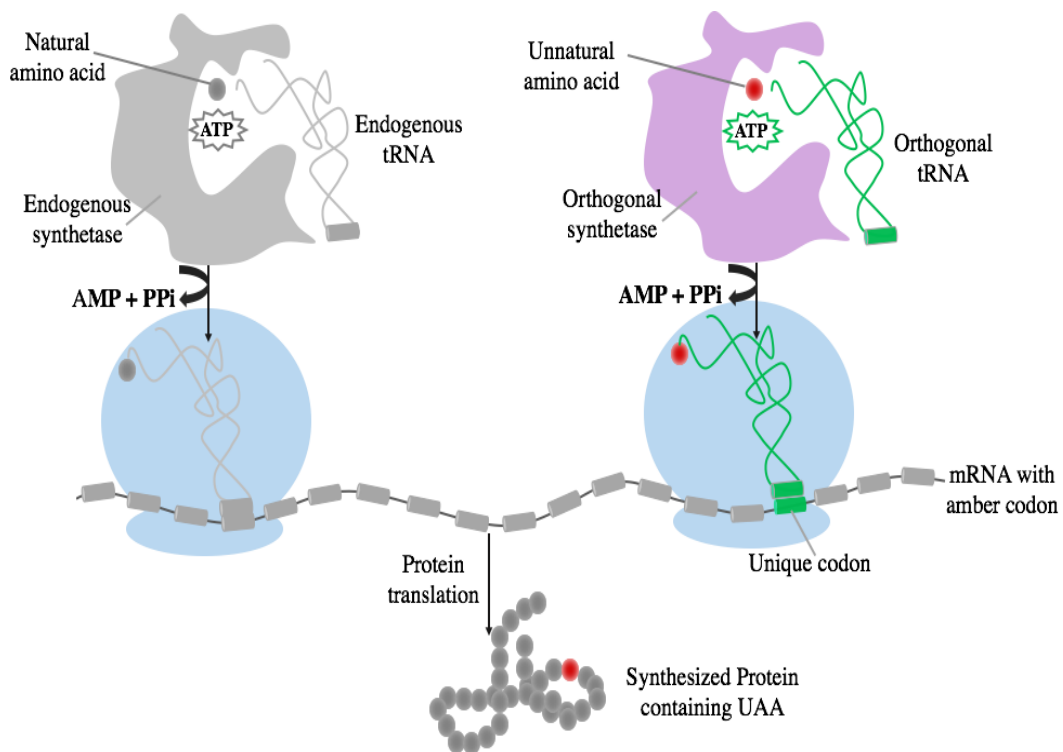


**Figure 1.4.** Schematic diagram showing a general method for genetic incorporation of unnatural acids (UAAs) in live cells. The orthogonal synthetase is engineered to charge the desired UAA onto the orthogonal tRNA, and the tRNA decodes a unique codon (such as the amber stop codon UAG) to incorporate the UAA into proteins through translation.

(*Mj*TyrRS/*Mjt*RNA<sub>CUA</sub>Tyr).<sup>47</sup> The *Mj*TyrRS/*Mjt*RNA<sub>CUA</sub>Tyr orthogonal pair was the first pair generated to introduce unnatural amino acids in *E. coli*. In Chapter 2 of this dissertation we incorporated *pAzF* into our probe to sense hydrogen sulfide (H<sub>2</sub>S), an important signaling molecule, in live mammalian cells using the above genetic code expansion strategy. The azido functional group in the unnatural amino acid *pAzF* acts as the recognition unit that is reduced to amino group in the presence of H<sub>2</sub>S. Consequently, by using the genetic code expansion method, we were able to monitor intracellular H<sub>2</sub>S.

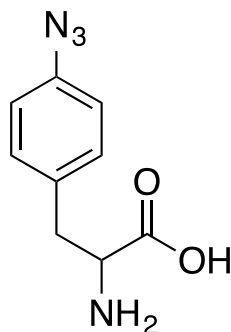


**Figure 1.5.** Chemical structure of p-Azido-L-phenylalanine (*pAzF*).

## 1.6. Cell Signaling via Hydrogen Sulfide and HIF-1 $\alpha$

### 1.6.1. Hydrogen Sulfide and Cell Signaling

Hydrogen sulfide (H<sub>2</sub>S), which was well known as a toxic gas, is increasingly recognized as an important signaling molecule in recent years. It is mainly produced from

L-cysteine in the mitochondria and cytosol of mammalian cells by enzymes. For example, the Pyridoxal 5'-phosphate-dependent cystathionine  $\beta$ -synthase (CBS) and cystathionine  $\gamma$ -lyase (CSE) catalyze the formation of H<sub>2</sub>S in the cytosol. Other enzymes such as cysteine aminotransferase (CAT) and 3-mercaptopyruvate sulfurtransferase (3-MST) convert L-cysteine to H<sub>2</sub>S in the mitochondria and the cytosol of mammalian cells. Cysteine lyase (CL) can also convert L-cysteine into H<sub>2</sub>S. While most emphasis has been on its enzymatic formation, endogenous production of H<sub>2</sub>S, also occurs via nonenzymatic pathways through the reduction of thiol and thiol-containing molecules, and from intracellular sulfur stores (bound sulfane sulfur) at certain physiological conditions.<sup>50</sup>

Since the discovery of its potential role in biological systems, extensive studies have been done to study the importance of H<sub>2</sub>S in cell signaling. H<sub>2</sub>S appears to be involved in sulfhydration, a post-translational modification of proteins, by modifying cysteines in a large number of proteins leading to the formation of persulfides (-S-SH). Emerging evidence has shown that physiological H<sub>2</sub>S acts as a neuromodulator, a regulator of cardiovascular and gastrointestinal systems and a relaxant of smooth muscles. It is also reported that H<sub>2</sub>S regulates ATP-sensitive K<sup>+</sup> (K<sub>ATP</sub>) channels, acts as a scavenger of reactive oxygen species (ROS), and play important roles in inflammation.<sup>50,51</sup> Although diverse physiological and pathological processes have been linked to H<sub>2</sub>S, more biological roles are yet to be identified.

### 1.6.2. Signaling via HIF-1 $\alpha$

Studies of the adaptation to low oxygen concentrations have identified the Hypoxia-Inducible Factor-1 (HIF-1) as the key component in the signaling pathway that controls the hypoxic response of mammalian cells. Cellular hypoxia, a decrease in oxygen concentration below normal, occurs in both physiological and pathological conditions. Adaptation to low oxygen concentration involves a signal transduction mechanism through post-translational modifications of the  $\alpha$  subunit of HIF-1. Hydroxylation, as well as other post-translational modifications, controls HIF-1 half-life and/or transcriptional activity.<sup>52</sup> HIF-1 consists of a heterodimer composed of a stable  $\beta$  subunit and an oxygen-regulated  $\alpha$  subunit that is rapidly degraded under normal conditions ( half-life is less than 5 min in 21% O<sub>2</sub> ) but stable under hypoxic conditions (~1-2 % O<sub>2</sub>).<sup>53</sup> Three isoforms of the  $\alpha$  subunit are identified: HIF-1 $\alpha$ , -2 $\alpha$ , and -3 $\alpha$ . Yet, HIF-1 $\alpha$  is the best characterized form.

In mammalian cells, three hypoxia-inducible factor prolyl 4-hydroxylases (PHD1-3) regulate the HIF-1 $\alpha$  by hydroxylating one or both proline residues in the oxygen-dependent degradation domain of its  $\alpha$  subunit. However, PHD2 appears to be the predominant form that regulates HIF-1 $\alpha$  *in vivo*.<sup>53</sup> In normal condition, hydroxylation of at least one of two proline residues generates a binding site for the von Hippel-Lindau tumor suppressor (pVHL) which acts as the recognition unit for the ubiquitin-dependent proteolysis of HIF-1 $\alpha$  by ubiquitin ligase. In contrast, the lack of oxygen inhibits hydroxylation of HIF-1 $\alpha$  so that it is no longer recognized by the pVHL and degraded but



instead translocate into the nucleus, dimerizes with HIF- $\beta$ , and activates the target genes. HIF-1 is responsible for the induction of more than 70 genes in hypoxic conditions including genes with roles in angiogenesis, erythropoiesis, energy metabolism, vasomotor function, and apoptotic/proliferation responses. It also plays a key role in many pathological conditions such as cardiovascular and inflammatory diseases as well as tumor growth. Moreover, it has been suggested that activation of HIF-1 signaling might act as a potential treatment for various conditions including ischemia, stroke, heart attack, inflammation, and wounding. One possible route of HIF-1 activation involves the inhibition of the HIF-1 prolyl 4-hydroxylases.<sup>54</sup>

### **1.7. Scope of this Dissertation**

This dissertation focuses on the development and characterization of genetically-encoded FRET-based sensors for the detection of H<sub>2</sub>S and prolyl hydroxylase enzyme in mammalian cells. In Chapter 2, we have designed, engineered, and characterized the first genetically encoded FRET-based probe, hsCY, for H<sub>2</sub>S. In this study, we have fused a genetically modified circularly permuted green fluorescent protein, cpGFP, with an enhanced blue fluorescent protein, EBFP2, to generate H<sub>2</sub>S-FRET sensor. Genetic code expansion strategy was utilized to incorporate the unnatural amino acid, p-azidophenylalanine (pAzF), into cpGFP that is served as the FRET acceptor to EBFP2. Upon reaction with H<sub>2</sub>S, the FRET ratio signal of cpGFP to EBFP2 increased indicating that the azido functional group has been reduced to an amino functional group. We tested hsCY *in vitro* and in mammalian cells, and demonstrated that hsCY could be used to

selectively monitor H<sub>2</sub>S in mammalian cells. hsCY thus represents a valuable addition to the toolbox for H<sub>2</sub>S detection and imaging.

In chapter 3 of this dissertation, we described a novel genetically encoded single-chain fluorescent biosensor, ProCY, which can ratiometrically respond to prolyl hydroxylases (PHD) activities *in vitro* and in live cells. We designed the biosensor by fusing a proline-containing substrate peptide derived from HIF-1 $\alpha$  and a small 10-kDa protein domain derived from the von Hippel-Lindau tumor suppressor (VHL) between an enhanced cyan FP (ECFP) and a yellow FP YPet. Hydroxylation of Pro564 of HIF-1 $\alpha$  by PHDs in normoxic condition induce the interaction of the peptide with the VHL domain, leading to a conformational change that alters the distance and/or relative orientation between ECFP and YPet and trigger a measurable change in the FRET efficiency. In this study, we demonstrated that ProCY could monitor hypoxia in mammalian cells. By targeting this novel genetically encoded biosensor to the cell nucleus or cytosol, we determined that the HIF-prolyl hydroxylase activity was mainly confined to the cytosol of HEK 293T cells under normoxic culture conditions. Our results collectively suggest broad applications of ProCY on evaluation of hypoxia and prolyl hydroxylase activities and understanding of pathways for the control of hypoxic responses.

In chapter 4 of this dissertation, we aimed to utilize ProCY probe in a high-throughput screening assay format to screen for inhibitors of PHDs. Essentially, a series of validation steps should be performed before adopting the assay to automation and scale up. We transiently transfected ProCY into HEK 293T cells, however, our results showed that this method is not effective for HTS as cells tend to wash off the plate during

transfection. Alternatively, a lentiviral packaging system was used to transduce ProCY into the target cells. Since High-titer viruses are essential for high transduction efficiency, our packaging system requires further optimization steps. In this chapter we show how to pack a virus and transduce ProCY into HEK 293T cells. We also show how we get high-titer viruses, a crucial step for live mammalian cells applications, before corroborating our assay compatibility with microtiter plates and screening for inhibitors of PHDs.

## References

- 1- Lakowicz, J. R.; "Principles of Fluorescence Spectroscopy (3rd ed.)" *Springer* 2006, New York.
- 2- Erbse, A. H.; Berlinberg, A. J.; Cheung, C.; Leung, W.; Falke, J. J.; "OS-FRET: A New One-Sample Method for Improved FRET Measurements" *Biochemistry* 2011, 50:451-457.
- 3- Carlson, H. J.; Campbell, R. E.; "Genetically encoded FRET-based biosensors for multiparameter fluorescence imaging" *Current opinions in Biotechnology* 2009, 20:19-27.
- 4- Piston, D. W.; Kremers, G.; "Fluorescent protein FRET: the good, the bad and the ugly" *Trends in Biochemical Sciences* 2007, 32:407-414.
- 5- Troung, K.; Ikura, M.; "The use of FRET imaging microscopy to detect protein-protein interactions and protein conformational changes *in vivo*" *Curr. Opin. Struct. Biol.* 2001, 11:573-578.
- 6- Ai, H.; Shaner, N. C.; Cheng, Z.; Tsien, R. T.; Cambell, R. E.; "Exploration of New Chromophore Structures Leads to the Identification of Improved Blue Fluorescent Proteins" *Biochemistry* 2007, 46:5904-5910.
- 7- Chen, S.; Chen, Z.; Ren, W.; Ai, H.; "Reaction-Based Genetically Encoded Fluorescent Hydrogen Sulfide Sensors", *J. Am. Chem. Soc.* 2012, 134:9589-9592.
- 8- Chen, Z.; Ren, W.; Wright, Q. E.; Ai, H.; "Genetically Encoded Fluorescent Probe for the Selective Detection of Peroxynitrite" *J. Am. Chem. Soc.* 2013, 135:14940-14943.
- 9- Carter, K. P.; Young, A. M.; Palmer, A. E.; "Fluorescent Sensors for Measuring Metal Ions in Living Systems" *Chem. Rev.* 2014, 114:4564-4601.
- 10-Palmer, A. E.; Qin, Y.; Park, J. G.; McCombs, J. E.; "Design and application of genetically encoded biosensors" *Trends in Biotechnology* 2011, 29:144-152.

- 11-Junichi, N.; Masamichi, O.; Keiji, I.; “A high signal-to-noise Ca<sup>2+</sup> probe composed of a single green fluorescent protein” *Nature Biotechnology* 2001, 19:137-141.
- 12-Vinkenborg, J. L.; Nicolson, T. J.; Bellomo, E. A.; Koay, M. S.; Guy A Rutter, G. A.; Merckx, M.; “Genetically encoded FRET sensors to monitor intracellular Zn<sup>2+</sup> homeostasis” *Nat. Methods* 2009, 6:737-740.
- 13-Okumoto, S.; Looger, L. L.; Micheva, K. D.; Reimer, R. J.; Smith, S. J.; Frommer, W. B.; “Detection of glutamate release from neurons by genetically encoded surface-displayed FRET nanosensors” *PNAS* 2005, 102:8740-8745.
- 14-Belousov, V., V.; Fradkov, A. F.; Lukyanov, K. A.; Staroverov, D. B.; Shakhbazov, K. S.; Terskikh, A. V.; Lukyanov, S.; “Genetically encoded fluorescent indicator for intracellular hydrogen peroxide” *Nat. Methods* 2006, 3:281-286.
- 15-Zhang, J.; Ma, Y.; Taylor, S. S.; Tsien, R. Y.; “Genetically encoded reporters of protein kinase A activity reveal impact of substrate tethering” *PNAS* 2001, 98: 14997–15002.
- 16-Xu, X.; Gerard, A. L.; Huang, B. C.; Anderson, D. C.; Payan, D. G.; Luo, Y.; “Detection of programmed cell death using fluorescence energy transfer” *Nucleic Acids Res.* 1998, 26: 2034-2035.
- 17-Dooley, C.T.; Dore, T.M.; Hanson, G.T.; Jackson, W.C.; Remington, S.J.; Tsien, R.Y.; “Imaging Dynamic Redox Changes in Mammalian Cells with Green Fluorescent Protein Indicators” *J. Biol. Chem.* 2004, 279:22284-22293.
- 18-Guerrero, G.; Siegel, M. S.; Roska, B.; Loots, E.; Esacoff, E. Y.; “Tuning FlaSh: redesign of the dynamics, voltage range, and color of the genetically encoded optical sensor of membrane potential” *Biophys. J.* 2002, 83:3607-3618.
- 19-VanEngelenburg, S. B.; Palmer, A. E.; “Fluorescent biosensors of protein function” *Curr. Opin. Chem. Biol.* 2008, 12:60-65.

- 20- Vinkenborg, J. L.; Evers, T. H.; Reulen, S. W. A.; Meijer, E. W.; Merkx, M.; “Enhanced Sensitivity of FRET-Based Protease Sensors by Redesign of the GFP Dimerization Interface” *ChemBioChem*. 2007, 8:1119-1121.
- 21- Mank, M.; Griesbeck, O.; “Genetically Encoded Calcium Indicators” *Chem. Rev.* 2008, 108:1550-1564.
- 22- Wang, L.; Xie, J.; Deniz, A. A.; Schultz, P. G.; “Unnatural Amino Acid Mutagenesis of Green Fluorescent Protein” *J. Org. Chem.* 2003, 68:174-176.
- 23- Heim, R.; Prasher, D. C.; Tsien, R. Y.; “Wavelength mutations and posttranslational autoxidation of green fluorescent protein” *PNAS* 1994, 91:12501-12504.
- 24- Niwa, H.; Inouye, S.; Hirano, T.; Matsuno, T.; Kojima, S.; Kubota, M.; Ohashi, M.; Tsuji, F. I.; “Chemical nature of the light emitter of the Aequorea green fluorescent protein” *PNAS* 1996, 93:13617-13622.
- 25- Tsien, R. Y.; “THE GREEN FLUORESCENT PROTEIN” *Annu. Rev. Biochem.* 1998, 67:509-544.
- 26- Craggs, T. D.; “Green fluorescent protein: structure, folding and chromophore maturation” *Chem. Soc. Rev.*, 2009, 38:2865-2875.
- 27- Remington, S. J.; “Fluorescent proteins: maturation, photochemistry and photophysics” *Curr. Opin. Struct. Biol.* 2006, 16, 6:714-721.
- 28- Kremers, G.; Gilbert, S. G.; Cranfill, P. J.; Davidson, M. W.; Piston, D. W.; “Fluorescent proteins at a glance” *J. Cell Sci.* 2011, 124:157-160.
- 29- Dedecker, P.; De Schryver, F. C.; Hofkens, J.; “Fluorescent Proteins: Shine on, You Crazy Diamond” *J. Am. Chem. Soc.* 2013, 135:2387-2402.
- 30- Ma, Y.; Sun, Q.; Zhang, H.; Peng, L.; Yu, J.; Smith, S. C.; “Theoretical Studies of Chromophore Maturation in the Wild-Type Green Fluorescent Protein: ONIOM(DFT:MM) Investigation of the Mechanism of Cyclization” *J. Phys. Chem. B* 2010, 114:9698-9705.

- 31-Ormo, M.; Cubitt, A. B.; Kallio, K.; Gross, L. A.; Tsien, R. Y.; Remington, S. J.; “Crystal structure of the *Aequorea victoria* green fluorescent protein” *Science* 1996, 273:1392-1395.
- 32-Reid B. G.; Flynn G. C.; “Chromophore Formation in Green Fluorescent Protein” *Biochemistry* 1997, 36:6786-6791
- 33-Hicks, B. W.; “Green Fluorescent Protein: Applications and Protocols” *Methods in Molecular Biology* 2002, 183, New Jersey.
- 34-Baird, G. B.; Zacharias, D. A.; Tsien, R. Y.; “Circular permutation and receptor insertion within green fluorescent proteins” *Proc. Natl. Acad. Sci. USA.* 1999, 96:11241-11246.
- 35-Turanov, A. A.; Lobanov, A. V.; Fomenko, D. E.; Morrison, H. G.; Sogin, M. L.; Klobutcher, L. A.; Hatfield, D. L.; Gladyshev, V. N.; “Genetic code supports targeted insertion of two amino acids by one codon” *Science* 2009, 323:259-261.
- 36-Davis, L.; Chin, J. W.; “Designer proteins: applications of genetic code expansion in cell biology” *Nature Reviews* 2012, 13:168-182.
- 37-Ambrogelly, A.; Palioura, S.; Soll, D.; “Natural expansion of the genetic code” *Nature Chemical Biology* 2007, 3:29-35.
- 38-Bock, A.; Forchhammer, K.; Heider, J.; Leinfelder, W.; Sawers, G.; Veprek, B.; Zinoni, F.; “Selenocysteine-the 21st aminoacid” *Molecular Microbiology* 1991, 5:515-520.
- 39-Srinivasan, G.; James, C. M.; Krzycki, J. A.; “Pyrrolysine encoded by UAG in Archaea: charging of a UAG-decoding specialized tRNA” *Science* 2002, 296:1459-1462.
- 40-Wilkinson, A. J.; Fersht, A. R.; Blow, D. M.; Winter, G.; “Site-Directed Mutagenesis as a Probe of Enzyme Structure and Catalysis: Tyrosyl-tRNA Synthetase Cysteine-35 to Glycine-35 Mutation” *Biochemistry* 1983, 22:3581-3586.

- 41- Karata, K.; Inagawa, T.; Wilkinson, A. J.; Tatsuta T.; Ogura, T.; “Dissecting the Role of a Conserved Motif (the Second Region of Homology) in the AAA Family of ATPases SITE-DIRECTED MUTAGENESIS OF THE ATP-DEPENDENT PROTEASE FtsH” *J. Biol. Chem.* 1999, 274:26225-26232.
- 42- Wang, L.; Xie, J.; Schultz, P. G.; “Expanding the genetic code” *Annu. Rev. Biophys. Biomol. Struct.* 2006, 35:225-249.
- 43- Carne, A. F.; “Chemical modification of proteins” *Methods Mol. Biol.* 1994, 32:311-32.
- 44- Kent, S. B. H.; “Chemical Synthesis of Peptides and Proteins” *Annu. Rev. Biochem.* 1988, 57:957-989.
- 45- Dawson, P. E.; Kent, S. B. H.; “Synthesis of native proteins by chemical ligation” *Annu. Rev. Biochem.* 2000, 69:923-960.
- 46- Evans Jr., T. C.; Xu, M.; “Intein-mediated protein ligation: harnessing nature's escape artists” *Biopolymers* 1999, 51:333-342.
- 47- Cload, S. T.; Liu, D. R.; Froland, W. A.; Schultz, P. G.; “Development of improved tRNAs for *in vitro* biosynthesis of proteins containing unnatural amino acids” *Chemistry & Biology* 1996, 3:1033-1038.
- 48- Chin, J. W.; Santoro, S. W.; Martin, A. B.; King, D. S.; Wang, L.; Schultz, P. G.; “Addition of p-Azido-l-phenylalanine to the Genetic Code of Escherichia coli” *J. Am. Chem. Soc.* 2002, 124:9026-9027.
- 49- Liu, C. C.; Schultz, P. G.; “Adding New Chemistries to the Genetic Code” *Annu. Rev. Biochem.* 2010, 79:413-444.
- 50- Li, L.; Rose, P.; Moore, P. K.; “Hydrogen sulfide and cell signaling” *Annu. Rev. Pharmacol. Toxicol.* 2011, 51:169-187.
- 51- Brahimi-Horn, C.; Mazure, N.; Pouyssegur, J.; “Signaling via the hypoxia-inducible factor-1alpha requires multiple posttranslational modifications” *Cell Signal.*, 2005, 17:1-9.



- 52-Berra, E.; Ginouves, A.; Pouyssegur, J.; “The hypoxia-inducible-factor hydroxylases bring fresh air into hypoxia signaling” *EMBO Rep.* 2006, 7:41-45.
- 53-Pan, Y.; Mansfield, K. D.; Bertozzi, C. C.; Rudenko, V.; Chan, D. A.; Giaccia, A. J.; Simon, M. C.; “Multiple Factors Affecting Cellular Redox Status and Energy Metabolism Modulate Hypoxia-Inducible Factor Prolyl Hydroxylase Activity *in Vivo* and *in Vitro*” *Mol. CELL. BIOL.* 2007, 27:912-925.
- 54-Hewitson, K. S.; Schofield, C. J.; Ratcliffe, P. J.; “Hypoxia-inducible factor prolyl-hydroxylase: purification and assays of PHD2” *Methods Enzymol.* 2007, 435:25-42.

## Chapter 2

### A FRET-Based Genetically Encoded Fluorescent Probe for Hydrogen Sulfide

#### 2.1. Abstract

Hydrogen sulfide (H<sub>2</sub>S) is an important gasotransmitter playing crucial roles in cell signaling. Incorporation of p-azidophenylalanine (pAzF) into fluorescent proteins (FPs) has been a successful strategy in developing intensity-based genetically encoded fluorescent sensors for H<sub>2</sub>S. However, currently there is no FRET-based genetically encoded fluorescent probe for H<sub>2</sub>S. Unlike intensity-based sensors, fluorescence resonance energy transfer (FRET)-based sensors eliminate most uncertainties in the detection by self-calibration of the two emission bands and they have been widely utilized for probing the dynamics of many molecules of biological interest. Here we report a genetically encoded reaction-based FRET H<sub>2</sub>S probe, hsCY, that can be used to selectively detect H<sub>2</sub>S. The chromophore of a circularly permuted green fluorescent protein (cpGFP) was modified with pAzF using genetic code expansion strategy. cpGFP-pAzF was served as an FRET acceptor to an enhanced blue fluorescent protein (EBFP2). FRET ratio signal of cpGFP to EBFP2 increases upon reaction with H<sub>2</sub>S indicative of reduction of the azido functional group to an amino functional group. We characterized hsCY *in vitro* and tested in mammalian cells. The results collectively demonstrated that hsCY could be used to selectively monitor H<sub>2</sub>S in mammalian cells.

## 2.2. Introduction

Hydrogen sulfide (H<sub>2</sub>S), which was long considered a toxic gas with wide range of cytotoxic effects, has been recognized as the third gasotransmitter following nitric oxide (NO) and carbon monoxide (CO) playing important roles in cell signaling.<sup>1</sup> H<sub>2</sub>S is a colorless, flammable, and water-soluble gas with a pK<sub>a1</sub> value of 6.6. At a mammalian body temperature of 37 °C, and at neutral pH, it equilibrates mainly with HS<sup>-</sup>.<sup>2,3</sup> Endogenous H<sub>2</sub>S can be produced enzymatically or non-enzymatically during sulfur metabolism through the reduction of thiol and thiol-containing molecules. Enzymes that catalyzes H<sub>2</sub>S production include cystathionine β-synthase (CBS), cystathionine γ-lyase (CGL) and cysteine aminotransferase/3-mercaptopyruvate sulfurtransferase (3-MST).<sup>4,5</sup> More recently, there has been a growing interest in elucidating the biological roles of H<sub>2</sub>S. H<sub>2</sub>S is involved in sulfhydrylation, a post-translational modification of proteins, by modifying cysteines in a large number of proteins leading to the formation of persulfides (-S-SH). S-sulfhydrylation have important roles in the regulation of inflammation, endoplasmic reticulum stress and vascular tension.<sup>6,7</sup> H<sub>2</sub>S has also been shown to mediate cardiovascular functions,<sup>2,8</sup> and to regulate ATP-sensitive K<sup>+</sup> (K<sub>ATP</sub>) channels.<sup>9,10</sup> Furthermore, accumulating evidences suggests that H<sub>2</sub>S functions as a signaling molecule in many biological processes such as neuromodulation, insulin release, anti-oxidation and angiogenesis.<sup>4,11-13</sup> Mis-regulation of H<sub>2</sub>S is related to diseases such as the Down syndrome,<sup>14</sup> Alzheimer's disease,<sup>15</sup> diabetes,<sup>16</sup> and hypertension.<sup>17</sup> Accordingly, dissection of the complex roles H<sub>2</sub>S play in biological and pathophysiological processes is highly needed. Yet the traditional H<sub>2</sub>S detection methods such as chromatographic,<sup>18</sup>

colorimetric,<sup>19</sup> and electrochemical analysis<sup>20</sup> methods does not allow for real-time and noninvasive detection.

Fluorescent probes are powerful tools for intracellular detection that allows a rapid and noninvasive investigation of physiological and pathological processes of interest with high spatiotemporal resolution.<sup>21</sup> In fact, many synthetic H<sub>2</sub>S- responsive fluorescent probes have been developed based on distinct chemical principles including the reduction of azido groups to amino groups,<sup>13,22-24</sup> reduction of nitro groups to amines,<sup>25-27</sup> nucleophilic reactions of H<sub>2</sub>S,<sup>28,29</sup> and copper sulfide precipitation.<sup>19,30-31</sup> Recently, two genetically encoded fluorescent probes, cpGFP-*pAzF* and hsGFP, containing the unnatural amino acid *p*-azidophenylalanine (*pAzF*) were developed for the detection of H<sub>2</sub>S in mammalian cells.<sup>32,33</sup> A genetic code expansion technology<sup>34</sup> was utilized in developing these sensors so that *pAzF* was introduced into the chromophore-forming Tyr67 position of a circularly permuted green fluorescent protein (cpGFP). Upon reaction with H<sub>2</sub>S, the azido group of *pAzF* is reduced into an amino group generating a fluorescent *p*-aminobenzylideneimidazolidone chromophore. Their genetic encodability allows them to be precisely localized to subcellular domains where H<sub>2</sub>S signaling occurs.<sup>35</sup> In addition, these single-FP based sensors have relatively large dynamic ranges. However, currently there are no fluorescence resonance energy transfer (FRET) based-sensors for H<sub>2</sub>S. A key advantage of FRET-based sensors is that they provide a ratiometric signal that is independent of sensor concentration, environment, and excitation intensity as compared to intensity-based fluorescent sensors.<sup>36-38</sup>

Herein, we present the design, engineering, and characterization of the first genetically encoded FRET-based probe, hsCY, for H<sub>2</sub>S. hsCY shows selective and sensitive response to H<sub>2</sub>S *in vitro* and allows ratiometric imaging of H<sub>2</sub>S in live mammalian cells.

## 2.3 Experimental Section

### 2.3.1. Materials, Reagents, and General Methodology

Synthetic DNA oligonucleotides for cloning and library construction were purchased from integrated DNA Technologies (San Diego, CA). Restriction endonucleases were purchased from New England Biolabs (Ipswich, MA, USA) or Thermo scientific Fermentas (Vilnius, Lithuania). Products of PCR and restriction digestion were purified by gel electrophoresis and extracted using Syd Laboratories Gel Extraction columns (Malden, MA, USA). Plasmid DNA was purified using Syd Laboratories miniprep columns. DNA sequence analysis was performed by the Genomic Core at the University of California, Riverside (UCR) or by Retrogen, Inc. Solutions for Functional Genomics, San Diego. All materials were obtained and used as previously described.<sup>34,41</sup> Live-cell microscopic imaging was carried out at the UCR Microscopy Core at the Institute for Integrative Genome Biology. Sodium hydrosulfide (NaHS) in 30 mM Tris-HCl (pH 7.4) was employed as the H<sub>2</sub>S donor throughout this work.

### 2.3.2. Construction of *Escherichia coli* Expression Plasmids and Libraries.

Polymerase chain reactions were utilized to amplify the gene fragments of the FRET donor and acceptor from pBAD-EBFP2 and pBAD-cpGFP, respectively.<sup>39,40</sup> In

particular, oligos BFP-For and BFP-Rev were utilized to amplify EBFP2 gene fragment. The PCR product was then digested with HindIII and XhoI and ligated into a predigested pCDF-1b expression vector to afford pCDF-1b-EBFP2. The resultant ligation product was used to transform *E. coli* DH10B competent cells, which was next plated on Luria-Bertani (LB) broth agar plates supplemented with spectinomycin (50 µg/mL). In the second PCR reaction, oligos GFP-For and GFP-Rev were used to amplify cpGFP gene fragment from pBAD-cpGFP. The resultant PCR product was then digested with NcoI and HindIII and ligated into a predigested pCDF-1b-EBFP2 plasmid to afford FRET-0.1. The ligation product was then transformed into DH10B *E. coli* competent cells and plated on LB agar plates supplemented with spectinomycin (50 µg/mL). To generate FRET-0.2, two separate PCR reactions were utilized. In the first PCR reaction, oligos BFP-For2, and BFP-Rev were utilized to amplify EBFP2 fragment from pBAD-EBFP2. The resulted PCR product was digested with HindIII and XhoI and ligated into a predigested pCDF-1b to afford pCDF-1b-BFP0.1. In the second PCR reaction, oligos GFP-For, and GFP-Rev2 were used to amplify cpGFP fragment from pBAD-cpGFP. The PCR product were digested with NcoI and HindIII and ligated into a predigested pCDF-1b-BFP0.1. The ligation product was used to transform DH10B *E. coli* competent cells and plated on LB agar plates supplemented with spectinomycin (50 µg/mL). To construct FRET-0.3, two separate PCR reactions were performed on pBAD-cpGFP to fully randomize residues H148, Thr203, and Ser205. In the first reaction H148X-For and TX-SX-Rev oligonucleotides containing degenerate NNK codons (in which N = A, T, G, or C, and K = G or T) were used, while in the second reaction TX-SX-For (containing degenerate

NNK codons) and GFP-Rev2 oligonucleotides were used. The products of these two reactions were then assembled using an overlap PCR-based strategy and outside primers to produce the full length gene. The amplified DNA fragment was then treated with NcoI and HindIII and ligated into a predigested pCDF-1b-BFP0.1. After screening the generated library for mutants that responds to H<sub>2</sub>S, FRET-0.3 was selected. To clone FRET-0.2 and FRET-0.3 into pBAD/His B, the gene fragments of both were separately digested with NcoI and XhoI restriction enzymes and ligated into a modified pBAD/ His B plasmid. To generate a library using error-prone PCR (ep-PCR), pBAD-FRET-0.2 and pBAD-FRET-0.3 were mixed and ep-PCR reaction were carried out using oligos pBAD-For and pBAD-Rev. The reaction was carried out with *Tag* DNA polymerase for 38 cycles in the presence of 200 μM MnCl<sub>2</sub> as previously described.<sup>41</sup> Mutagenic PCR products were combined, separated by agarose gel electrophoresis, and digested with NcoI and XhoI. The resulting fragment was ligated into a modified pBAD/ His B, and the crude ligation mixture was transformed into *E. coli* DH10B cells by electroporation.

### 2.3.3. Library Screening

To screen the library generated by randomizing residues H148, Thr203, and Ser205 for mutants that responds to H<sub>2</sub>S, the gene Library in the pCDF-1b plasmid was used to cotransform *E. coli* BL21(DE3) competent cells with pEvol-*pAzF* by electroporation.<sup>42</sup> Cells were grown on LB agar plates supplemented with 50 μg/mL spectinomycin and 50 μg/mL chloramphenicol and incubated at 37 °C for 24 h. Random colonies were picked into 96 well plates containing LB broth supplemented with 50 μg/mL spectinomycin, 50

$\mu\text{g/mL}$  chloramphenicol, 1mM IPTG, 0.02 % L-Arabinose and 1mM *pAzF*. The 96 well plates were first incubated at 37 °C and 250 rpm overnight, and next at room temperature and 200 rpm for another 12 h. Crude proteins were extracted with B-PER Bacterial Extraction Reagents (Pierce, Rockford, IL) and tested with a final concentration of 1mM NaHS prepared in Tris-HCl buffer (pH 7.4). The fluorescence responses were monitored using a monochromator-based Synergy Mx Microplate Reader (BioTek, Winooski, VT) with excitation wavelength of 385 nm and emission scan between 405 nm and 600 nm. FRET-0.3 was then selected from the library based on the emission ratio of cpGFP to EBFP2. To screen the library generated from ep-PCR, the gene library in the modified pBAD/ His B plasmid was used to cotransform *E. coli* DH10B competent cells with pEvol-*pAmF* by electroporation. pEvol-*pAmF* was prepared by introducing 5 mutations (Y32T, E107T, D158P, I159L, and V164A) in both copies of the *M. jannaschii* aminoacyl-tRNA synthetase (AARS) of the pEvol-*pAzF* to afford pEvol-*pAmF*.<sup>44</sup> Cells were grown on LB agar plates supplemented with 100  $\mu\text{g/mL}$  ampicillin, 50  $\mu\text{g/mL}$  chloramphenicol, 0.04% L-arabinose, and 1mM p-aminophenylalanine, *pAmF*. LB agar plates were incubated at 37 °C for 24 h followed by incubation for 4-12 h at room temperature. Fluorescent colonies were selected and grown in Liquid LB medium and induced with 0.04% L-arabinose for protein expression. Crude proteins were extracted



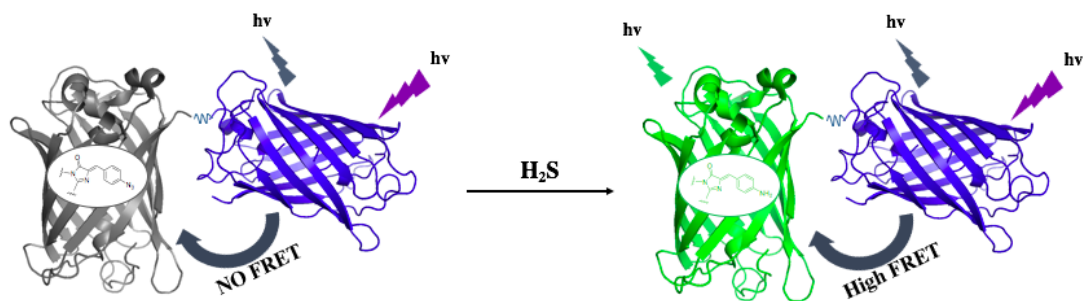


**Figure 2.1.** Illustration of the FRET change of the genetically encoded dual-emission ratiometric fluorescent sensor, hsCY. Upon addition of  $\text{H}_2\text{S}$ , the azido group of the cpGFP chromophore is reduced to an amino group forming the mature chromophore, and inducing FRET enhancement upon illuminating EBFP2. The chemical structures of the chromophore before and after conversion are shown. The basic tertiary structure schematic is adopted from Protein Data bank entries 3EVP (grey and green) and 2B3P (blue).

with B-PER, and FRET ratios were measured using a Synergy Mx Microplate Reader. After each round of screening, the best mutant was selected for the next round of ep-PCR.

#### 2.3.4 Protein Expression and Purification.

To express hsCY, pEvol-*pAzF* and pBAD-hsCY were cotransformed into DH10B competent cells by electroporation and grown on LB agar containing 100 µg/mL ampicillin and 50 µg/mL chloramphenicol at 37 °C overnight. One single colony was grown in 5 mL of LB broth supplemented with the appropriate antibiotics and allowed to grow at 37 °C overnight with shaking. A saturated started culture was diluted 100-fold into 2YT medium containing the appropriate antibiotic and grown under the same conditions. When the OD<sub>600</sub> reached 0.8, the expression culture was induced with 0.2% L-arabinose and 1mM *pAzF*. Culture flasks were then wrapped with aluminum foil to avoid the light-activated conversion of *pAzF* to *pAmF*, transferred to room temperature, and allowed to shake for 24 h before harvesting the cells. Pellets were then suspended in phosphate-buffered saline (PBS), lysed, and affinity-purified with nickel-nitrilotriacetic acid (Ni-NTA) agarose beads under native conditions. The concentration of the protein was determined with a Bradford assay in comparison to a series of bovine serum albumin (BSA) standards.

#### 2.3.5. In Vitro Characterization.

A final protein concentration of 1 µM was used in all *in vitro* assays. All assays were performed in Tris-HCl buffer (pH 7.4) at room temperature. Fluorescence emission

spectra were measured before and after reaction of hsCY with various concentrations of NaHS in Tris-HCl (pH 7.4) for 30 min. Kinetics experiments were performed by measuring the point fluorescence emissions at 450 nm and 500 nm using the excitation wavelength of 385 nm over 30 min at 2 min intervals. Selectivity assays were performed by incubating hsCY with various redox-active molecules (all solutions were prepared as previously described<sup>39</sup>) for 30 min at room temperature. FRET ratios of fluorescence emission intensities at 500 nm over emission intensities at 450 nm were calculated and represented as means  $\pm$  SD from three independent measurements.

#### *2.3.6. Construction of Mammalian Expression Plasmids*

The GFP gene sequence of pBAD-hsCY was amplified using hsCY-HindIII-F and hsCY-EcorI-R oligonucleotides. After digestion with HindIII and EcorI, the product was ligated into a predigested pcDNA3 plasmid resulting in pcDNA3-GFP. Next, the BFP gene sequence of pBAD-hsCY was amplified with oligonucleotides hsCY-EcorI-F and hsCY-ApaI-R. The PCR product was treated with EcorI and ApaI and ligated into a predigested pcDNA3-GFP to afford pcDNA3-hsCY. To improve the mammalian expression of hsCY, we cloned hsCY into pMAH-POLY plasmid<sup>39</sup> by digesting pcDNA3-hsCY with HindIII and ApaI. The digested product was then separated on agarose gel electrophoresis, and ligated into a predigested pMAH-POLY vector to afford POLY-hsCY.

### *2.3.7. Mammalian Cell Culture and Imaging.*

Human Embryonic Kidney (HEK) 293T cells were cultured in Dulbecco's Eagle's Medium (DMEM) supplemented with 10% fetal bovine serum. Cells were incubated at 37 °C with 5% CO<sub>2</sub> in humidified air for 24 h. HEK 293T cells were then co-transfected with 1.5 µg PMAH-POLY and 1.5 µg POLY-hsCY in the presence of 9 µg PEI (polyethyleneimine, linear, M.W. 25KDs). After transfection, cells were cultured in special DMEM containing 1 mM *pAzF* but not L- methionine or L-cystine for 48 h. Cells were then cultured in fresh special growth medium without *pAzF* for an additional 12 h to deplete free *pAzF*. Next, cells in DPBS were imaged under a Leica SP5 confocal fluorescence microscope. Time-lapse imaging experiment was set at one frame per min for 31 minutes. The excitation laser was set at 380 nm, and emission was collected between 400 and 600 nm. NaHS (100 µM) in DPBS was directly added to cells after 3 initial frames.

## **2.4 Results and Discussion**

### *2.4.1. Laboratory Engineering of hsCY*

To construct a FRET-based sensor for H<sub>2</sub>S, we selected cpGFP as the acceptor because of its favorable spectral properties and efficiency in protein folding and maturation.<sup>39</sup> We hypothesized that these favorable properties make it an excellent FRET acceptor when fused to EBFP2 donor. EBFP2, an improved version of blue fluorescent proteins derived previously,<sup>40</sup> serves as an excellent candidate based on its spectral properties and significant overlap with the spectra of GFP, and thus, would maximize the FRET signal.

We envisioned if we could incorporate a H<sub>2</sub>S-reactive functional group into cpGFP such as *pAzF*, an efficient FRET transfer from the donor EBFP2 to the genetically modified cpGFP acceptor could be achieved upon reaction with H<sub>2</sub>S and subsequently illumination of EBFP2 (Figure 2.1). For this reason, we constructed FRET-0.1 by fusing EBFP2 using a short floppy peptide linker (Figure 2.2). The construct was cloned into a pCDF-1b vector and expressed in BL21 (DE3) *E. coli* bacterial cells along with pEvol-*pAzF* in the presence of *pAzF*. Crude proteins were extracted with B-PER and tested with 1 mM H<sub>2</sub>S. Results of this reaction showed a small FRET ratio change upon reaction with H<sub>2</sub>S (Figure A1, Appendix A). Because the sensor is a reaction-based probe, we speculated that reducing the length between the two FPs induces an efficient energy transfer from the FRET donor to the acceptor. We thus cut the small floppy peptide linker and the first few amino acid residues at N-terminal of EBFP2 (FRET-0.2, Figure 2.2). FRET-0.2 was then co-expressed with pEvol-*pAzF* in BL21 *E. coli* cells in the presence of *pAzF*. Reaction of crude proteins extracted from *E. coli* cells with 1 mM H<sub>2</sub>S showed only a small FRET ratio improvement (Figure S1). Next, we aimed to improve the FRET efficiency by improving the spectral properties of the cpGFP acceptor. Consequently, we generated a library by fully randomizing three amino acid residues in FRET-0.2 namely H148, Thr203, and Ser205 (Figure 2.2). These residues appear to stabilize the phenolate ion of the chromophore in the wild type GFP through H-bonds interactions as shown in

```

FRET-01      145                               171                               193
MGSSTYNSHKVYITADKQKNGIKVNFKIRHNVEDGQVQLADHYQQNTPIGDGPVLLPDNH
FRET-02      MGSSTYNSHKVYITADKQKNGIKVNFKIRHNVEDGQVQLADHYQQNTPIGDGPVLLPDNH
FRET-03      MGSSTYNSHKVYITADKQKNGIKVNFKIRHNVEDGQVQLADHYQQNTPIGDGPVLLPDNH
hsCY         MGSSTYNSNKVYITADKQKNGIKVNFKIRHNVEDGQVQLADHYQQNTPIGDGPVLLPDNH

FRET-01      201                               221                               238                               11
YLSTQSVLSKDPNEKRDHMLLEFVTAAGITLGMDELYKVDGGSGGTGVSKGEEELFTGVV
FRET-02      YLSTQSVLSKDPNEKRDHMLLEFVTAAGITLGMDELYKVDGGSGGTGVSKGEEELFTGVV
FRET-03      YLSVQSVLSKDPNEKRDHMLLEFVTAAGITLGMDELYKVDGGSGGTGVSKGEEELFTGVV
hsCY         YLSVQSMLSKDPNEKRDHMLLEFVTAAGITLGMDELYKVDGGPGGTGVSKGEEELFTGVV

FRET-01      21                               31                               41                               51                               61                               71
PILVELDGDVNGHKFSVRGEGEGDATNGKLTLLKFICTTGKLPVPWPTLVTTLTZGVQCFS
FRET-02      PILVELDGDVNGHKFSVRGEGEGDATNGKLTLLKFICTTGKLPVPWPTLVTTLTZGVQCFS
FRET-03      PILVELDGDVNGHKFSVRGEGEGDATNGKLTLLKFICTTGKLPVPWPTLVTTLTZGVQCFS
hsCY         PILVELDGDVNGHKFSVRGEGEGDATNGKLTLLKFICTTGKLPVPWPTLVTTLTZGVQCFS

FRET-01      81                               91                               101                              111                              121                              131
YPDHMKQHDFFKSAMPEGYVQERTIFFKDDGTYKTRAEVKFEGDTLVNRIELKGIDFKED
FRET-02      YPDHMKQHDFFKSAMPEGYVQERTIFFKDDGTYKTRAEVKFEGDTLVNRIELKGIDFKED
FRET-03      YPDHMKQHDFFKSAMPEGYVQERTIFFKDDGTYKTRAEVKFEGDTLVNRIELKGIDFKED
hsCY         YPDHMKQHDFFKSAMPEGYVQERTIFFKGDGTYKTRAEVKFEGDTLVNRIELKGIDFKED

FRET-01      141  N+1                               6
GNILGHKLEYNTHHGGSKLMVSKGEEELFTGVV
FRET-02      GNILGHKLEYNTHH-----KLEELFTGVV
FRET-03      GNILGHKLEYNTHH-----KLEELFTGVV
hsCY         GNILGHKLEYNMHH-----KLEELFTGVV
EBFP2
EBFP2
EBFP2
EBFP2

```

**Figure 2.2.** Sequence alignment of hsCY and the different designs developed in this study. Residues forming the chromophores are boxed in green. pAzF is shown as Z (colored green). The mutations of hsCY are colored in blue. Residues are numbered according to the sequence of wild-type GFP.

the crystal structure of EGFP.<sup>44</sup> *pAzF* was incorporated into FRET-0.2 library to synthesize *pAzF*-containing proteins, and the library was screened for H<sub>2</sub>S-induced changes in bacterial colonies. Bacterial colonies were randomly picked and cultured in liquid media for protein expression. Their FRET ratios were quantitatively measured before and after reaction with H<sub>2</sub>S. After multiple rounds of bacterial screening, FRET-0.3 (Figure 2.2) was chosen as our template for the next step. Reaction of FRET-0.3 with 1 mM H<sub>2</sub>S showed a substantial FRET enhancement compared to FRET-0.2 (Figure A1-Appendix A). We then mixed FRET-0.2 and FRET-0.3 to build a library using random error-prone mutagenesis technology. The library was cloned into a modified pBAD/His B vector instead to pCDF-1b used before to avoid cell toxicity generated by adding IPTG. We introduced *pAmF* to the generated library instead of *pAzF* by co-expressing the generated library in DH10B cells with pEvol-*pAmF*, a pEvol-vector containing two copies of *M. jannaschii* aminoacyl -tRNA synthetase (AARS) with 5 mutations (Y32T, E107T, D158P, I159L, and V164A) in both copies compared to pEvol-*pAzF*.<sup>43</sup> GFP/BFP ratios of the *pAmF*-incorporated proteins was used as a measure to evaluate the maximum FRET signal we could get upon H<sub>2</sub>S-induced conversion of the azido groups to amino groups. Through the screening process, we identified a promising mutant showing a large GFP/BFP ratio signal. This mutant was selected and tested with H<sub>2</sub>S after incorporating *pAzF*. Results showed a > 2.7- fold of FRET ratio change in response to 1 mM H<sub>2</sub>S. We named this mutant hsCY and performed more experiments to characterize it *in vitro* and live cell.

#### 2.4.2 Spectroscopic Responses of hsCY to H<sub>2</sub>S

We next measured the fluorescence spectrum change of hsCY to various concentrations of H<sub>2</sub>S (Figure 2.3). Upon reaction with H<sub>2</sub>S, hsCY showed a decrease in emission intensity at 450 nm, and a concomitant increase of emission intensity peak at 500 nm suggesting an increase of energy transfer between the donor and acceptor in response to H<sub>2</sub>S. The peak formed at 500 nm upon addition of H<sub>2</sub>S suggests that p-azidobenzylideneimidazolidone chromophore was reduced to aminobenzylideneimidazolidone and that excitation of the EBFP2 caused an efficient energy transfer to this newly formed chromophore when excited at 385 nm. This fact also suggests that the reduced p-aminobenzylideneimidazolidone is highly fluorescent.

To measure the kinetics of the reaction, and to determine the sensitivity of hsCY to H<sub>2</sub>S, we monitored the FRET ratio (GFP/BFP) of hsCY in response to various concentrations of H<sub>2</sub>S. We found that the reaction was completed within 30 minutes (Figure 2.4). The result also showed that upon reaction of hsCY with 100 μM or 1 mM H<sub>2</sub>S, the ratio increased from 0.62 to 0.96 and 1.73, respectively (corresponding to a change of 154 % and 279% respectively). To further investigate the relationship between the concentration of H<sub>2</sub>S and FRET signal, we plotted the ratio change of hsCY upon treating it with different concentrations of H<sub>2</sub>S from 1 to 100 μM (Figure 2.5). The graph showed a linear relationship between the FRET ratio signal and the concentration of H<sub>2</sub>S suggesting that the formation of the chromophore, and the subsequent fluorescence resonance energy transfer is concentration-dependent. Next, we tested the selectivity of hsCY in response to different redox-active molecules commonly generated by cells,



including thiols, and reactive oxygen, nitrogen, and sulfur molecules at physiological concentrations or higher (Figure 2.6). Except for H<sub>2</sub>S, hsCY showed limited or no responses to all other redox-active species tested suggesting that hsCY is highly selective toward H<sub>2</sub>S.

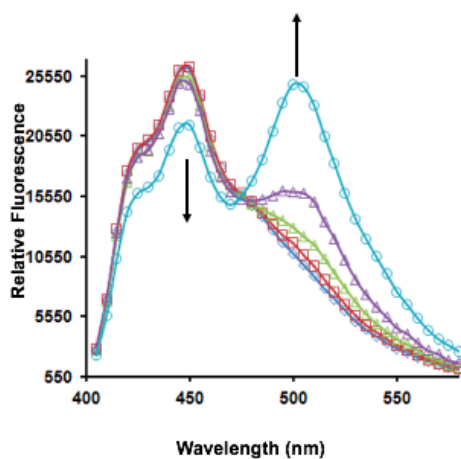


**Figure 2.3.** Fluorescence emission spectra of hsCY (1 μM ) in response to various concentrations of H<sub>2</sub>S ( H<sub>2</sub>S concentrations are 1 mM, 100 μM, 50 μM , 20 μM , and 0 μM from top to bottom) with arrows indicating the decrease of the emission intensity at 450 nm and the increase of emission intensity at 500 nm.

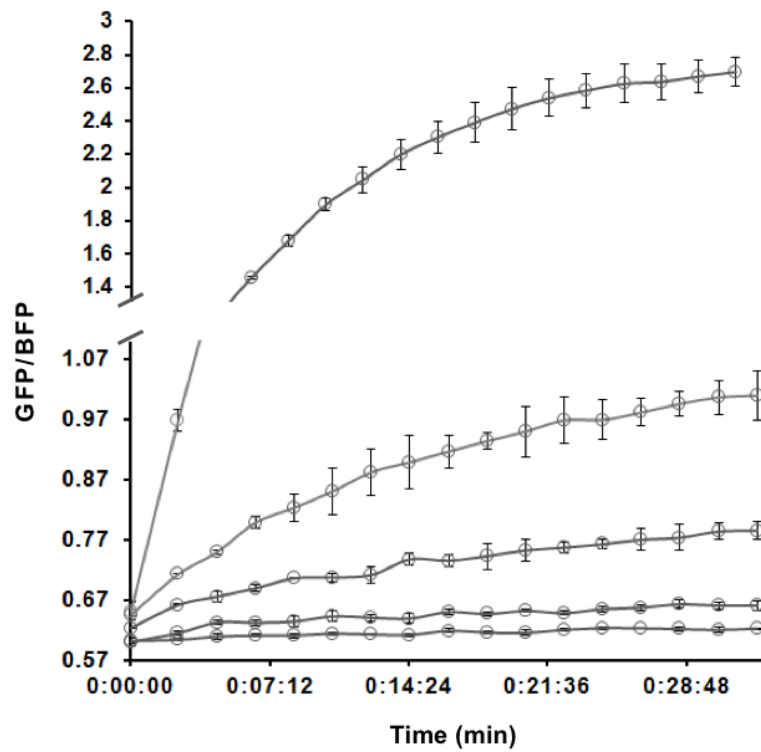


**Figure 2.4.** GFP/BFP ratio changes of hsCY (1  $\mu$ M) in response to 1 mM H<sub>2</sub>S, 100  $\mu$ M, 50  $\mu$ M, 20  $\mu$ M, and 0  $\mu$ M from top to bottom.

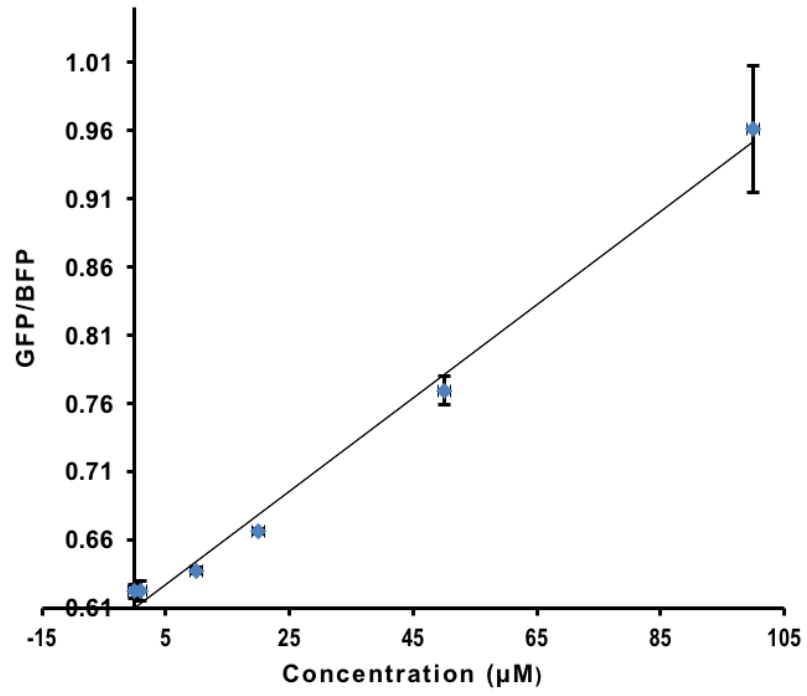


**Figure 2.5.** GFP/BFP Ratios of hsCY (1  $\mu\text{M}$ ) to  $\text{H}_2\text{S}$  up to 100  $\mu\text{M}$ .

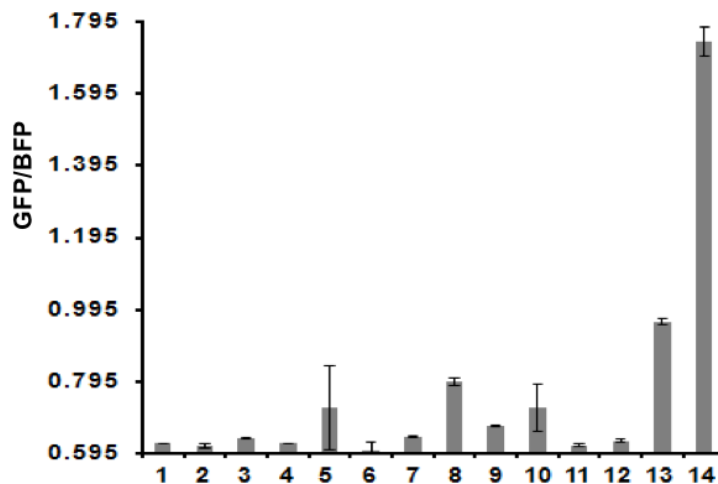


**Figure 2.6.** Chemoselectivity of hsCY against various redox-active chemicals: (1) Tris-HCl, (2) 1 mM H<sub>2</sub>O<sub>2</sub>, (3) 100 μM HOCl, (4) 100 μM HOOtBu, (5) 100 μM ·OH (1 mM Fe<sup>2+</sup> and 100 μM H<sub>2</sub>O<sub>2</sub>), (6) 100 μM ·OtBu (1 mM Fe<sup>2+</sup> and 100 μM HOOtBu), (7) 1 mM Vitamin C, (8) 1 mM DTT, (9) 5 mM L-cysteine (10) 100 μM O<sub>2</sub><sup>-</sup>, (11) 100 μM ONOO<sup>-</sup>, (12) 100 μM Noc-5 (NO<sup>·</sup> donor) (13) 100 μM H<sub>2</sub>S, and (14) 1 mM H<sub>2</sub>S.

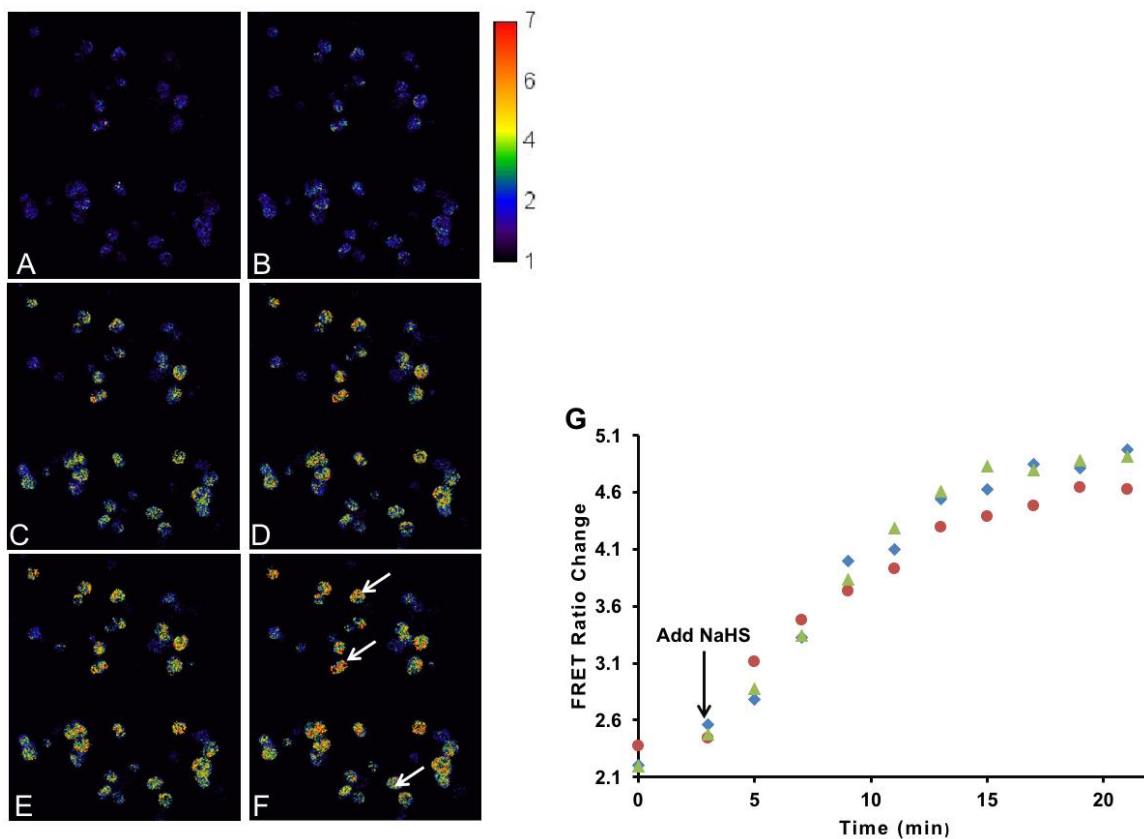


**Figure 2.7.** Live cell imaging of HEK 293T cells expressing hsCY. (A-F) Pseudo-colored ratiometric imaging of HEK 293T cells treated with 100  $\mu$ M H<sub>2</sub>S at (A) 0 min, (B) 5 min, (C) 10 min, (D) 15 min, (E) 20 min, and (F) 30 min. (G) Calculated FRET ratios of individual cells indicated by arrows in F.

### 2.4.3 Expression of *hsCY* in live Mammalian Cells

To validate the use of *hsCY* for H<sub>2</sub>S imaging in living mammalian cells, we transiently co-transfected PMAH-*hsCY* and PMAH- POLY containing the orthogonal synthetase/tRNA pair that incorporates *pAzF* into *hsCY* in HEK 293T cells in the presence of *pAzF*. Upon treating the cells with 100 μM H<sub>2</sub>S, a large increase in the FRET ratio signal was observed within 30 minutes when excited at 405 nm (Figure 2.7A-F). FRET ratio analysis of cells showed a ~214 % FRET change that reached its maximum within 20 minutes (Figure 2.7G). The larger dynamic range of the probe in mammalian cells as compared to the *in vitro* experiments, is also observed in the previously reported H<sub>2</sub>S probes, *hsGFP* and *cpGFP-pAzF*.<sup>32,33</sup> Better protein folding and higher fidelity of mammalian *pAzF* synthetase have been proposed to account for this observation. Taken together, we show that *hsCY* is a robust ratiometric probe for H<sub>2</sub>S both in *E. coli* and in mammalian cells.

## 2.5 Conclusion

To conclude, we developed *hsCY*, the first genetically-encoded ratiometric probe for H<sub>2</sub>S by combining genetic code expansion and FP-based FRET technology. *hsCY* showed selective H<sub>2</sub>S-induced FRET ratio change by modulation of the donor fluorescence intensity. When tested in live mammalian cells, *hsCY* exhibited a large ratiometric response to H<sub>2</sub>S. *hsCY* thus represents a valuable addition to the toolbox for H<sub>2</sub>S detection and imaging. In addition, our sensor design and optimization strategy may

be applied to derive similar FRET-based probes for other cellular reactive chemical species.

### **Appendix Material**

List of primers used, % FRET change of all the constructs studied in this chapter with 1 mM H<sub>2</sub>S, and full protein sequence of hsCY. This material is in Appendix A.

## References

- 1- Elord, J. W.; Calvert, J. W.; Morrison, J.; Doeller, J. E.; Kraus, D. W.; Tao, L.; Jiao, X.; Scalia, R.; Kiss, L.; Szabo, C.; Kimura, H.; Chow, C. W.; Lefer, D. J.; "Hydrogen sulfide attenuates myocardial ischemia-reperfusion injury by preservation of mitochondrial function" *Proc. Natl. Acad. Sci. U. S. A.* 2007, 104:15560-15565.
- 2- Liu Y-H.; Lu, M.; Hu, L.F.; Wong, P. T.; Webb, G. D.; Bian, J. S.; "Hydrogen Sulfide in the Mammalian Cardiovascular System" *Antioxid. Redox Signal.* 2012, 17:141-185.
- 3- Whitfield, N. L.; Kreimier, E. L.; Verdial, F. C.; Skovgaard, N.; Olson, K. R.; "Reappraisal of H<sub>2</sub>S/sulfide concentration in vertebrate blood and its potential significance in ischemic preconditioning and vascular signaling" *Am. J. Physiol. Regul. Integr. Comp. Physiol.* 2008, 249:1930-1937.
- 4- Abe, K.; Kimura, H.; "The possible role of hydrogen sulfide as an endogenous neuromodulator" *J. Neurosci.* 1996, 16:1066-1071.
- 5- Kamoun, P.; "Endogenous production of hydrogen sulfide in mammals" *Amino Acids* 2004, 26:243-254.
- 6- Paul, B. D.; Snyder, S. H.; "H<sub>2</sub>S signaling through protein sulfhydration and beyond" *Nature Reviews Molecular Cell Biology* 2012, 13:499-507.
- 7- Zanardo, R. C.; Brancaleone, V.; Distrutti, E.; Fiorucci, S.; Cirino, G.; Wallace, J. L.; "Hydrogen sulfide is an endogenous modulator of leukocyte-mediated inflammation" *FASEB J.* 2006, 20:2118-2120.
- 8- Else, D. J.; Fowkes, R. C.; Baxter, G. F.; "Regulation of cardiovascular cell function by hydrogen sulfide (H<sub>2</sub>S)" *Cell Biochem. Funct.* 2010, 28:95-106.
- 9- Fitzgerald, R. S.; Shirahta, M.; Chang, I.; Kostuk, E.; Kiihl, S.; "The impact of hydrogen sulfide (H<sub>2</sub>S) on neurotransmitter release from the cat carotid body" *Respir Physiol Neurobiol* 2011, 176:80-89.



- 10- Wang R.; “Two’s company, three’s a crowd: can H<sub>2</sub>S be the third endogenous gaseous transmitter?” *FASEB J.* 2002, 16:1792-1798.
- 11- Kimura, H.; Shibuya, N.; Kimura, Y.; “Hydrogen sulfide is a signaling molecule and a cytoprotectant” *Antioxid Redox Signal.* 2012, 17:45-57.
- 12- Li, L.; Rose, P.; Moore, P. K.; “Hydrogen sulfide and cell signaling” *Annu. Rev. Pharmacol. Toxicol.* 2011, 51:169-187.
- 13- Peng, H.; Cheng, Y.; Dai, C.; King, A. L.; Predmore, B. L.; Lefer, D. J.; Wang, B.; “A Fluorescent Chemoprobe for Fast and Quantitative Detection of Hydrogen Sulfide in Blood” *Angew. Chem. Int. Ed.* 2011, 50:9672-9675.
- 14- Kamoun, P.; Belardinelli, M. C.; Chabli, A.; Lallouchi, K.; Chadefaux-Vekemans, B.; “Endogenous hydrogen sulfide overproduction in down syndrome” *Am J Med Genet A.* 2003, 116:310-311.
- 15- Eto, K.; Asada, T.; Arima, K.; Makifuchi, T.; Kimura, H.; “Brain hydrogen sulfide is severely decreased in Alzheimer's disease” *Biochem Biophys, Res, Commun.* 2002, 293:1485-1488.
- 16- Wu, L.; Yang, W.; Jia, X.; Yang, G.; Duridanova, D.; Cao, K.; Wang, R.; “Pancreatic islet overproduction of H<sub>2</sub>S and suppressed insulin release in Zucker diabetic rats” *Lab. Invest.* 2009, 89:59-67.
- 17- Yang, G.; Wu, L.; Jiang, B.; Yang, W.; Qi, J.; Cao, K.; Meng, Q.; Mustafa, A. K.; Mu, W.; Zhang, S.; Snyder, S. H.; Wang, R.; “H<sub>2</sub>S as a physiologic vasorelaxant: hypertension in mice with deletion of cystathionine gamma-lyase” *Science.* 2008, 322:587-590.
- 18- Radford-Knoery, J.; Cutter, G. A.; “Determination of carbonyl sulfide and hydrogen sulfide species in natural waters using specialized collection procedures and gas chromatography with flame photometric detection” *Anal. Chem.* 1993, 65:976-982.
- 19- Choi, M. G.; Cha, S.; Lee, H.; Jeon, H. L.; Chang, S. K.; “Sulfide-selective chemosignaling by a Cu<sup>2+</sup> complex of dipicolylamine appended fluorescein” *Chem Commun.* 2009, 47:7390-7392.

- 20- Searcy, D. G.; Peterson, M. A.; “Hydrogen sulfide consumption measured at low steady state concentrations using a sulfidostat.” *Anal. Biochem.* 2004, 324:269-275.
- 21- Yu, F.; Han, X.; Chen, L.; “Fluorescent probes for hydrogen sulfide detection and bioimaging” *Chem. Commun.* 2014, 50:12234-12249.
- 22- Lippert A. R.; New, E. J.; Chang, C. J.; “Reaction-Based Fluorescent Probes for Selective Imaging of Hydrogen Sulfide in Living Cells” *J. Am. Chem. Soc.* 2011, 133:10078-10080.
- 23- Lin V. S.; Lippert, A. R.; Chang, C. J.; “Cell-trappable fluorescent probes for endogenous hydrogen sulfide signaling and imaging H<sub>2</sub>O<sub>2</sub>-dependent H<sub>2</sub>S production” *Proc. Natl. Acad. Sci. U. S. A.* 2013, 110:7131-7135.
- 24- Zhang, H.; Wang, P.; Chen, G.; Cheung, H. Y.; Sun, H.; “A highly sensitive fluorescent probe for imaging hydrogen sulfide in living cells” *Tetrahedron Lett.* 2013, 54:4826-4829.
- 25- Wang, R.; Yu, F.; Chen, L.; Chen, H.; Wang, L.; Zhang, W.; “A highly selective turn-on near-infrared fluorescent probe for hydrogen sulfide detection and imaging in living cells” *Chem. Commun.* 2012, 48:11757-11759.
- 26- Wu, M.; Li, K.; Hou, J.; Huang, Z.; Yu, X.; “A selective colorimetric and ratiometric fluorescent probe for hydrogen sulfide” *Org. Biomol. Chem.* 2012, 10:8342-8347.
- 27- Montoya, L. M.; Pluth, M. D.; “Selective turn-on fluorescent probes for imaging hydrogen sulfide in living cells” *Chem. Commun.* 2012, 48:4767-4769.
- 28- Qian, Y.; Karpus, J.; Kabil, O.; Zhang, S. Y.; Zhu, H. L.; Banerjee, R.; Zhao, J.; He, C.; “Selective fluorescent probes for live-cell monitoring of sulphide” *Nat. Commun.* 2011, 2:495-501.
- 29- Liu, C.; Pan, J.; Li, S.; Zhao, Y.; Wu, L. Y.; Berkman, C. E.; Whorton, A. R.; Xian, M.; “Capture and visualization of hydrogen sulfide by a fluorescent probe” *Angew. Chem., Int. Ed.* 2011, 50:10327-10329.

- 30-Cao, X.; Lin, W.; He, L.; “A Near-Infrared Fluorescence Turn-On Sensor for Sulfide Anions” *Org. Lett.* 2011, 13:4716-4719.
- 31-Sasakura, K.; Hanaoka, K.; Shibuya, N.; Mikami, Y.; Kimura, Y.; Komatsu, T.; Ueno, T.; Terai, T.; Kimura, H.; Nagano, T.; “Development of a Highly Selective Fluorescence Probe for Hydrogen Sulfide” *J. Am. Chem. Soc.* 2011, 133:18003-18005.
- 32-Chen, S.; Chen, Z.; Ren, W.; Ai, H.; “Reaction-Based Genetically Encoded Fluorescent Hydrogen Sulfide Sensors” *J. Am. Chem. Soc.* 2012, 134:9589-9592.
- 33-Chen, Z.; Ai, H.; “A Highly Responsive and Selective Fluorescent Probe for Imaging Physiological Hydrogen Sulfide” *Biochemistry* 2014, 53:5966-5974.
- 34-Ai, H.; “Biochemical analysis with the expanded genetic lexicon” *Anal. Bioanal. Chem.* 2012, 403:2089-2102.
- 35-Ren, W.; Ai, H.; “Genetically Encoded Fluorescent Redox Probes” *Sensors* 2013, 13:15422-15433.
- 36-Liu, B.; Zeng, F.; Wu, G.; Wu, S.; “A FRET-based ratiometric sensor for mercury ions in water with multi-layered silica nanoparticles as the scaffold” *Chem. Commun.* 2011, 47:8913-8915.
- 37-Yu, C.; Li, X.; Zeng, F.; Zheng, F.; Wu, S.; “Carbon-dot-based ratiometric fluorescent sensor for detecting hydrogen sulfide in aqueous media and inside live cells” *Chem. Commun.* 2013, 49:403-405.
- 38-Hussain, S. A.; Dey, D.; Chakraborty, S.; Saha, J.; Roy, A. D.; Chakraborty, S.; Debnath, P.; Bhattacharjee, D.; “Fluorescence Resonance Energy Transfer (FRET) sensor” *Sci. Lett. J.* 2015, 4:1-16.
- 39-Chen, Z.; Ren, W.; Wright, Q. E.; Ai, H.; “Genetically Encoded Fluorescent Probe for the Selective Detection of Peroxynitrite” *J. Am. Chem. Soc.* 2013, 135:14940-14943.

- 40- Ai, H.; Shaner, N. C.; Cheng, Z.; Tsien, R. Y.; Campbell, R. E.; "Exploration of New Chromophore Structures Leads to the Identification of Improved Blue Fluorescent Proteins" *Biochem.* 2007, 46:5904-5910.
- 41- Griesbeck, O.; Baird, G. S.; Cambell, R. E.; Zacharias, D. A.; Tsien, R. T.; "Reducing the Environmental Sensitivity of Yellow Fluorescent Protein - MECHANISM AND APPLICATIONS" *J. Biol. Chem.* 2001, 276:29188-29194.
- 42- Chin, J. W.; Santoro, S. W.; Martin, A. B.; King, D. S.; Wang, L.; Schultz, P. G.; "Addition of p-azido-L-phenylalanine to the genetic code of Escherichia coli." *J. Am. Chem. Soc.* 2002, 124:9026-9027.
- 43- Kolev, J. N.; Zaengle, J. M.; Ravikumar, R.; Fasa, R.; "Enhancing the Efficiency and Regioselectivity of P450 Oxidation Catalysts by Unnatural Amino Acid Mutagenesis" *ChemBioChem.* 2014, 15:1001-1010.
- 44- Wang, Q.; Shui, B.; Kotlikoff, M. I.; Sondermann, H.; "Structural basis for calcium sensing by GCaMP2" *Structure* 2008, 16:1817-1827.

## Chapter 3

### A Genetically Encoded FRET Sensor for Hypoxia and Prolyl Hydroxylases

#### 3.1. Abstract

Oxygen is vital for all aerobic life forms. Oxygen-dependent hydroxylation of hypoxia-inducible factor (HIF)-1 $\alpha$  by prolyl hydroxylase domain enzymes (PHDs) is an important step for controlling the expression of oxygen-regulated genes in metazoan species, thereby constituting a molecular mechanism for oxygen sensing and response. Herein, we report a genetically encoded dual-emission ratiometric fluorescent sensor, ProCY, which responds to PHD activities *in vitro* and in live cells. We demonstrated that ProCY could monitor hypoxia in mammalian cells. By targeting this novel genetically encoded biosensor to the cell nucleus or cytosol, we determined that the HIF-prolyl hydroxylase activity was mainly confined to the cytosol of HEK 293T cells under normoxic culture conditions. The results collectively suggest broad applications of ProCY on evaluation of hypoxia and prolyl hydroxylase activities and understanding of pathways for the control of hypoxic responses

#### 3.2. Introduction

Oxygen is required for all aerobic organisms on Earth for metabolism and energy production. In the meanwhile, oxygen overexposure may increase the production of reactive oxygen species (ROS), leading to oxidative damage.<sup>1</sup> Therefore, biological

systems have evolved complex mechanisms to sense oxygen concentration changes and respond accordingly to maintain homeostasis. Hypoxia-inducible factor (HIF)-1 is an important component of a cellular signaling cascade responsible for oxygen-dependent responses in various animals.<sup>2</sup> HIF-1 is a transcription factor, which regulates the expression of a number of downstream genes, whereas the stability of the  $\alpha$ -subunit of HIF-1 (HIF-1 $\alpha$ ) is controlled by oxygen-dependent hydroxylation of conserved proline residues by prolyl hydroxylase domain enzymes (PHDs), thereby leading to subsequent ubiquitination and proteosomal degradation of HIF-1 $\alpha$  (Figure 3.1).<sup>2-5</sup> Consequently, HIF-1 $\alpha$  and its prolyl hydroxylation serve as a mechanism to transduce the cellular oxygen level into changes in gene expression.<sup>6,7</sup>

Under normoxia, PHDs use molecular oxygen (O<sub>2</sub>) as a substrate to generate proline-hydroxylated HIF-1 $\alpha$ , which next binds to von Hippel-Lindau (VHL) protein to trigger polyubiquitylation and proteosomal degradation. Under hypoxia, PHD activity is reduced because of low oxygen levels, so HIF-1 $\alpha$  is stabilized and enters the nucleus to bind hypoxia responsive elements (HREs) to induce the expression of downstream genes.

Hypoxia, a condition defined by low oxygen levels, has been linked to diverse pathophysiological processes and diseases, such as cancer, anemia, ischemia, and stroke.<sup>8-11</sup> Because of the high sensitivity and versatility of fluorescence measurements, hypoxia-responsive fluorescent probes are considered important research tools.<sup>12,13</sup> Previous studies have reported several synthetic fluorescent probes sensitive to bioreduction reactions under hypoxia, such as synthetic molecules containing a nitro group,<sup>14-16</sup> a quinone group,<sup>17</sup> an azo group,<sup>18,19</sup> or a xanthine ring<sup>20</sup> as their sensory

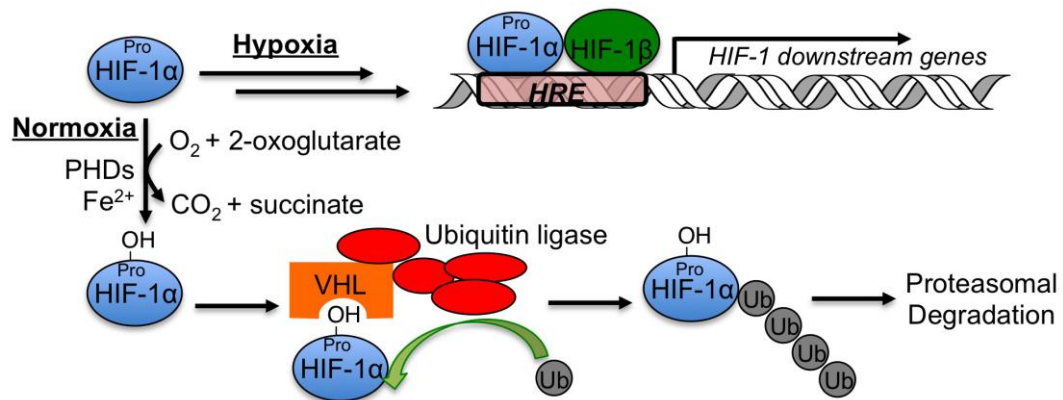


**Figure 3.1.** Schematic illustration of the regulation of HIF-1 $\alpha$ .

moieties. Despite the progress, none of these aforementioned fluorescent probes directly senses the hydroxylation of the HIF-1 $\alpha$  proline by PHDs. Instead, their fluorescence change is often dependent of the activities of endogenous reductases under hypoxia. Moreover, it is not trivial to deliver these synthetic dyes to specific subcellular locations. In other studies, fluorescent proteins (FPs) have been fused downstream to tandem repeats of the hypoxia transcriptional response element (HRE) to afford genetic tools for monitoring the transcriptional activity of HIF-1.<sup>21</sup> Because prolyl hydroxylation is not the only regulatory mechanism for HRE-dependent transcription,<sup>2</sup> the fluorescence of the FP reporters does not necessarily reflect oxygen abundance and the activities of PHDs. Herein, we describe a novel genetically encoded single-chain fluorescent biosensor, which can ratiometrically respond to PHD activities *in vitro* and in live cells. We also

show that the Förster resonance energy transfer (FRET) ratios of the biosensor are indicative of hypoxic and normoxic conditions in living systems.

### **3.3. Experimental Section**

#### *3.3.1. Materials, Reagents, and General Methodology*

Ascorbic acid was purchased from Spectrum Chemical (New Brunswick, NJ). Disodium 2-oxoglutarate was purchased from TCI America (Portland, OR). Iron (II) sulfate heptahydrate was purchased from Thermo Fisher Scientific (Hanover Park, IL). Catalase from Bovine Liver was purchased from Sigma-Aldrich (St. Louis, MO). IOX2 was purchased from Cayman Chemical (Ann Arbor, MI). Gases for cell culture were purchased from Airgas USA (Lynwood, CA). SuperSignal West Pico Chemiluminescent substrate (Prod # 34077) and HRP-conjugated HIF-1 $\alpha$  antibody (Prod # PA5-22779) were from Thermo Fisher Scientific (Rockford, IL). HRP-conjugated antibody to c-Myc was from Abcam (Cambridge, UK). Colorimetric One-Component TMB Membrane Peroxidase Substrate (Prod # 50-77-18) was purchased from Kierkegaard & Perry Laboratories (Gaithersburg, MD). Synthetic DNA oligonucleotides were purchased from Integrated DNA Technologies (San Diego, CA). HA-Egln1-pcDNA3 (Plasmid # 18963) was purchased from Addgene (Cambridge, MA). Restriction endonucleases were purchased from New England Biolabs (Ipswich, MA) or Thermo Scientific Fermentas (Vilnius, Lithuania). PCR products and products of restriction digestion were purified by gel electrophoresis and extracted using Syd Laboratories Gel Extraction columns



(Malden, MA). Plasmid DNA was purified using Syd Laboratories Miniprep columns. DNA sequence analysis was performed by Retrogen (San Diego, CA).

### 3.3.2. Construction of *E. Coli* Expression Plasmids

To construct ProCY, polymerase chain reactions (PCR) were utilized to amplify the pVHL fragment from a synthetic gene block (IDT, San Diego, CA), the PHD2 sequence from HA-Egln1-pcDNA3, and YPet and ECFP from a previously reported Src sensor.<sup>1</sup> In particular, YPet was amplified with oligos YPet-For and YPet-Rev. The PCR product was digested with KpnI and HindIII and ligated into a compatible pre-digested pBAD plasmid to afford YPet-pBAD plasmid. In the next step, two PCR reactions were performed to amplify ECFP and pVHL and add sequences for linkers and a HIF-1 $\alpha$  derived peptides. Oligonucleotides ECFP-For and pVHL-Rev were used in the first reaction, and oligos Pst1-For, Kpn1-Rev1, Kpn-Rev2 and Kpn-Rev3 were used in the second PCR reaction, respectively. Products of these two reactions were then assembled using an overlap PCR to produce the full length gene containing ECFP, pVHL, the linkers, and a HIF-1 $\alpha$  derived peptide. The PCR product was digested with XhoI and KpnI, and ligated into a pre-digested YPet-pBAD plasmid. To construct ProCY-B, two separate PCR reactions were done on ProCY using oligos ECFP-For, GGSG-Rev, and GGSG-For, Kpn-Rev2 respectively. The products of the two reactions were assembled using overlap PCR, followed by digestion with XhoI and KpnI and ligation to a predigested YPet-pBAD to generate ProCY-B. To create ProCY-C, two separate PCR reactions were performed on ProCY-B template. In the first PCR reaction, oligos ECFP-

For, and MidFloppy-R were used, while in the second reaction, MidFloppy-F1, MidFloppy-F2, and pBAD-Rev were used. The two PCR reactions were assembled using overlap PCR and outside primers, digested with XhoI and HindIII, and ligated into a compatible pre-digested pBAD/His B vector. To construct ProCY-D, we did a PCR reaction on ProCY-B using oligos HIF-Rigid-F and pBAD-Rev. The PCR product was digested with KpnI and HindIII and ligated into a pre-digested ProCY-B vector to afford the full length gene sequence in ProCY-D. To make ProCY-E, a PCR reaction was performed on ProCY using oligos ECFP-For and SacI-Rev. The generated PCR product was digested with XhoI and SacI and ligated with a pre-digested ProCY to afford ProCY-E. The control construct ProCY-N was generated by carrying out a PCR reaction on ProCY using ECFP-For and PAPA-Rev. The resulted product was digested with XhoI and KpnI and ligated to a pre-digested YPet-pBAD. The ligation products were then used to transform *E. coli* DH10B competent cells, which were next plated on LB agar plates supplemented with ampicillin (100 µg/mL) and L-arabinose (0.04%, w/v%). Similarly, PCR was used to amplify PHD2 gene using PHD2-Kpn1-F and PHD2-HindIII-R primers. The PCR product was digested with Kpn1 and HindIII restriction enzymes and ligated into a compatible pre-digested PCDF-1b plasmid. The ligation product was used to transform *E. coli* DH10B competent cells, which were next plated on LB agar plates supplemented with spectinomycin (50 µg/mL).

### *3.3.3. Optimization of FRET Efficiency by Linker Modification*

To optimize the FRET efficiency change of ProCY, the length of the linkers between PVHL and HIF-1 $\alpha$  were varied. The amino acid sequences of all linkers tested in this study are provided in Figure 3.4 (and Figure B1, Appendix B). Linkers were modified using a PCR procedure in which the cDNA encoding the ECFP-PVHL gene fragment of ProCY was amplified with appropriately modified forward and reverse primers.

### *3.3.4. Protein Expression and Purification in E. coli*

To express FRET-based proteins, DH10B cells were co-transformed with a pBAD/His B containing the gene of interest and pGro7 chaperone plasmid by electroporation and grown on LB agar containing 100  $\mu$ g/mL ampicillin and 50  $\mu$ g/mL chloramphenicol at 37 °C overnight. A single colony was grown in a starter culture of 5 mL of LB broth with appropriate antibiotics at 37 °C and 220 rpm overnight. A saturated starter culture was diluted 100-fold into 2YT medium containing the appropriate antibiotics and grown under the same conditions. When the OD<sub>600</sub> reached 0.8, the expression culture was induced with 0.2% L-arabinose. Culture flasks were then moved to room temperature where growth continued with vigorous shaking for 48 hours. Cells were then harvested, suspended in 1xPBS supplied with protease inhibitor, and then lysed. The hexa-His-tagged proteins were affinity-purified with nickel-nitrilotriacetic acid(Ni-NTA) agarose beads (Qiagen) under native conditions according to the manufacturer's instruction and then buffer-exchanged into Tris-HCl (30 mM, pH 7.4)

using Thermo Scientific Snakeskin dialysis tubing (7 k molecular cutoff). Proteins were further purified by size exclusion column chromatography (Amersham Superdex 75 prep) and concentrated using a 3K molecular weight cutoff Amicon Ultra centrifugal filter (Millipore, Billerica, MA). The concentration was determined using Beer's Law and extinction coefficients of ECFP and YPet. PHD2 enzyme expression was done by transforming pCDF-1bPHD2 into BL21 cells by electroporation and grown on LB agar dishes containing 50 µg/mL Spectinomycin 37°C overnight. A single colony was grown in 5mL LB culture medium supplied with appropriate antibiotics at 37°C shaker overnight. The cell culture was then diluted 100-fold into 2YT medium containing the appropriate antibiotics and grown under the same conditions. When the OD600 reached 0.8, the protein was induced by adding IPTG to a final concentration of 1mM. Cell culture was next allowed to grow for 24 hours at room temperature. Cells were then harvested and lysed. The 6-His-tagged PHD2 enzyme was affinity purified with nickel-nitrilotriacetic acid (Ni-NTA) agarose beads (Qiagen) and dialyzed in 30 mM Tris-HCl buffer as mentioned above. The protein was then stored immediately at -80°C after adding 10% glycerol.

### *3.3.5. Spectroscopic Characterization*

A monochromator-based Synergy MixMicroplate Reader (BioTek, Winooski, VT) was used to record all absorbance and fluorescence spectra. To record the emission spectra, the excitation wavelength was set at 434 nm, and the emission was scanned from 455 nm to 600 nm. FRET ratios were calculated by dividing fluorescence intensity of

YPet over fluorescence intensity of ECFP. For single point measurements, excitation at 434 nm and emission at 477 nm and 525 nm were used to calculate FRET ratio. Absorbance spectra were recorded by scanning from 250 nm to 600 nm, and a blank solution was used to subtract the background.

### *3.3.6. PHD2 Activity Assay*

Freshly made stock solutions were all prepared in 30 mM Tris (PH 7.4) buffer solution. A final protein concentration of 1  $\mu$ M and PHD2 final concentration of 2  $\mu$ M were used in all the measurements. The PHD2 activity assay was carried out by mixing 2 mg/mL BSA, 1mM DTT, 2mM ascorbic acid, 0.6 mg/mL catalase, 25  $\mu$ M Fe (II) solution (prepared as 500 mM stock in 20mM HCL and diluted with distilled water) with 1  $\mu$ M ProCY in a black 96-well plate and incubated for 20 min at room temperature. PHD2 enzyme (2  $\mu$ M) was then added to the reaction mixture but not to the control solution and the reaction was initiated by adding 200  $\mu$ M 2-oxoglutarate. The 96-well plate was next incubated at 37°C for 40 min. Excitation at 434 nm was used to measure the emission spectrum from 455 nm to 600 nm. FRET ratio was calculated by dividing the emission intensity at 525 nm over the emission intensity at 480 nm.

### *3.3.7. Construction of Mammalian Reporter Plasmids*

To insert the ProCY and ProCY-N genes into the mammalian expression vector pcDNA3, primers HydpcDNA3-F and HydpcDNA3-R were used to amplify both genes separately and add HindIII and XbaI restriction sites at N- and C-terminals respectively.

The HydpcDNA3-F primer also includes a kozak sequence and a start codon for efficient translational initiation. Each PCR product was digested with HindIII and XbaI, and inserted into a compatible pre-digested pcDNA3 plasmid. In a similar way PHD2 gene was amplified using PHD2-pcDNA3-F and PHD2-pcDNA3-R primers, digested with HindIII and XbaI restriction enzymes and ligated into a compatible pre-digested pcDNA3 vector. To add myc-tag at C-terminal of PHD2 for western blot analysis, pcDNA3-F, and mycPHD2-R were used. The PCR product was then digested with HindIII and XbaI and ligated into a pre-digested pcDNA3 plasmid. To create a plasmid for nuclear expression of ProCY, we used oligonucleotides PLJMI-NheI-F, and pHP-Nuc-R to amplify ProCY gene fragment from pBAD-ProCY. The PCR product was digested with NheI and XhoI and ligated into a predigested pECFP-Nuc-derived plasmid containing three copies of a nuclear localization sequence (DPKKKRKV) added to the C-terminal in the final target plasmid pNuc-ProCY. To construct a plasmid for cytosolic expression, we used oligonucleotides NES-HP-F1, NES-HP-F2, and NES-HP-XbaI-R to amplify the ProCY gene fragment from pBAD-ProCY and further extend it to include an N-terminal nucleus export signal (LQLPPLERLTL). The product was digested with HindIII and XbaI, and then ligated into a predigested pcDNA3-derived plasmid containing two repeats of the nuclear export signal to afford pNES-ProCY.

### *3.3.8. Experimental Design of Hypoxia Chambers*

Hypoxia chambers were manually constructed. Briefly, tightly sealed 150 x 15 mm petri dish was used as a hypoxia chamber with two holes drilled in the lid. A valve was

placed in each hole, one allowing gas in and one allowing gas out. To establish hypoxia, we placed transfected (or non-transfected) HEK 293T cells in the hypoxia chamber along with a dish containing distilled water to humidify the incoming gas. The chamber was then sealed and a gas mixture containing 93% N<sub>2</sub> containing 5% CO<sub>2</sub> and 2% O<sub>2</sub> was allowed to run through the inlet valve for at least 4-6 minutes. Next, the chambers were incubated for 48 hours at 37°C. Gas mix was allowed to run through the hypoxic chamber inlet valve every 12-14 hours.

### *3.3.9. Mammalian Cell Culture and Imaging*

Human Embryonic Kidney (HEK) 293T cells were cultured in Dulbecco's Modified Eagle's Medium (DMEM) supplemented with 10% fetal bovine serum (FBS). Cells were incubated at 37°C with 5% CO<sub>2</sub> in humidified air for 24 hours. HEK 293T cells were then co-transfected with 2 µg pcDNA3-ProCY and 2 µg pcDNA3-PHD2 in the presence of 12 µg PEI (polyethyleneimine, linear, M.W. 25 kDs). As a control, HEK 293T cells on a 35-mm plastic culture dish were co-transfected with 2 µg empty pcDNA3 and 2 µg pcDNA3-ProCY in the presence of 12 µg PEI. Transfected cells were then divided in two groups. The first group was cultured in complete media under normoxic conditions for 48 hours, and the second group of transfected cells was cultured in complete media in the hypoxic chambers for 48 hours. Hypoxic gas mixture was allowed to run every 12-14 hours into the hypoxic chamber. Another group of Transfected HEK 293T cells were treated with 10 µM IOX2 inhibitor for 48 hours. All media were replaced with Dulbecco's Phosphate Buffered Saline (DPBS) before imaging.

### 3.3.10. Western blotting

HEK 293T cells seeded on a 100 mm dishes were exposed to hypoxia conditions for 48 hours. Cells were then harvested and nuclear proteins were extracted using an established nuclear protein extraction protocol.<sup>36</sup> Proteins were then allowed to run on a polyacrylamide gel electrophoresis (SDS-PAGE) and next transferred into nitrocellulose membranes. Membranes were blocked with 5% low fat milk for 1 hour followed by incubation with (HRP)-conjugated HIF-1 alpha antibody. The signal was detected using an enhanced chemiluminescence western blotting substrate. Western blot analysis of PHD2-Myc proteins was done by transfecting PHD2-Myc plasmid into HEK 293T cells and exposing them to either normoxia or hypoxia conditions. Cell lysates were then allowed to run on polyacrylamide gel electrophoresis (SDS-PAGE) followed by blotting on a nitrocellulose membrane. The membrane was next blocked with 5% low fat milk for 1 hour followed by an overnight incubation with (HRP)-conjugated c-Myc antibody at 4°C. Signals were detected using colorimetric One-Component TMB Membrane Peroxidase Substrate.

## 3.4. Results and Discussion

The biosensor was designed by sandwiching a proline-containing substrate peptide derived from HIF-1 $\alpha$  and a small 10-kDa protein domain derived from the von Hippel-Lindau tumor suppressor (VHL) between an enhanced cyan FP (ECFP) and a yellow FP (YPet) (Figure 3.2). We selected a 22-aa peptide from HIF-1 $\alpha$  (residues 556 to 577 with a hydroxylation site at residue 564), because of its reasonable length and excellent



substrate activity for various PHDs.<sup>22,23</sup> The hydroxylation of Pro564 can greatly enhance the interaction of the peptide with VHL, whereas residues 60-154 of VHL form a distinct domain responsible for the interaction (Figure 3.3).<sup>24</sup> ECFP and YPet were selected, because they form a highly optimized FRET pair, which typically leads to relatively large dynamic ranges in FP-based biosensors.<sup>25,26</sup> We reasoned that the oxygen-dependent hydroxylation of the HIF-1 $\alpha$  derived peptide by PHDs might induce the interaction of the peptide with the VHL domain, leading to a conformational change that alters the distance and/or relative orientation between ECFP and YPet to further trigger a measurable change in the FRET efficiency.<sup>26</sup>

We constructed five genetic variants, which differ from each other in terms of the length and composition of the linkers (Figures 3.4, 3.5, and Figure B1 of Appendix B). We expressed all fusion proteins in *Escherichia coli*, by co-expressing GroEL and GroES chaperones to assist protein folding.<sup>27</sup> We next purified the proteins in two steps using Ni-NTA affinity chromatography and size-exclusion columns, and determined their fluorescence responses to a catalytically active fragment of PHD2 (*a.k.a.* HIF-P4H-2, or EglN1) using an *in vitro* enzyme assay.<sup>28</sup> We named the variant showing the largest dynamic range (defined as the ratio of the acceptor-to-donor emission ratios before and after treatment with PHD2) ProCY. It contains a 21-amino acid Gly- and Ser- rich linker between the VHL domain and the HIF-1 $\alpha$  derived peptide; all other elements were fused with short dipeptide sequences (Figure 3.6 A). The FRET ratio (YPet/ECFP) of this variant changed from 2.95 to 1.76 after addition of PHD2, corresponding to a dynamic range of 168% (Figure 3.6 B). We further constructed a negative-control fluorescent

probe, ProCY-N, which is identical to ProCY except for that both proline residues (Pro564 and Pro567) in the HIF-1 $\alpha$  derived peptide were mutated to alanine (Figure 3.6 A). The fluorescence of ProCY-N is irresponsive to the PHD2 activity (Figure 3.6 C).

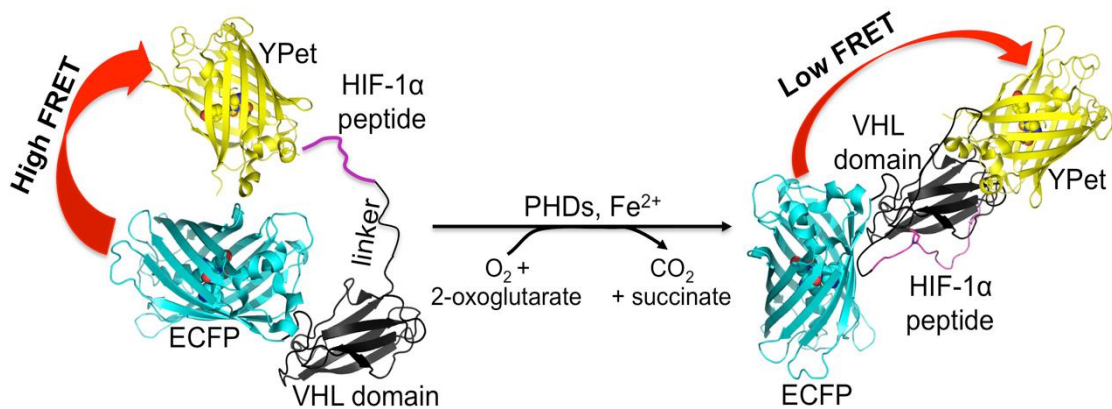


**Figure 3.2.** Illustration of the FRET change of the genetically encoded dual-emission ratiometric fluorescent sensor, ProCY, upon the actions of PHDs.

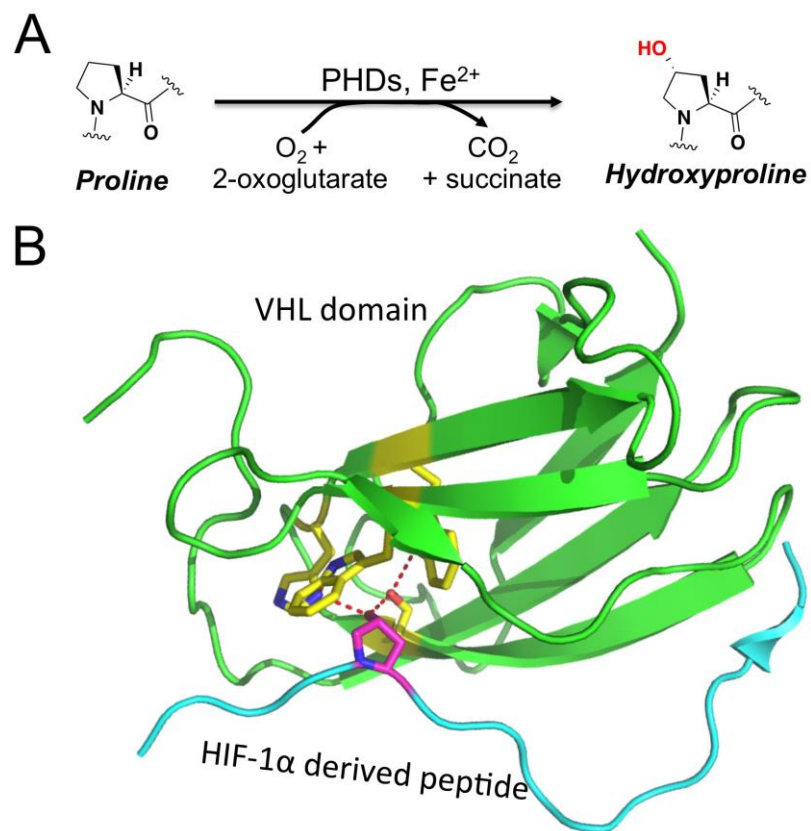


**Figure 3.3.** (A) Chemical reaction for conversion of proline into 4-hydroxyproline by prolyl hydroxylase domain enzymes (PHDs). (B) Interactions between a VHL domain (residues 60-154) and a HIF-1 $\alpha$  derived peptide, showing several interfacial H-bonds through the hydroxyl group of 4-hydroxyproline (residue 564). The structure is redrawn based on Protein Data Bank (PDB) entry 4AJY.

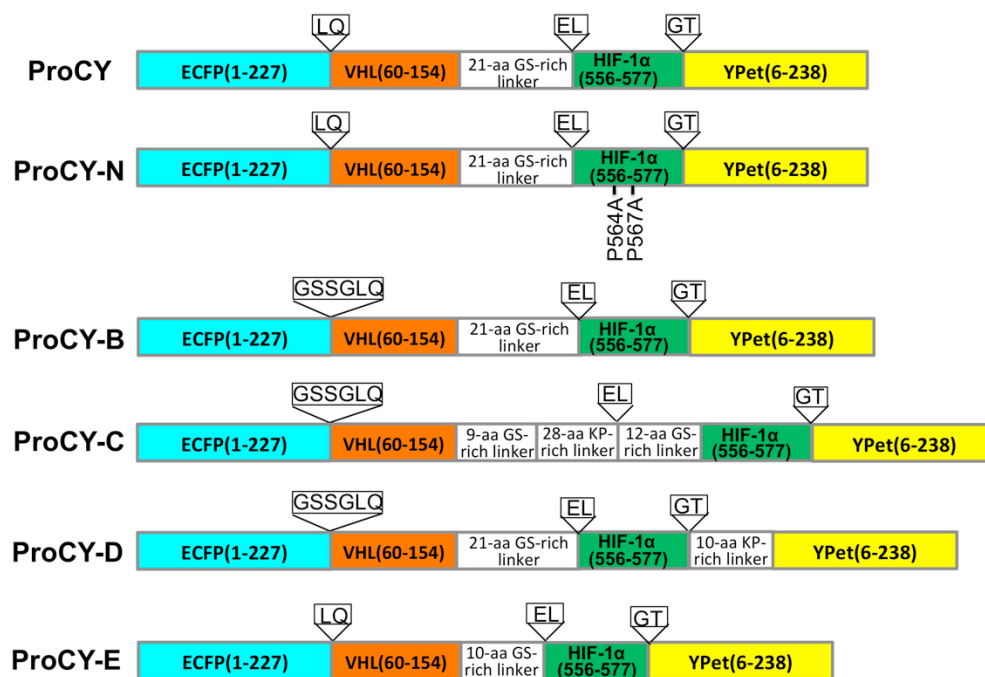


**Figure 3.4.** Domain arrangements of biosensors constructed in this study. Residues are numbered by following PDB entries 2WSN and 4AJY.

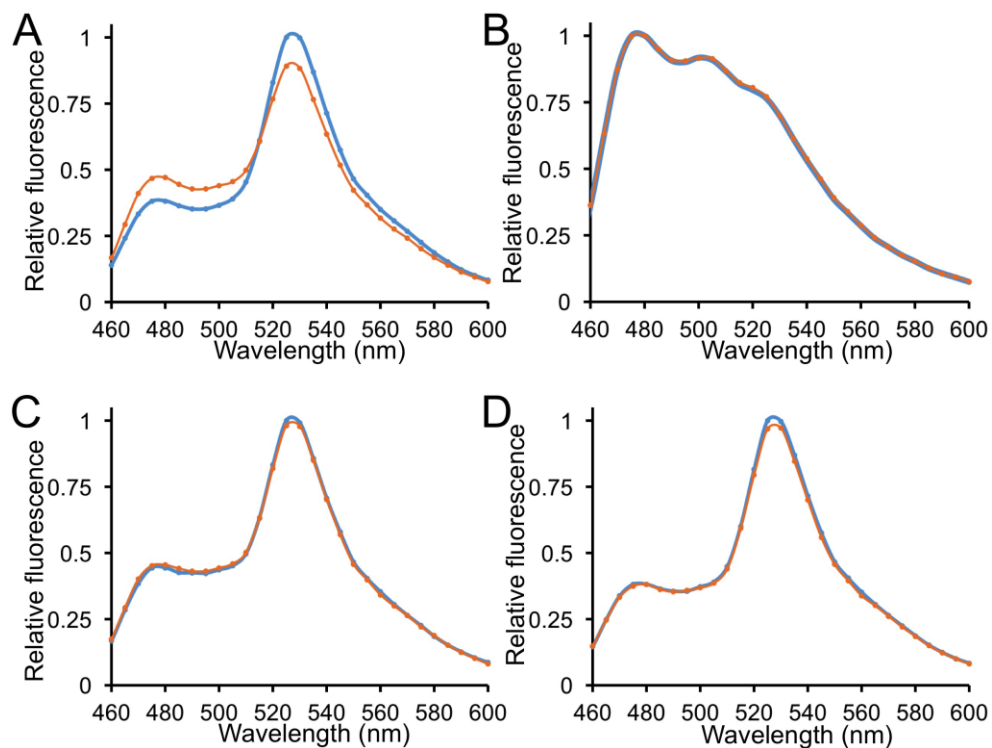


**Figure 3.5.** Fluorescent emission spectra for (A) ProCY-B, (B) ProCY-C, (C) ProCY-D, and (D) ProCY-E before (blue) and after (orange) treatment with a catalytically active PHD2 fragment.

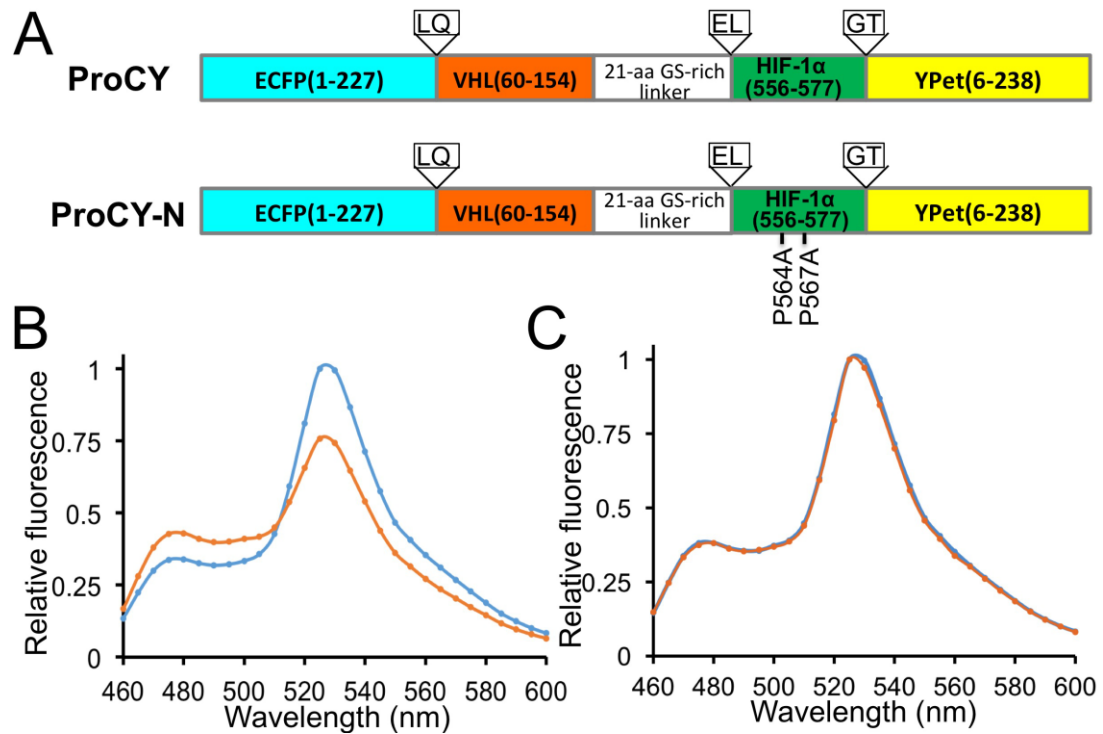


**Figure 3.6.** (A) Domain arrangements of ProCY and the negative-control probe, ProCY-N. (B) Fluorescent emission spectra for ProCY before (blue) and after (orange) treatment with a catalytically active PHD2 fragment. (C) Fluorescent emission spectra for ProCY-N, showing no response to PHD2 treatment.

We next expressed ProCY in human embryonic kidney (HEK) 293T cells, and examined its responses to intracellular PHD activities. We cultured cells in a typical cell culture incubator (~ 20% O<sub>2</sub>), or in a hypoxic chamber supplied with 2% O<sub>2</sub>. A lower FRET ratio was observed for the cells under normoxia (Figure 3.7 A) than the cells under hypoxia (Figure 3.7 B), corroborating our *in vitro* characterization with purified proteins. Under normoxia, addition of 10 μM IOX2,<sup>29</sup> a commercially available PHD inhibitor, brought the FRET ratio back to a level close to that of cells under hypoxia (Figure 3.7 C). We further co-expressed ProCY with the catalytic fragment of PHD2 in HEK 293T cells. Under all conditions, the FRET ratios of the cells overexpressing the PHD2 fragment were essentially indistinguishable from the ratios of the cells without PHD2 overexpression (Figures 3.7 D-F and 3.8 A), indicating that the endogenous PHD level in HEK 293T cells is high and it is not the limiting factor for the intracellular prolyl hydroxylation reaction. To further confirm that the FRET changes of ProCY were caused by intracellular PHD activities, we expressed the negative-control probe, ProCY-N, in HEK 293T cells under normoxia and hypoxia, and no FRET ratio change was observed (Figures 3.8 A and 3.9). All data collectively support that ProCY is an effective sensor for monitoring the PHD activities and hypoxia in mammalian cells. We also utilized Western blot to probe the expression levels of PHD2 and HIF-1α in HEK 293T (Figure 3.8 B). PHD2 was observed for cells under both normoxia and hypoxia, whereas HIF-1α was only observed for cells under hypoxia. The result is aligned with previous reports,<sup>2</sup> indicating that our experimental conditions were well controlled.

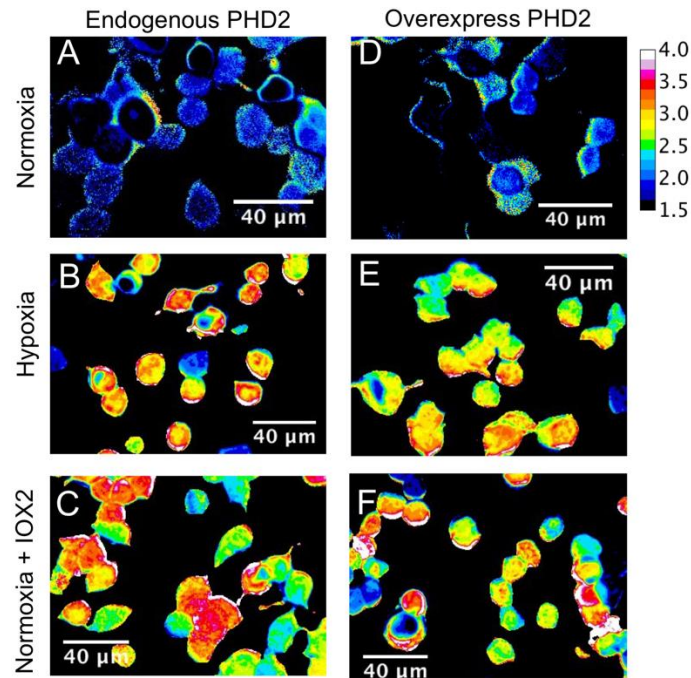


**Figure 3.7.** Pseudocolored ratio images of representative ProCY-expressing HEK 293T cells without (A-C) or with (D-F) overexpression of PHD2. The cells were cultured under either normoxia (A and D) or hypoxia (B and E), or treated with a PHD2 inhibitor, IOX2, under normoxia (C and F). The color bar represents the ratio of sensitized YPet fluorescence emission to direct ECFP donor emission (YPet/ECFP).



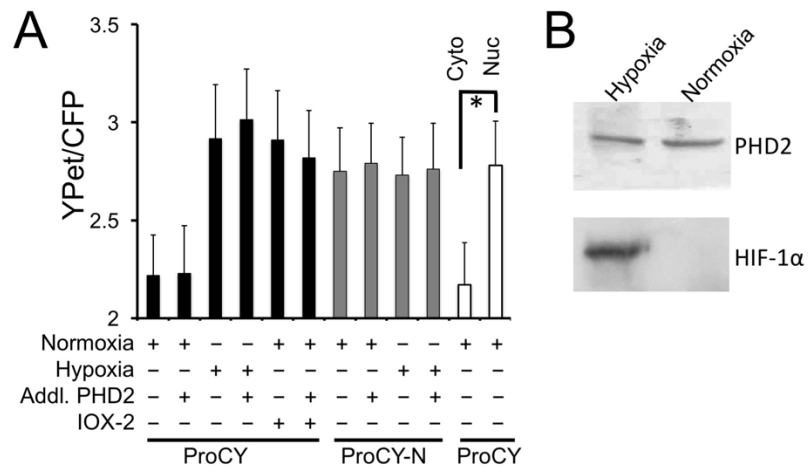


**Figure 3.8.** (A) The FRET ratios of ProCY or ProCY-N in HEK 293T cells under the corresponding conditions. PHD2 overexpression had little effect, indicating the endogenous PHD level was high. Compartmental expression of ProCY suggests a higher PHD activity in the cytosol than the nucleus of HEK 293T cells (\* $p < 0.05$ ). (B) Western blot of PHD2 and HIF-1 $\alpha$  for cells under hypoxia or normoxia.

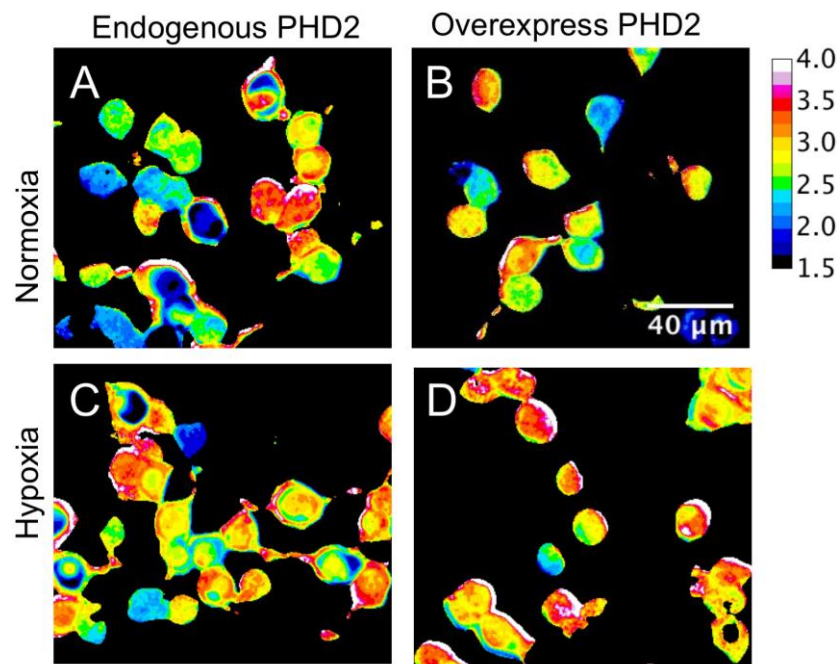


**Figure 3.9.** Pseudocolored ratio images of representative ProCY-N expressing HEK 293T cells under normoxia (A and B) or hypoxia (C and D). PHD2 was overexpressed in cells in panels B and D. The color bar represents the ratio of sensitized YPet fluorescence emission to direct ECFP donor emission (YPet/ECFP).

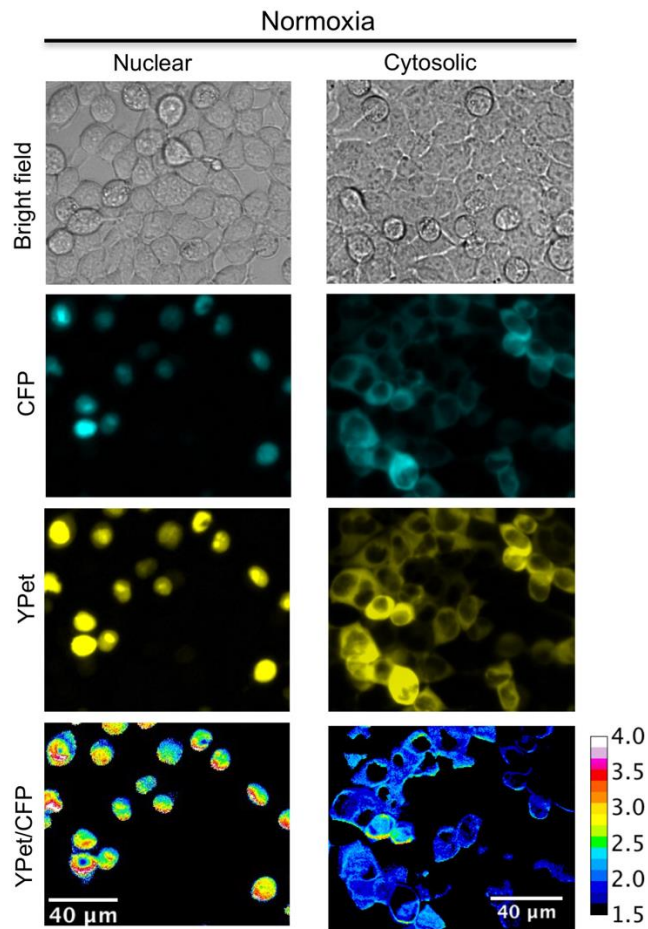


**Figure 3.10.** Microscopic images of representative HEK 293T cells expressing nuclear or cytosolic ProCY. The ratio images are pseudocolored and the color bar represents the ratio of sensitized YPet fluorescence emission to direct ECFP donor emission (YPet/ECFP).

It is generally accepted that the localization of PHDs in distinct subcellular compartments is regulated.<sup>30,31</sup> Their localization and translocation are important mechanisms for the control of hypoxic responses.<sup>31,32</sup> In recent studies, the subcellular localization of PHDs has even been linked to tumor development and resistance to radiotherapy.<sup>33-35</sup> Despite that a number of studies have sought to elucidate intracellular distribution of PHD enzymes, conflicting results have been reported. This discrepancy may be attributed to different cell types used in these studies, or may be caused by the inaccuracy of their detection methods. Since ProCY is a genetically encoded indicator for the HIF-prolyl hydroxylase activity, we simply fused ProCY with a nuclear localization sequence (NLS) or a nuclear export signal (NES) to achieve the complete localization of ProCY in either the nucleus or the cytosol. When HEK 293T cells were cultured in normoxia, reduced FRET ratios were observed for cytosolic ProCY, but not for nuclear ProCY (Figures 3.8 A and 3.10). The result suggests that the endogenous HIF-prolyl hydroxylase activity is mainly in the cytosol of HEK 293T cells. This experiment demonstrates the use of ProCY to directly image subcellular HIF-prolyl hydroxylase activities. The method may be applied to different cell lines to investigate cell-type specific impacts and to elucidate molecular mechanisms that control the shuttling of PHDs between subcellular domains.

### **3.5. Conclusion**

In summary, we have developed a novel genetically encoded dual-emission ratiometric fluorescent biosensor for HIF-prolyl hydroxylase activities, by sandwiching a

proline-containing HIF-1 $\alpha$  derived peptide and a 4-hydroxyproline interacting domain between an FP-based FRET pair. We demonstrated that the probe could be utilized to monitor hypoxia and PHD activities in live mammalian cells. We targeted this biosensor to the nucleus or cytosol, and determined that, under normoxia, the HIF-prolyl hydroxylase activity was mainly confined to the cytosol of HEK 293T cells. Our data collectively suggest broad applications of ProCY on evaluation of hypoxia and prolyl hydroxylase activities and understanding of relevant molecular mechanisms. Moreover, as HIF-prolyl hydroxylases have emerged as promising drug targets for a variety of diseases, such as myocardial infarction, stroke, cancer, diabetes, and severe anemia, ProCY may be utilized in high-throughput assays to identify inhibitors or activators of PHDs.

### **Appendix Material**

List of primers used, and protein sequence alignment of all the biosensors studied in this chapter. This material is in Appendix B.

## References

- 1- Berkelhamer, S. K.; Kim, G. A.; Radder, J. E.; Wedgwood, S.; Czech, L.; Steinhorn, R. H.; Schumacker, P. T.; " Developmental differences in hyperoxia-induced oxidative stress and cellular responses in the murine lung" *Free Radic. Biol. Med.* 2013, 61:51-60.
- 2- Semenza, G. L.; "Hydroxylation of HIF-1: Oxygen Sensing at the Molecular Level" *Physiol.* (Bethesda) 2004, 19:176-182.
- 3- Huang, L. E.; Gu, J.; Schau, M.; Bunn, H. F.; "Regulation of hypoxia-inducible factor 1 $\alpha$  is mediated by an O<sub>2</sub>-dependent degradation domain via the ubiquitin-proteasome pathway" *Proc. Natl. Acad. Sci. U. S. A.* 1998, 95:7987-7992.
- 4- Van Molle, I.; Thomann, A.; Buckley, D. L.; So, E. C.; Lang, S.; Crews, C. M.; Ciulli, A.; "Dissecting fragment-based lead discovery at the von Hippel-Lindau protein: hypoxia inducible factor 1 $\alpha$  protein-protein interface" *Chem. Biol.* 2012, 19:1300-1312.
- 5- Ivan, M.; Kondo, K.; Yang, H.; Kim, W.; Valiando, J.; Ohh, M.; Salic, A.; Asara, J. M.; Lane, W. S.; Kaelin, W. G., Jr.; "HIF $\alpha$  targeted for VHL-mediated destruction by proline hydroxylation: Implications for O<sub>2</sub> sensing" *Science* 2001, 292:464-468.
- 6- Jiang, B. H.; Semenza, G. L.; Bauer, C.; Marti, H. H.; "Hypoxia-inducible factor 1 levels vary exponentially over a physiologically relevant range of O<sub>2</sub> tension" *Am. J. Physiol.* 1996, 271:C1172-1180.
- 7- Giaccia, A. J.; Simon, M. C.; Johnson, R.; "The biology of hypoxia: the role of oxygen sensing in development, normal function, and disease" *Genes Dev.* 2004, 18:2183-2194.
- 8- Vaupel, P.; Mayer, A.; "Hypoxia and Aggressive Tumor Phenotype: Implications for Therapy and Prognosis" *Cancer Metastasis Rev.* 2007, 26:225-239.
- 9- Zhao, S.; Wu, J.; "Hypoxia Inducible Factor Stabilization as a Novel Strategy to Treat Anemia" *Curr. Med. Chem.* 2013, 20:2697-2711.

- 10- Vannucci, S. J.; Hagberg, H. J.; "Hypoxia–ischemia in the immature brain" *Exp. Biol.* 2004, 207:3149-3154.
- 11- Shi, H.; "Hypoxia inducible factor 1 as a therapeutic target in ischemic stroke" *Curr. Med. Chem.* 2009, 16:4593-4600.
- 12- Wu, Y.; Zhang, W.; Li, J.; Zhang, Y.; "Optical imaging of tumor microenvironment" *Am. J. Nucl. Med. Mol. Imaging.* 2013, 3:1-15.
- 13- Papkovsky, D. B.; Dmitriev, R. I.; "Biological detection by optical oxygen sensing" *Chem. Soc. Rev.* 2013, 42:8700-8732.
- 14- Cui, L.; Zhong, Y.; Zhu, W.; Xu, Y.; Du, Q.; Wang, X.; Qian, X.; Xiao, Y.; "A New Prodrug-Derived Ratiometric Fluorescent Probe for Hypoxia: High Selectivity of Nitroreductase and Imaging in Tumor Cell" *Org. Lett.* 2011, 13:928-931.
- 15- Wang, S.; Liu, H.; Mack, J.; Tian, J.; Zou, B.; Lu, H.; Li, Z.; Jiang, J.; Shen, Z.; "A BODIPY-based 'turn-on' fluorescent probe for hypoxic cell imaging" *Chem. Commun. (Camb.)* 2015, 51:13389-13392.
- 16- Li, Z.; Li, X.; Gao, X.; Zhang, Y.; Shi, W.; Ma, H.; "Nitroreductase Detection and Hypoxic Tumor Cell Imaging by a Designed Sensitive and Selective Fluorescent Probe, 7-[(5-Nitrofuranyl) methoxy]-3H-phenoxazin-3-one" *Anal. Chem.* 2013, 85:3926-3932.
- 17- Komatsu, H.; Harada, H.; Tanabe, K.; Hiraoka, M.; Nishimoto, S. I.; "Indolequinone-rhodol conjugate as a fluorescent probe for hypoxic cells: Enzymatic activation and fluorescence properties" *MedChemComm* 2010, 1:50-53.
- 18- Kiyose, K.; Hanaoka, K.; Oshiki, D.; Nakamura, T.; Kajimura, M.; Suematsu, M.; Nishimatsu, H.; Yamane, T.; Terai, T.; Hirata, Y.; Nagano, T.; "Hypoxia-sensitive fluorescent probes for *in vivo* real-time fluorescence imaging of acute ischemia" *J. Am. Chem. Soc.* 2010, 132:15846-15848.

- 19- Cai, Q.; Yu, T.; Zhu, W.; Xu, Y.; Qian, X.; “A turn-on fluorescent probe for tumor hypoxia imaging in living cells: *Chem. Commun. (Camb.)* 2015, 51:14739-14741.
- 20- Takahashi, S.; Piao, W.; Matsumura, Y.; Komatsu, T.; Ueno, T.; Terai, T.; Kamachi, T.; Kohno, M.; Nagano, T.; Hanaoka, K.; “Reversible Off–On Fluorescence Probe for Hypoxia and Imaging of Hypoxia–Normoxia Cycles in Live Cells” *J. Am. Chem. Soc.* 2012, 134:19588-19591.
- 21- Vordermark, D.; Shibata, T.; Brown, J. M.; “Green Fluorescent Protein is a Suitable Reporter of Tumor Hypoxia Despite an Oxygen Requirement for Chromophore Formation” *Neoplasia* 2001, 3:527-534.
- 22- Hirsila, M.; Koivunen, P.; Gunzler, V.; Kivirikko, K. I.; Myllyharju, J.; “Characterization of the Human Prolyl 4-Hydroxylases That Modify the Hypoxia-inducible Factor” *J. Biol. Chem.* 2003, 278:30772-30780.
- 23- Koivunen, P.; Hirsila, M.; Kivirikko, K. I.; Myllyharju, J.; “The Length of Peptide Substrates Has a Marked Effect on Hydroxylation by the Hypoxia-inducible Factor Prolyl 4-Hydroxylases” *J. Biol. Chem.* 2006, 281:28712-28720.
- 24- Hon, W. C.; Wilson, M. I.; Harlos, K.; Claridge, T. D.; Schofield, C. J.; Pugh, C. W.; Maxwell, P. H.; Ratcliffe, P. J.; Stuart, D. I.; Jones, E. Y.; “Structural basis for the recognition of hydroxyproline in HIF-1 $\alpha$  by pVHL” *Nature* 2002, 417:975-978.
- 25- Ouyang, M.; Sun, J.; Chien, S.; Wang, Y.; “Determination of hierarchical relationship of Src and Rac at subcellular locations with FRET biosensors” *Proc. Natl. Acad. Sci. U. S. A.* 2008, 105:14353-14358.
- 26- Ai, H. W.; “Fluorescent-protein-based probes: general principles and practices” *Anal. Bioanal. Chem.* 2015, 407:9-15.
- 27- Nishihara, K.; Kanemori, M.; Kitagawa, M.; Yanagi, H.; Yura, T.; “Chaperone Coexpression Plasmids: Differential and Synergistic Roles of DnaK-DnaJ-GrpE and GroEL-GroES in Assisting Folding of an Allergen of Japanese Cedar Pollen, Cryj2, in *Escherichia coli*” *Appl. Environ. Microbiol.* 1998, 64:1694-1699.



- 28-Hewitson, K. S.; Schofield, C. J.; Ratcliffe, P. J.; "Hypoxia-inducible factor prolyl-hydroxylase: purification and assays of PHD2" *Methods Enzymol.* 2007, 435:25-42.
- 29-Chowdhury, R.; Candela-Lena, J. I.; Chan, M. C.; Greenald, D. J.; Yeoh, K. K.; Tian, Y. M.; McDonough, M. A.; Tumber, A.; Rose, N. R.; Conejo-Garcia, A.; Demetriades, M.; Mathavan, S.; Kawamura, A.; Lee, M. K.; van Eeden, F.; Pugh, C. W.; Ratcliffe, P. J.; Schofield, C. J.; "Selective Small Molecule Probes for the Hypoxia Inducible Factor (HIF) Prolyl Hydroxylases" *ACS Chem. Biol.* 2013, 8:1488-1496.
- 30-Metzen, E.; Berchner-Pfannschmidt, U.; Stengel, P.; Marxsen, J. H.; Stolze, I.; Klinger, M.; Huang, W. Q.; Wotzlaw, C.; Hellwig-Burgel, T.; Jelkmann, W.; Acker, H.; Fandrey, J.; "Intracellular localisation of human HIF-1 $\alpha$  hydroxylases: implications for oxygen sensing" *J. Cell Sci.* 2003, 116:1319-1326.
- 31-Pientka, F. K.; Hu, J.; Schindler, S. G.; Brix, B.; Thiel, A.; Jöhren, O.; Fandrey, J.; Berchner-Pfannschmidt, U.; Depping, R. J.; "Oxygen sensing by the prolyl-4-hydroxylase PHD2 within the nuclear compartment and the influence of compartmentalisation on HIF-1 signalling" *Cell Sci.* 2012, 125:5168-5176.
- 32-Steinhoff, A.; Pientka, F. K.; Mockel, S.; Kettelhake, A.; Hartmann, E.; Kohler, M.; Depping, R.; "Cellular oxygen sensing: Importins and exportins are mediators of intracellular localisation of prolyl-4-hydroxylases PHD1 and PHD2" *Biochem. Biophys. Res. Commun.* 2009, 387:705-711.
- 33-Jokilehto, T.; Rantanen, K.; Luukkaa, M.; Heikkinen, P.; Grenman, R.; Minn, H.; Kronqvist, P.; Jaakkola, P. M.; "Overexpression and Nuclear Translocation of Hypoxia-Inducible Factor Prolyl Hydroxylase PHD2 in Head and Neck Squamous Cell Carcinoma Is Associated with Tumor Aggressiveness" *Clin. Cancer Res.* 2006, 12:1080-1087.
- 34-Jokilehto, T.; Jaakkola, P. M.; "The role of HIF prolyl hydroxylases in tumour growth" *J. Cell. Mol. Med.* 2010, 14:758-770.
- 35-Luukkaa, M.; Jokilehto, T.; Kronqvist, P.; Vahlberg, T.; Grenman, R.; Jaakkola, P.; Minn, H.; "Expression of the cellular oxygen sensor PHD2 (EGLN-1) predicts radiation sensitivity in squamous cell cancer of the head and neck" *Int. J. Radiat. Biol.* 2009, 85:900-908.

36- Schreiber, E.; Matthias, P.; Muller, M. M.; Schaffner, W.; "Rapid detection of octamer binding proteins with 'mini-extracts', prepared from a small number of cells" *Nucleic Acids*. 1989, 17:6419

## Chapter 4

### Toward a Cell-Based Screening Assay for Inhibitors of PHDs

#### 4.1. Abstract

Hypoxia, a condition defined by the reduction of oxygen supply to a tissue below physiological levels, has been linked to diverse pathophysiological processes and diseases, such as cancer, anemia, ischemia, and stroke. Studies of the adaptation to low oxygen levels have identified the Hypoxia Inducible Factor proteins (HIF) and the HIF prolyl hydroxylase domain enzymes (PHDs) as the key components in the signaling pathway that controls the hypoxic response of mammalian cells. As part of the cellular adaptation to hypoxia, the expression of more than 70 genes is activated by the upregulation of HIFs. Consequently, upregulation of HIF through the inhibition of its hypoxia sensors, PHDs, could be a potential therapy for a wide range of diseases linked to hypoxia. Herein, we aimed to utilize ProCY to screen for inhibitors of PHDs in a high throughput screening (HTS) assay. As part of the required validation steps for HTS assays, we utilized a lentiviral vector production system to transduce ProCY into HEK 293T cells. The system could be potentially used in the HTS assay for inhibitors of PHDs. However, further optimization and validation steps are still needed.

## 4.2. Introduction

Tissue hypoxia results when supply of oxygen from the bloodstream fails to meet the demand of O<sub>2</sub>-consuming cells. Hypoxia can occur in physiologic settings such as exercising muscle, embryonic development, and in pathologic conditions including anemia, ischemia, stroke, inflammation, and tumor formation.<sup>1</sup> The levels of HIF- $\alpha$  isoforms are regulated by the activity of the HIF prolyl hydroxylase domain (PHD) enzymes in an oxygen-dependent manner. As stated in chapter 3, hydroxylation at either or both of two prolyl residues of HIF- $\alpha$  by PHDs greatly enhances the recognition of HIF- $\alpha$  by the von Hippel-Lindau protein (pVHL) and the subsequent ubiquitination and proteosomal degradation of HIFs in normoxic conditions. On the contrary, the activity of PHDs is suppressed in hypoxic conditions, resulting in HIF- $\alpha$  stabilization and activation of the HIF system. Accordingly, therapeutic activation of the HIF system in hypoxia-triggered diseases could be achieved by inhibiting its hypoxia sensors (i.e. PHDs).

PHDs are members of the class of enzymes known as 2-oxoglutarate-dependent dioxygenases. These enzymes catalyze the incorporation of oxygen into organic substrates. This is a mechanism that requires 2-oxoglutarate, Fe<sup>2+</sup>, and ascorbate (Figure 4.1).<sup>2</sup> Recently, there has been a growing interest in developing potent and selective inhibitors of PHDs for conditions including anemia and ischemic/vascular diseases.<sup>3</sup> Indeed, various compounds have been reported as PHD inhibitors in the academic and patent literature.<sup>4</sup> Some of these compounds compete with iron in its binding to the active site of PHDs (e.g. CoCl<sub>2</sub>), others are analogues of 2-oxoglutarate (2OG) that bind in the pocket occupied by 2OG (e.g. DMOG, DFO, and IOX2).<sup>5,6</sup> Despite the progress, the

need to develop more inhibitor compounds is still growing. Correspondingly, applying efficient assays to validate PHD inhibitors in a HTS format is an objective of the academic and the commercial research at the chemistry-biology interface.

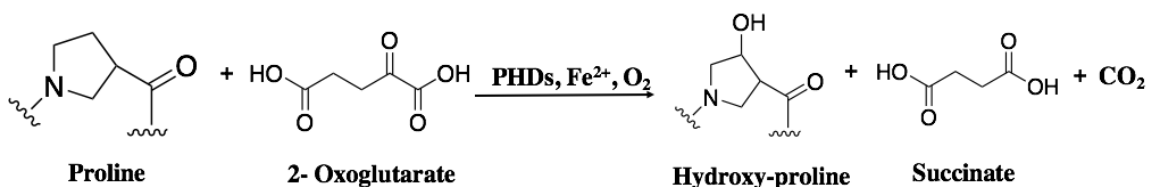


**Figure 4.1.** The reaction catalyzed by the HIF prolyl hydroxylases in the hypoxic response.

In chapter 3 of this dissertation, we developed a ratiometric sensor, ProCY, that can be effectively used to monitor hypoxia in mammalian cells. In this chapter, we are interested in using ProCY and fluorescence imaging technology in a high-throughput screening assay (HTS) to identify inhibitor compounds of PHDs that can be used to validate new drug targets for hypoxia-related diseases. Our assay provides a key advantage in that the small molecule compounds to be tested do not require modification or immobilization; the compound can be directly added to the cell culture media to detect a FRET signal change.

Typically, once an assay format is chosen for HTS, a series of assay development and validation steps must be performed to demonstrate that the method is acceptable for its intended purpose. This includes steps for pre-study, in-study, and cross validation.<sup>7</sup> The pre-study validation steps involve specifically choosing the reagents, control compounds, and detection method. In-study validation steps involve scaling up the assay to at least 96-well plate and using proper control samples to test plate acceptance, check signal variability and procedural errors, and evaluate the stability of the assay over time. Cross-validation steps involve screening a subset of compounds and comparing the agreement in results to predefined criteria, which specify the allowable performance for HTS, to verify that an acceptable level of agreement exists in analytical results (Figure 4.2).

Lentiviruses, such as the Human Immunodeficiency Virus (HIV), are unique and robust vehicles for gene delivery. They are capable of transducing a wide range of cell types and integrating into the host genome of both dividing and non-dividing cells, resulting in long-term expression of the transgene both *in vitro* and *in vivo*.<sup>8</sup> Herein, we show that utilizing ProCY directly in HEK 293T cells in a 96-well plate is not efficient for HTS of PHD inhibitors. Alternatively, we utilized a lentiviral vector production system to transduce ProCY into HEK 293T cells. Our preliminary steps showed that the lentiviral production protocol needs optimization before proceeding to the next validation steps. Optimization steps are in progress as we highly believe that this system can be potentially applied for HTS assays of PHD inhibitors.

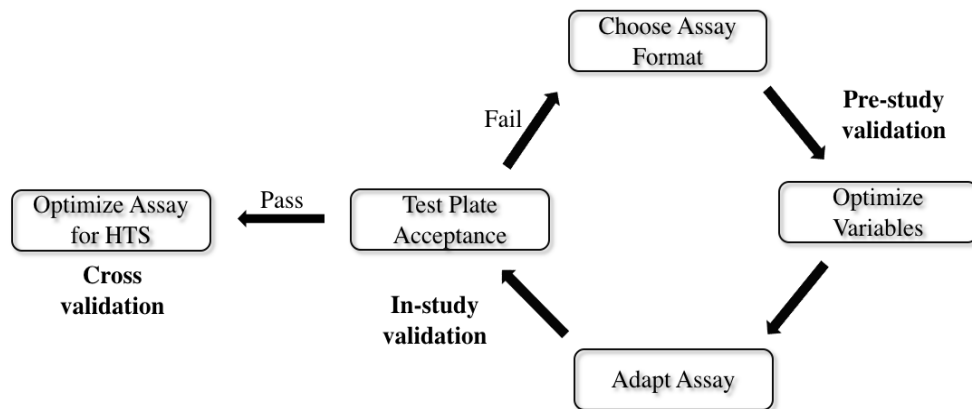


**Figure 4.2.** Assay Development Cycle for HTS.

### 4.3. Experimental Methods

#### 4.3.1 Materials, Reagents, and General Methodology

IOX2 was purchased from Cayman Chemical (Ann Arbor, MI). Synthetic DNA oligonucleotides were purchased from Integrated DNA Technologies (San Diego, CA). pLJM1-EGFP (Plasmid # 19319), pRSV-Rev (Plasmid # 12253), pMDLg.pRRE (Plasmid # 12251), and pMD2.G (Plasmid # 12259) were purchased from Addgene (Cambridge, MA). Restriction endonucleases were purchased from New England Biolabs (Ipswich, MA) or Thermo Scientific Fermentas (Vilnius, Lithuania). PCR products and products of restriction digestion were purified by gel electrophoresis and extracted using Syd Laboratories Gel Extraction columns (Malden, MA). Plasmid DNA was purified

using Syd Laboratories Miniprep columns. DNA sequence analysis was performed by Retrogen (San Diego, CA).

#### *4.3.2. Mammalian Cell Culture, Imaging, and Screening.*

Human Embryonic Kidney (HEK) 293T cells were cultured in Dulbecco's Modified Eagle's Medium (DMEM) supplemented with 10% fetal bovine serum (FBS) in a 96-well plate. Cells were incubated at 37°C with 5% CO<sub>2</sub> in humidified air for 24 hours. HEK 293T cells were next transfected with 4 µg pcDNA3-ProCY in the presence of 12 µg PEI (polyethyleneimine, linear, M.W. 25 kDs). 10 µM of the inhibitor control compound, IOX2, was added to the control wells, and cells were incubated for 48 hours. All media were replaced with Dulbecco's Phosphate Buffered Saline (DPBS) before imaging. Initial screening experiments were done using a monochromator-based Synergy Mx Microplate Reader. The instrument was set to area scan the plate. Excitation was set at 434 nm, and emission was recorded at 477 and 525 nm.

#### *4.3.3. Construction of the Lentivirus Reporter Plasmid*

Polymerase chain reaction was utilized to amplify the gene fragment of ProCY using oligos pLJM1-NheI-F and pLJM1-EcoRI-R. The PCR product was then digested with NheI and EcoRI and ligated into a predigested pLJM1-EGFP lentivirus expression vector to afford pLJM1-ProCY. The resultant ligation product was used to transform E. coli DH10B competent cells, which was next plated on Luria-Bertani (LB) broth agar plates supplemented with ampicillin (50 µg/mL).



#### 4.3.4. Lentivirus Production and Purification

Lentivirus vectors were prepared as previously described.<sup>9</sup> Briefly, human Embryonic Kidney (HEK) 293T cells were split to 6 x 10 cm dishes from a confluent T75 cm flask. Cells were cultured in Dulbecco's Modified Eagle's Medium (DMEM) supplemented with 10% fetal bovine serum (FBS) and incubated at 37°C with 5% CO<sub>2</sub> in humidified air for 24 hours. For the 6 x 10 cm dishes, a plasmid mix was prepared by mixing 48.9 µg pLJM1-ProCY transfer plasmid, 31.86 µg pMDLg/pRRE and 12.3 µg pRSV-Rev packaging plasmids, 17.16 µg pMD2.G envelope expressing plasmid, and 440.8 µg PEI (polyethyleneimine, linear, M.W. 25 kDs) in the presence of 14.4 mL DMEM solution. The solution was mixed gently and allowed to incubate for 15 min at room temperature. Next, transfection mixture was carefully added to each dish and the cells were incubated at 37°C with 5% CO<sub>2</sub> in humidified air for 24 hours. After 24 hours, we harvested the supernatant and added fresh DMEM supplemented with 10% fetal bovine serum (FBS) to each dish. Following 24-hour incubation period at 37°C, the supernatant was collected from the dishes and pooled with the first harvest. We next cleared the supernatant of cell debris by filtering through a 0.45-µm filter. The cleared supernatant was used directly to transduce HEK 293T cells.

#### 4.4. Results and Discussion

In chapter 3 of this dissertation, we demonstrated that ProCY could be effectively used to monitor hypoxia and evaluate PHD2 activity in mammalian cells. Owing to its ability to provide a detectable FRET signal in response to PHD2 activity in hypoxia and

normoxia, we envisioned that ProCY could be effectively used to screen for inhibitors of PHDs in a HTS assay. In general, as mentioned above, a series of validation steps are required when developing an assay for HTS. Our assay has passed the pre-study validation steps, as we had carefully optimized our probe and transfection procedure as well as selected the reagents and control compounds. Next, we wanted to validate our assay compatibility with microtiter plate formats, typically a 96-well plate, so we transiently transfected HEK 293T cells seeded in a 96-well plate and used IOX2, a commercially available inhibitor, as the control compound. Subsequently, the area was scanned for FRET using the plate reader. Unfortunately, our results did not meet expectations. We attributed this to the uneven cell density on the plate surface caused by cells being washed off the plate when changing media during transfection, the difference in transfection efficiency between cells, and the inevitable cell death occurring regardless of the transfection method used (Figure 4.3). We consequently used a lentiviral vector production system to transduce ProCY into HEK 293T cells. Owing to their robustness and effectiveness in transgene delivery in both dividing and non-dividing cells, we hypothesized that lentiviral vectors derived from HIV-1 would be able to infect all HEK 293T cells on a 96-well plate without the need to wash or change media on cells. We used the third-generation packaging system that consists of four plasmids with Rev gene encoded on a separate packaging plasmid for increased biosafety. We cloned ProCY into the transfer viral vector pLJM1 and used HEK 293T cells to produce lentivirus vectors following a previously reported method<sup>9</sup> (summarized in Figure 4.4). We imaged the transfected cells and confirmed fluorescence, so we harvested the viral particles and

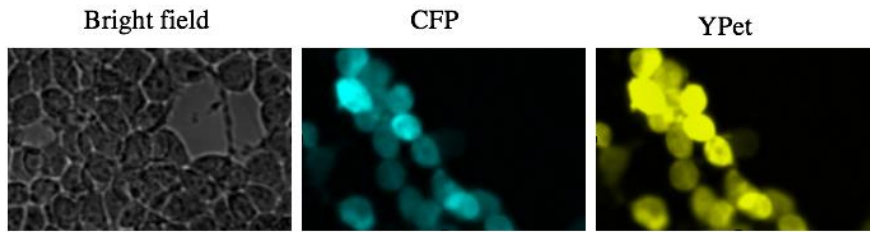


**Figure 4.3.** Microscopic images of representative HEK 293T cells expressing ProCY. The cells were cultured under normoxia in a 96-well plate and treated with IOX2.

stored them at 4 °C. Following the second harvest, we added the un-concentrated viral vectors directly on HEK 293T cells and imaged the cells. Unfortunately, the cells were not fluorescent indicative of low transduction efficiency which may be attributed to having low-titer lentivirus particles ( $< 10^6$  TU/mL). Also, although some reports claims that lentivirus particles could be stored at 4 °C for up to 3-4 days without loss of activity,<sup>8,9</sup> a more recent study shows that the infection efficiency of both concentrated and un-concentrated lentivirus decreases rapidly when viruses are stored at 4 °C ( $\tau \approx 1.9$  days), and that ultracentrifugation with relative centrifugal force (RCF) exceeding 90,000 g is crucial to remove impurities and produce high-titer lentivirus ( $> 10^9$  TU/ml) with high infection rate.<sup>10</sup> Consequently, our lentivirus production system needs to be optimized to produce high titer-lentivirus particles with high infection efficiency to effectively transduce mammalian cells with our target sensor ProCY.

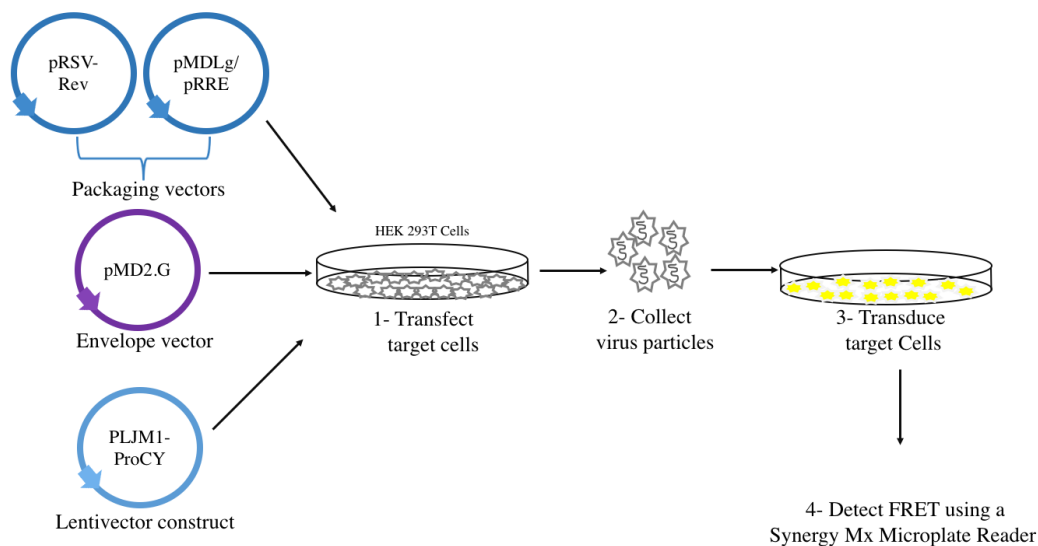


**Figure 4.4.** Schematic representation of the third generation lentiviral production and transduction system.

#### 4.5. Conclusion and Future Direction

To conclude, we have presented an assay format using ProCY and a monochromator-based Microplate Reader to screen for inhibitors of PHD2 that could be potentially used to target hypoxia-related diseases. Adopting our screening assay to automation and scale up requires validation steps to demonstrate that the method is acceptable for HTS. This requires testing our assay in a microtiter plate, typically a 96-well plate. Since the plate reader scans the area occupied by cells to detect a FRET signal, we used a lentiviral vector production system to transduce ProCY into our target cells. Apparently, high-titer viruses are required for high transduction efficiency and therefore, method optimization of our lentiviral packaging system is required. Interestingly, Jiang *et*

*al<sup>10</sup>* proposed an alternative method to ultracentrifugation to produce high-titer viruses based on sucrose gradient centrifugation with a regular tabletop centrifuge (relative speed  $\leq 10,000$  g). We next aim to test their reported method and subsequently, we will continue to validate our assay as we strongly believe it could be potentially used to screen for inhibitors of PHDs to treat hypoxia-related diseases.

### **Appendix Material**

List of primers used is in Appendix C.

## Reference

- 1- Papandreou, I.; Cairns, R. A.; Fontana, L.; Lim, A. L.; Denko, N. C.; “HIF-1 mediates adaptation to hypoxia by actively downregulating mitochondrial oxygen consumption”, *Cell Metabolism*, 2006; 3:187-197
- 2- Smith, T. G.; Talbot, N. P.; “Prolyl Hydroxylases and Therapeutics”, *Antioxid. & Redox Signal.*, 2010; 12:431-433
- 3- McNeill, L. A.; Flashman, E.; Buck, M. R. G.; Hewitson, K. S.; Clifton, I. J.; Jeschke, G.; Claridge, T. D. W.; Ehrismann, D.; Oldham, N. J.; Schofield, C. J.; “Hypoxia-inducible factor prolyl hydroxylase 2 has a high affinity for ferrous iron and 2-oxoglutarate”, *Mol. BioSyst.*, 2005; 1:321-324
- 4- Chan, M. C.; Atasoylu, O.; Hodson, E.; Tumber, A.; Leung, I. K. H.; Chowdhury, R.; Gomez-Perez, V.; Demetriades, M.; Rydzik, A. M.; Holt-Martyn, J.; Tian, Y.; Bishop, T.; Claridge, T. D. W.; Kawamura, A.; Pugh, C. W.; Ratcliffe, P. J.; Schofield, C. J.; “Potent and Selective Triazole-Based Inhibitors of the Hypoxia-Inducible Factor Prolyl-Hydroxylases with Activity in the Murine Brain”, *PLOS ONE*, 2015, 1-17
- 5- Rabinowitz, M. H.; “Inhibition of Hypoxia-Inducible Factor Prolyl Hydroxylase Domain Oxygen Sensors: Tricking the Body into Mounting Orchestrated Survival and Repair Responses”, *J. Med. Chem.*, 2013, 56:9369-9402
- 6- Chowdhury, R.; Candela-Lena, J. I.; Chan, M. C.; Greenald, D. J.; Yeoh, K. K.; Tian, Y.; McDonough, M. A.; Tumber, A.; Rose, N. R.; Conejo-Garcia, A.; Demetriades, M.; Mathavan, S.; Kawamura, A.; Lee, M. K.; Eeden, F. V.; Pugh, C. W.; Ratcliffe, P. J.; Schofield, C. J.; “Selective Small Molecule Probes for the Hypoxia Inducible Factor (HIF) Prolyl Hydroxylases”, *ACS Chem. Biol.*, 2013, 8:1488-1496
- 7- Eastwood, B. J.; Iturria, S. J.; Iversen, P. W.; Montrose, C.; Moore, R.; Sittampalam, G. S.; “Guidance for Assay Development & HTS” *Eli Lilly and Company and the National Institutes of Health Chemical Genomics Center* 2007, 5:1-316

- 8- Wang, X.; McManus, M.; “Lentivirus Production” *J Vis Exp.* 2009, 32:1499
- 9- Tiscornia, G.; Singer, O.; Verma, I. M.; “Production and purification of Lentiviral vectors” *Nature Protocols* 2006, 1:241-245
- 10- Jiang, W.; Hua, R.; Wei, M.; Li, C.; Qiu, Z.; Yang, X.; Zhang, C.; “An optimized method for high-titer lentivirus preparations without ultracentrifugation” *Sci. Rep.* 2015, **5**, 13875.

## Chapter 5

### Concluding Remarks and Future Direction

In this dissertation, we have combined FRET technology with fluorescence microscopy and fluorescent proteins to design genetically encoded FRET-based probes for live cell imaging. We utilized fluorescent proteins of different hues and applied random mutagenesis, site directed mutagenesis, and the genetic code expansion strategy in designing and constructing our FRET-based sensor, hsCY (chapter 2). Our sensors could be effectively used to detect FRET changes in live cells with improved spatial and temporal resolution (chapter 2 and 3). Since they are genetically encoded, the probes could be targeted to subcellular compartments such as the cytosol and the nucleus (chapter 3). Moreover, we used a lentiviral packaging system to transduce a genetically encoded sensor into HEK 293T cells toward a lab-HTS assay of inhibitors of PHD2 (Chapter 4).

In Chapter 2, we have developed the first genetically-encoded FRET-based probe, hsCY, for the detection of H<sub>2</sub>S in mammalian cells. In this work, we have fused cpGFP to EBFP2 and used the genetic code expansion strategy to incorporate *pAzF* into cpGFP. Upon reaction with H<sub>2</sub>S, hsCY showed selective H<sub>2</sub>S-induced FRET ratio change by modulation of the donor fluorescence intensity. We tested the selectivity of hsCY against a panel of redox-active molecules commonly generated by cells. Except for H<sub>2</sub>S, hsCY showed little or no response to the tested molecules. When tested in live mammalian



HEK 293T cells, hsCY showed a large ratiometric response to H<sub>2</sub>S. Collectively, our results showed that hsCY could be used to sensitively and selectively detect H<sub>2</sub>S in mammalian cells. hsCY thus represents a valuable addition to the toolbox for H<sub>2</sub>S detection and imaging. In future studies, the same sensor design and optimization strategy could be applied to derive similar FRET-based probes for other cellular reactive chemical species.

In chapter 3, we have developed a novel genetically encoded FRET-based biosensor, ProCY, for HIF-prolyl hydroxylase activities. We fused a proline-containing HIF-1 $\alpha$  derived peptide and a 4-hydroxyproline interacting domain (VHL) between an ECFP and YPet pair. We showed that the FRET ratio (YPet/ECFP) of this ProCY changed from 2.95 to 1.76 corresponding to a dynamic range of 168% upon addition of PHD2 while the P564A mutant (ProCY-N) did not respond to PHD2 addition. This result clearly indicated that PHD2 hydroxylation of the P564 residue of HIF-1  $\alpha$  induced a conformational change that altered the distance and/or relative orientation between ECFP and YPet. We also tested ProCY in live mammalian cells, and showed that FRET increased in hypoxic conditions compared to normoxic conditions demonstrating that the probe could be utilized to monitor hypoxia and PHD activities in live mammalian cells. When targeted to the nucleus and the cytosol under normoxic conditions, ProCY showed that the HIF-prolyl hydroxylase activity was mainly confined to the cytosol of HEK 293T cells. Our data collectively suggest broad applications of ProCY on evaluation of hypoxia and prolyl hydroxylase activities and understanding of relevant molecular mechanisms. Increasing interest in HIF-prolyl hydroxylases as promising drug targets for a variety of

diseases, such as myocardial infarction, stroke, cancer, diabetes, and severe anemia, motivates us to utilize ProCY in high-throughput assays in future studies to identify inhibitors or activators of PHDs.

In chapter 4, we proposed a high-throughput screening assay format to screen for PHD2 inhibitors utilizing ProCY. To validate the assay for HTS, we transiently transfected HEK 293T cells in a 96-well plate with ProCY and used IOX2 as a control compound. FRET results obtained by the plate reader did not agree with the expected ratios mainly due to uneven cell attachment on the plate surface caused by washing out the cells from the plate during transfection, and by the difference in transfection efficiency between cells. Alternatively, we used a lentiviral vector production system to transduce ProCY into our target cells. Since high-titer viruses are required for high transduction efficiency in mammalian cells, our lentiviral packaging method needed optimization. Previous reports claim that ultracentrifugation with relative centrifugal force (RCF) exceeding 90,000 g is crucial to remove impurities and produce high-titer lentivirus ( $> 10^9$  TU/ml) with high infection rate. Unfortunately, an ultracentrifuge is not a common instrument in labs. More recently, a sucrose gradient centrifugation with a regular tabletop centrifuge (relative speed  $\leq 10,000$  g) has been reported to replace ultracentrifugation and produce high-titer viruses. In our future studies, we will test the sucrose gradient method, and subsequently we will continue validating our assay toward developing an assay to screen for PHD2 inhibitors for hypoxia-related diseases.

## Appendix A

### Supporting Information for Chapter 2

#### A FRET-Based Genetically Encoded Fluorescent Probe for Hydrogen Sulfide

**Table A1. List of Oligonucleotides used in this study**

<b>Primer name</b>	<b>Nucleotide sequence</b>
GFP-For	TACCCCATGGGCTCGAGCACTTACAAC
GFP-Rev	GGCTAAGCTTGCTCCCACCATGGTGCGTGTTGTA
BFP-For	CTACGAAAGCTTATGGTGAGCAAGGGCGAG
BFP-Rev	CTACTGCTCGAGTTAATGATGATGATGATGATGCTTGTACA GCTCGTC
BFP-For2	CTAGGAAAGCTTGAGGAGCTGTTCACCGGG
GFP-Rev2	TCGGAAGCTTATGGTGCGTGTTGTACTC
H148X-For	TACCCCATGGGCTCGAGCACTTACAACAGCNNKAAGGTCT ATATCACCGCCGAC
TX-SX-Rev	GTCTTTGCTCAGCACMNNCTGMNNGCTCAGGTAGTGGTT
TX-SX-For	AACCACTACCTGAGCNNKCAGNNKGTGCTGAGCAAAGAC
pBAD-F	ATGCCATAGCATTTTTATCC
pBAD-R	GATTTAATCTGTATCAGG
hsCY-HindIII-F	CTTAAGCTTGCCGCCACCATGGGCTCCAGCACTTAC
hsCY-EcorI-F	ACCATGAATTCGAGGAGCTGTTCACCGGG
hsCY-EcorI-R	TCCTCGAATTCATGGTGATGTTGTA
hsCY-ApaI-R	AAACGGGCCCTTAATGATGATGATGATGATGCTTGTACAG CTCGTCCAT

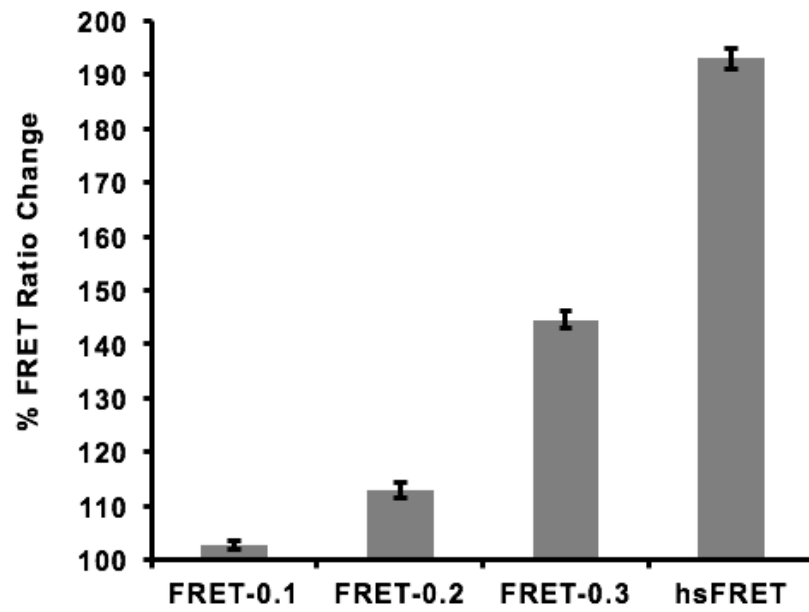


**Figure A1.** % FRET change of the different designs constructed in this study. Crude proteins were extracted with B-PER from *E. coli* cells and tested with 1 mM H<sub>2</sub>S.

MGSSTYNSNKVYITADKQKNGIKVNFKIRHNVEDGSVQLADHYQQNTPIGDGPVLLPDNH  
YLSVQSMLSKDPNEKRDHMLLEFVTAAGITLGMDELYKVDGGPGGTGVSKGEELFTGVV  
PILVELDGDVNGHKFSVRGEGEGDATNGKLTCLKFICTTGKLPVPWPTLVTLT**TZG**VQCFSR  
YPDHMKQHDFFKSAMPEGYVQERTIFFKGDGTYKTRAEVKFEGDTLVNRIELKGIDFKED  
GNILGHKLEYNMHHKLEELFTGVVPILVELDGDVNGHKFSVRGEGEGDATNGKLTCLKFIC  
TTGKLPVPWPTLVTTL**SHG**VQCFARYPDHMKQHDFFKSAMPEGYVQERTIFFKDDGTYKT  
RAEVKFEGDTLVNRIELKGVDFKEDGNILGHKLEYNFNHNYIMAVKQKNGIKVNFKIR  
HNVEDGSVQLADHYQQNTPIGDGPVLLPDSHYLSTQSVLSKDPNEKRDHMLLEFRTAAG  
ITLGMDELYK HHHHHH

**Figure A2.** Full protein sequence of hsCY. The chromophores of cpGFP and EBFP2 are colored in green and blue, respectively.

## Appendix B

### Supporting Information for Chapter 3

#### A Genetically Encoded FRET Sensor for Hypoxia and Prolyl Hydroxylases

**Table B1. List of Oligonucleotides used in this study**

Primer name	Nucleotide sequence
YPet-For	GATTGGTACCGAGTTATTCAGTGGTGTT
YPet-Rev	TTCTAAGCTTAGAATTCTTTGTACAATTCATT
ECFP-For	AGGGCTCGAGCATGGTGAGCAAGGGCGA
PVHL-Rev	CAGCACTGGGCGCTGCAGGGCGGCGGTCACGAACTC
Pst1-For	CCGCCCTGCAGCGCCAGTGCTGCGCAGC
Kpn1-Rev1	GGGGATGTATGGAGCCAACATCTCTAAATCAAGGTCGAGC TCACCACCTGCTGAACCTGC
Kpn-Rev2	ACTCGGTACCAAACTGCGAAGCTGGAAGTCATCATCCAT GGGGATGTATGGAGCCAA
Kpn-Rev3	ACCACCTGCTGAACCTGCTCCGCTACCACCGGCAGAGCCA CC
GGSG-For	GGAGGCAGCGGACGCCAGTGCTGCGCAGC
GGSG-Rev	GCGTCCGCTGCCTCCGGCGGCGGTCACGAACTC
MidFloppy-R	GAATGAGCTCTTTAGGCTTAGGTTTGGGCTTCGGCTTTGGT TTGCCACCTGCGCTTGA
MidFloppy-F1	CTTAGAGCTCCCCAAGCCAAAACCAAAGCCCAAGCCGAAG CCAAAGCCGAAGCCC
MidFloppy-F2	CCAAAGCCGAAGCCCAGCGGTGGTAGCGGAGCAGGTTTCAG CAGGTGGTAAGCTC
pBAD-Rev	GATTTAATCTGTATCAGG
HIF-Rigid-F	ATTAGGTACCAAGCCCAAGCCGAAGCCAAAGCCGAAGCCC GAGTTATTCAGTGGTGTT
SacI-Rev	GGTCGAGCTCAGAGCCACCTGCGCT
PAPA-Rev	ACTCGGTACCAAACTGCGAAGCTGGAAGTCATCATCCAT TGCGATGTAAGCAGCCAA
PHD2-Kpn1-F	CGTGGGTACCATGCCCAACGGGCAGACGAAG
PHD2-HindIII-R	AAGCGAAGCTTAGAAGACGTCTTTACCGAC
HydpcDNA3-F	CGCCTAAGCTTGCCGCCACCATGGTGAGCAAGGGCGAG

HydpcDNA3-R	ACCTTCTAGATTAGAATTCTTTGTACAATTCATT
PHD2-pcDNA3-F	TCGCCTAAGCTTGCCGCCACCATGGGTCCCAACGGGCAGACGAAG
PHD2-pcDNA3-R	GATCTCTAGATTAGAAGACGTCTTTACCGACCGA
mycPHD2-R	CCCTCTAGATTACAGATCCTCTTCTGAGATGAGTTTTTTGTTCGAAGACGTCTTTACCGAC
NES-HP-F1	CCCAAGCTTGCCGCCACCATGGCACTTCAACTTCCTCCTCTTGAACG
NES-HP-F2	CAACTTCCTCCTCTTGAACGTCTTACTCTTGTGAGCAAGGGCGAGGAG
NES-HP-XbaI-R	GCATTCTAGAGAATTCTTTGTACAATTCA
PLJMI-NheI-F	TCCGCTAGCGCCGCCACCATGGGAGCAAGGGCGAGG
pHP-Nuc-R	TCAGCTCGAGAGAACTCTTTGTACAATTCATT

```

ProCY      MRGSHHHHHHGMASMTGGQQMGRDLYENLYFQGSMSVSKGEELFTGVVPIILVELDGDVNG
ProCY-N   MRGSHHHHHHGMASMTGGQQMGRDLYENLYFQGSMSVSKGEELFTGVVPIILVELDGDVNG
ProCY-B   MRGSHHHHHHGMASMTGGQQMGRDLYENLYFQGSMSVSKGEELFTGVVPIILVELDGDVNG
ProCY-C   MRGSHHHHHHGMASMTGGQQMGRDLYENLYFQGSMSVSKGEELFTGVVPIILVELDGDVNG
ProCY-D   MRGSHHHHHHGMASMTGGQQMGRDLYENLYFQGSMSVSKGEELFTGVVPIILVELDGDVNG
ProCY-E   MRGSHHHHHHGMASMTGGQQMGRDLYENLYFQGSMSVSKGEELFTGVVPIILVELDGDVNG

ProCY      HRFVSVSGELEGDATYGKLTLLKFICTTGKLPVPWPPTLVTTLTWGVQCFSRYPDHMKQHDF
ProCY-N   HRFVSVSGELEGDATYGKLTLLKFICTTGKLPVPWPPTLVTTLTWGVQCFSRYPDHMKQHDF
ProCY-B   HRFVSVSGELEGDATYGKLTLLKFICTTGKLPVPWPPTLVTTLTWGVQCFSRYPDHMKQHDF
ProCY-C   HRFVSVSGELEGDATYGKLTLLKFICTTGKLPVPWPPTLVTTLTWGVQCFSRYPDHMKQHDF
ProCY-D   HRFVSVSGELEGDATYGKLTLLKFICTTGKLPVPWPPTLVTTLTWGVQCFSRYPDHMKQHDF
ProCY-E   HRFVSVSGELEGDATYGKLTLLKFICTTGKLPVPWPPTLVTTLTWGVQCFSRYPDHMKQHDF

ProCY      KSAMPEGYVQERTIFFKDDGNYKTRAEVKFEGDTLVNRIELKIDFKEDGNILGHKLEYN
ProCY-N   KSAMPEGYVQERTIFFKDDGNYKTRAEVKFEGDTLVNRIELKIDFKEDGNILGHKLEYN
ProCY-B   KSAMPEGYVQERTIFFKDDGNYKTRAEVKFEGDTLVNRIELKIDFKEDGNILGHKLEYN
ProCY-C   KSAMPEGYVQERTIFFKDDGNYKTRAEVKFEGDTLVNRIELKIDFKEDGNILGHKLEYN
ProCY-D   KSAMPEGYVQERTIFFKDDGNYKTRAEVKFEGDTLVNRIELKIDFKEDGNILGHKLEYN
ProCY-E   KSAMPEGYVQERTIFFKDDGNYKTRAEVKFEGDTLVNRIELKIDFKEDGNILGHKLEYN

ProCY      YISHNVYITADKQKNGIKAHFKIRHNIEDGSVQLADHYQQNTPIGDGPVLLPDNHYLSTQ
ProCY-N   YISHNVYITADKQKNGIKAHFKIRHNIEDGSVQLADHYQQNTPIGDGPVLLPDNHYLSTQ
ProCY-B   YISHNVYITADKQKNGIKAHFKIRHNIEDGSVQLADHYQQNTPIGDGPVLLPDNHYLSTQ
ProCY-C   YISHNVYITADKQKNGIKAHFKIRHNIEDGSVQLADHYQQNTPIGDGPVLLPDNHYLSTQ
ProCY-D   YISHNVYITADKQKNGIKAHFKIRHNIEDGSVQLADHYQQNTPIGDGPVLLPDNHYLSTQ
ProCY-E   YISHNVYITADKQKNGIKAHFKIRHNIEDGSVQLADHYQQNTPIGDGPVLLPDNHYLSTQ

ProCY      SALSXPDPNEKRDHMLLEFVTA----LQRPVLRVSNRSREPSQVIFCNRSRPRVLPVWLN
ProCY-N   SALSXPDPNEKRDHMLLEFVTA----LQRPVLRVSNRSREPSQVIFCNRSRPRVLPVWLN
ProCY-B   SALSXPDPNEKRDHMLLEFVTAAGGSGLRQRPVLRVSNRSREPSQVIFCNRSRPRVLPVWLN
ProCY-C   SALSXPDPNEKRDHMLLEFVTAAGGSGLRQRPVLRVSNRSREPSQVIFCNRSRPRVLPVWLN
ProCY-D   SALSXPDPNEKRDHMLLEFVTAAGGSGLRQRPVLRVSNRSREPSQVIFCNRSRPRVLPVWLN
ProCY-E   SALSXPDPNEKRDHMLLEFVTA----LQRPVLRVSNRSREPSQVIFCNRSRPRVLPVWLN

ProCY      FDGEPQPYPTLPPGTGRRIHSGRHLWLFDRDAGTHDGLLVNQTELVFVPSLNVDGQPIFAN
ProCY-N   FDGEPQPYPTLPPGTGRRIHSGRHLWLFDRDAGTHDGLLVNQTELVFVPSLNVDGQPIFAN
ProCY-B   FDGEPQPYPTLPPGTGRRIHSGRHLWLFDRDAGTHDGLLVNQTELVFVPSLNVDGQPIFAN
ProCY-C   FDGEPQPYPTLPPGTGRRIHSGRHLWLFDRDAGTHDGLLVNQTELVFVPSLNVDGQPIFAN
ProCY-D   FDGEPQPYPTLPPGTGRRIHSGRHLWLFDRDAGTHDGLLVNQTELVFVPSLNVDGQPIFAN
ProCY-E   FDGEPQPYPTLPPGTGRRIHSGRHLWLFDRDAGTHDGLLVNQTELVFVPSLNVDGQPIFAN

ProCY      ITLPGSAGSSAGG-----SAGGSAGSAGGELDLDDLEM
ProCY-N   ITLPGSAGSSAGG-----SAGGSAGSAGGELDLDDLEM
ProCY-B   ITLPGSAGSSAGG-----SAGGSAGSAGGELDLDDLEM
ProCY-C   ITLPGSAGSSAGGKPKPKPKPKELPKPKPKPKPKPKPAGGSAGSAGKLDLDDLEM
ProCY-D   ITLPGSAGSSAGG-----SAGGSAGSAGGELDLDDLEM
ProCY-E   ITLPGSAGSSAG-----GSELDLDDLEM

ProCY      LAPYIPMDDDFQLRSFGT-----ELFTGVVPIILVELDGDVNGHKFVSVEGEGDA
ProCY-N   LAAYIAMDDDFQLRSFGT-----ELFTGVVPIILVELDGDVNGHKFVSVEGEGDA
ProCY-B   LAPYIPMDDDFQLRSFGT-----ELFTGVVPIILVELDGDVNGHKFVSVEGEGDA
ProCY-C   LAPYIPMDDDFQLRSFGT-----ELFTGVVPIILVELDGDVNGHKFVSVEGEGDA
ProCY-D   LAPYIPMDDDFQLRSFGTKPKPKPKPKPELFTGVVPIILVELDGDVNGHKFVSVEGEGDA
ProCY-E   LAPYIPMDDDFQLRSFGT-----ELFTGVVPIILVELDGDVNGHKFVSVEGEGDA

ProCY      TYGKLTLLKLLCTTGKLPVPWPPTLVTTLGYGVCQFARYPDHMKQHDFFKSAMPEGYVQERT
ProCY-N   TYGKLTLLKLLCTTGKLPVPWPPTLVTTLGYGVCQFARYPDHMKQHDFFKSAMPEGYVQERT
ProCY-B   TYGKLTLLKLLCTTGKLPVPWPPTLVTTLGYGVCQFARYPDHMKQHDFFKSAMPEGYVQERT
ProCY-C   TYGKLTLLKLLCTTGKLPVPWPPTLVTTLGYGVCQFARYPDHMKQHDFFKSAMPEGYVQERT
ProCY-D   TYGKLTLLKLLCTTGKLPVPWPPTLVTTLGYGVCQFARYPDHMKQHDFFKSAMPEGYVQERT
ProCY-E   TYGKLTLLKLLCTTGKLPVPWPPTLVTTLGYGVCQFARYPDHMKQHDFFKSAMPEGYVQERT

ProCY      IFFKDDGNYKTRAEVKFEGDTLVNRIELKIDFKEDGNILGHKLEYNNSHNVYITADKQ
ProCY-N   IFFKDDGNYKTRAEVKFEGDTLVNRIELKIDFKEDGNILGHKLEYNNSHNVYITADKQ
ProCY-B   IFFKDDGNYKTRAEVKFEGDTLVNRIELKIDFKEDGNILGHKLEYNNSHNVYITADKQ
ProCY-C   IFFKDDGNYKTRAEVKFEGDTLVNRIELKIDFKEDGNILGHKLEYNNSHNVYITADKQ
ProCY-D   IFFKDDGNYKTRAEVKFEGDTLVNRIELKIDFKEDGNILGHKLEYNNSHNVYITADKQ
ProCY-E   IFFKDDGNYKTRAEVKFEGDTLVNRIELKIDFKEDGNILGHKLEYNNSHNVYITADKQ

ProCY      KNGIKANFKIRHNIEDGGVQLADHYQQNTPIGDGPVLLPDNHYLSYQSALFKDPNEKRDH
ProCY-N   KNGIKANFKIRHNIEDGGVQLADHYQQNTPIGDGPVLLPDNHYLSYQSALFKDPNEKRDH
ProCY-B   KNGIKANFKIRHNIEDGGVQLADHYQQNTPIGDGPVLLPDNHYLSYQSALFKDPNEKRDH
ProCY-C   KNGIKANFKIRHNIEDGGVQLADHYQQNTPIGDGPVLLPDNHYLSYQSALFKDPNEKRDH
ProCY-D   KNGIKANFKIRHNIEDGGVQLADHYQQNTPIGDGPVLLPDNHYLSYQSALFKDPNEKRDH
ProCY-E   KNGIKANFKIRHNIEDGGVQLADHYQQNTPIGDGPVLLPDNHYLSYQSALFKDPNEKRDH

ProCY      MVLLEFLTAAGITEGMNELYKEF-
ProCY-N   MVLLEFLTAAGITEGMNELYKEF-
ProCY-B   MVLLEFLTAAGITEGMNELYKEF-
ProCY-C   MVLLEFLTAAGITEGMNELYKEF-
ProCY-D   MVLLEFLTAAGITEGMNELYKEF-
ProCY-E   MVLLEFLTAAGITEGMNELYKEF-

```

**Figure B1.** Alignment of protein sequences of the biosensors constructed in this study.



## Appendix C

### Supporting Information for Chapter 4

#### Toward a Lab-Cell Screening Assay for Inhibitors of PHDs

**Table C1. List of Oligonucleotides used in this study**

<b>Primer name</b>	<b>Nucleotide sequence</b>
pLJM1-NheI-F	TCCGCTAGCGCCGCCACCATGGTGAGCAAGGGCGAGG
pLJM1-EcoRI-R	CGAGAATTCTTAGAACTCTTTGTACAATTCATTC